University of Stavanger

Faculty of Science and Technology

MASTER'S THESIS

Study program/ Specialization: Petroleum Technology / Well Engineering	Spring semester, 2020 Open
Writer: Diego Arturo Pinto Ariza	…… (Writer's signature)
Faculty supervisor: Dan Sui External supervisor(s): Ahmad Mirhaj (MHWirth)	
Thesis title: Effect of fluid forces on wellbore mechanics	
Credits (ECTS): 30 ECTS	
Key words: Drilling, Hook load, fluid, forces, viscous forces, hydrodynamic forces, inertial force	Pages: ……79…… + enclosure: …26…… Stavanger, …14/07/2020….. Date/year

Front page for master thesis
Faculty of Science and Technology

Abstract

In the present situation of rig operations, the procedure of drill string design is crucial for the successful enlargement of any kind project. Besides of a pipe reliable material, the hoisting system of the rig must be prepared both for pulling out and moderating the velocity of tripping in. Therefore, the term Hook Load is introduced to evaluate the axial forces experienced by the drill string. This expression will be approached carefully through this work, since it still brings some uncertainty within drilling operations and it should be evaluated through an indirect method of measurement. This circumstance denotes one of the principal incentives of this master thesis, which aims to improve the Hook Load measurement and calculation, performing a better understanding of the forces exerted by fluids in drill pipes, quantifying the effect and running sensitivity analysis. The partnership of the company involved in this project allowed to achieve fruitfully the objectives planned.

Each step of modelling will be accurately supported by physical and mathematical models giving through WellPlan™ simulator. Classic and modern approaches of the fluid forces studies will be developed in this master thesis, analysing them individually also as a group, because it is vital to know the effect of each downhole parameter to make efficient and innocuous choices into the oil well drilling.

Key Words: Fluid forces, Hook Load, Buoyancy, viscous force, inertial force, piston force, torque and drag.

Table of Contents

Acknowledgement

First of all, I would like to thank Ahmad Mirhaj of MHWirth Norway for setting the objective of this thesis, a very interesting and challenging one. My gratitude to Dan Sui, Professor at the University of Stavanger for the guidance and support. They were always available to clarify doubts and take me to into the right path to finalize the project.

Acronyms

BHA- Bottom Hole Assembly

CF- Coefficient factor

DC- Drill Collar

DLS- Dog Leg Severity

DP- Drill Pipe

HWDP- Heavy Weight Drill Pipe

HB- Herschel Bulkley

IBOP-Internal Blow-Out Preventer

MD- Measured Depth

MWD- Measurement While Drilling

PDC- Polycrystalline Diamond Cutters

POOH-Pulling Out Of the Hole

RIH-Running Into the Hole

ROP- Rate of penetration

SD-Side force

TOR-Torque On Bit

TVD – True Vertical Depth

WOB-Weight On Bit

YS-Yield Stress

List of Figures

List of Tables

Chapter 1: Introduction

The primary goal of this study is to implement a hook load model that take in account the impact of the fluid forces. In order to fulfil that purpose, it is necessary to approach some concepts commonly used in hydrodynamics such a buoyancy, pressure area, inertial and viscous force. The enlargement of those previous mentioned concepts is needed to develop a reliable and complete downhole torque and drag model that can consider the influence of the fluids additional to the existent terms as torque, tension, friction, weight on bit and drag.

In this initial chapters, one and two, the context of drilling mud, rheologic models, drilling circulation system, including drill string mechanics, friction forces and hook load will be exposed. A chronologic overview of previous works and their limitations is also part of the introductory path. On chapter three, the focus will be in the mathematical access to the forces in investigation. The next stage, chapter four, will explain the source of data used into the model developed, for this case the guidance of MHWirth and the access to Downhole Simulator ® which allowed to use input values, similarly there is some parameters that must be commuted which base in some assumption that will allow to simplify some calculations, then the data calculated must be interpreted and explained how to applied step by step, each force at the time and finally the impact of the results in the torque and drag model including some sensibility. Furthermore, the conclusion will take place in the fifth chapter with the potential improvements for future work in order to encourage the reader to improve and go beyond the scopes of the thesis.

Within this project a lot of concepts will be clarified regarding terms that usually are misunderstood and overlapped inside the drill string mechanics examination. And hopefully formulate an enhanced procedure of torque and drag modelling.

Chapter 2: Literature Review

2.1 Background

Fluid Types

It is necessary to define:

- ***Shear rate:*** The rate of change of velocity at which one layer of fluid passes over an adjacent layer.
- ***Shear stress:*** *"*Applied force, F, acting along a unit surface are, A, tending to deform the fluid element" [9].
- ***Yield stress (YS):*** Stress required to initiate flow.
- ***Plastic viscosity (μ_p):*** "Resistance of the fluid to flow due to mechanical friction within the fluid" [9]

The relationship between shear rate and shear stress for a fluid defines how that fluid flows, then, viscosity links these two magnitudes:

$$Viscosity\ (\mu) = \frac{Shear\ stress\ (\tau)}{Shear\ rate\ (\gamma)} \qquad Eq.2.1$$

Based on their flow behaviour, fluids can be classified into two different types:

a. ***Newtonian fluid:*** For these fluids the shear stress is directly proportional to the shear rate. Viscosity of a Newtonian fluid is the slope of this shear-stress / shear-rate line also the yield stress will always be zero. Newtonian fluids will not suspend cuttings and weight material under static conditions.

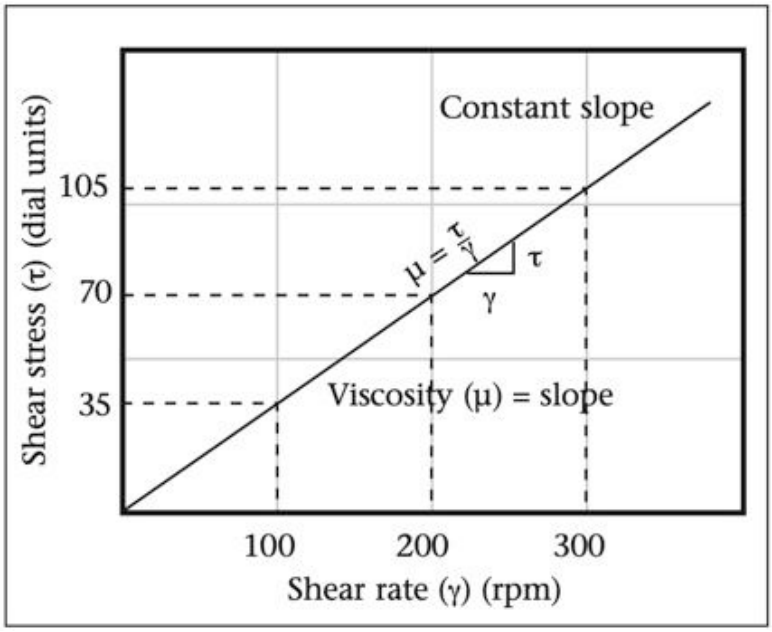

Figure 2.1 Shear stress vs shear rate graph Newtonian fluid (Mi-Swaco, 2006)

b. ***Non-Newtonian fluids:*** When a fluid contains clays or colloidal particles, these particles tend to "bump" into one another, increasing the shear stress or force

necessary to maintain a given flow rate. If these particles are long compared to their thickness, the particle interference will be large when they are randomly oriented in

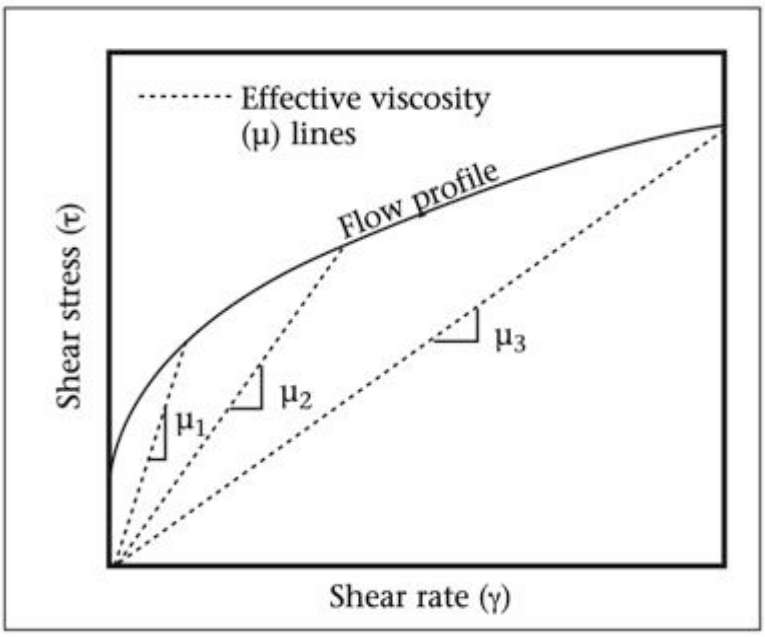

Figure 2.2 Shear stress vs shear rate graph for Non-Newtonian fluid (Mi-Swaco, 2006)

the flow streams. When shear rate is increased, the particle will "straight up" in the flow stream and the effect of a particle interaction is decreased. These fluids dos not have a single constant viscosity that describes its flow behaviour at all shear rates.

The drilling fluids are non-Newtonian and the next scenarios are presented:

a. At high velocities (high shear rates) in the drill string and through the bit, the mud shear thins to low viscosities. This reduces the circulating pressure and pressure losses.

b. At the lower velocities (lower shear rates) in the annulus, the mud has a higher viscosity that aids in hole cleaning.

c. At ultra-low velocity the mud has its highest viscosity and when not circulating will develop gel strengths that aid in suspending weight material and cuttings.

The relationship between the shear stress and shear rate is defined as Rheological model. These models have been developed to describe the flow behaviour of non-Newtonian fluids.

- ***Bingham Plastic model:*** It is one of the older rheological models currently in use. This model describes a fluid in which a finite force is required to initiate flow (yield point) and then shows a constant viscosity with increasing shear rate (plastic viscosity), Eq.2.2 exhibits the behaviour:

$$\tau = \tau_0 + \mu_p \gamma \qquad Eq.2.2$$

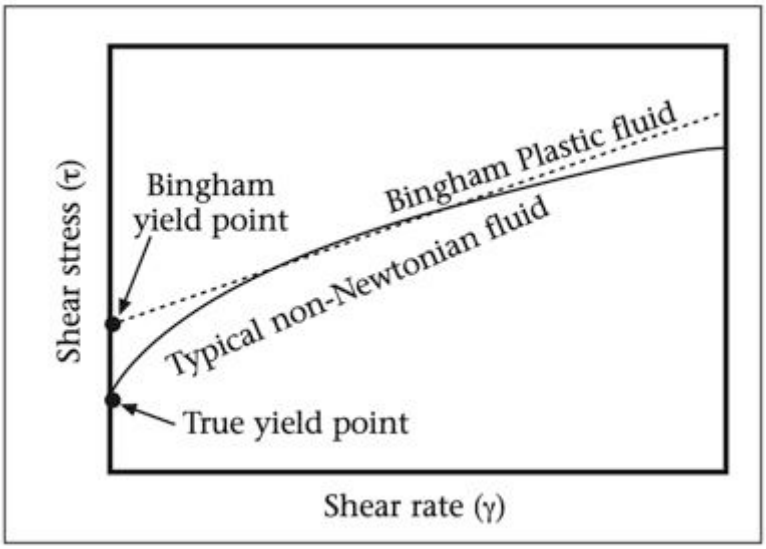

Figure 2.3 Shear stress vs shear rate graph for Bingham fluid (Mi-Swaco, 2006)

Where:

τ	$Shear\ stress$
τ_0	$Yield\ point\ or\ shear\ stress\ at\ zero\ shear\ rate\ (Y-intercept)$
μ_p	$Plastic\ viscosity\ or\ rate\ of\ increase\ of\ shear\ stress\ with\ increasing\ shear\ rate$
γ	$Shear\ rate$

- ***Power Law model:*** Attempts to solve shortcomings of the previous model at low shear rates. It does not assume a linear relationship between shear stress and shear rate. Power Law equation is expressed as:

$$\tau = K\gamma^n \qquad Eq.2.3$$

The way to find Power Law index 'n' is plotting on a log-log graph, shear stress vs shear rate, and calculating the slope of the straight line. Consistency index 'K' is the interception with the Y-axis.

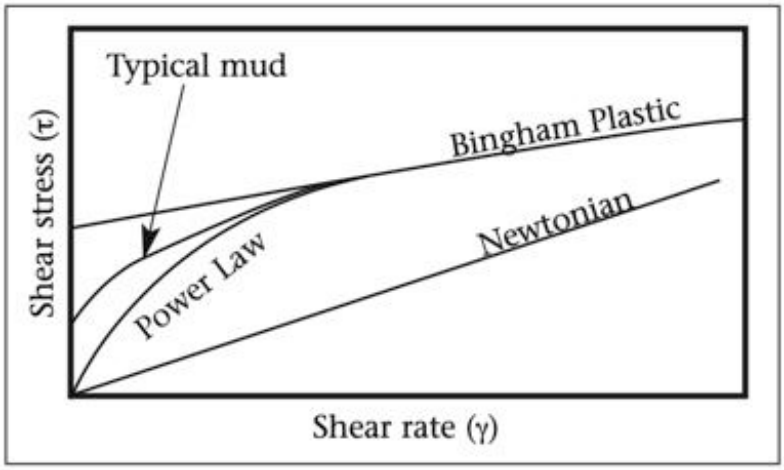

Figure 2.4 Shear stress vs shear rate graph for Power Law fluid (Mi-Swaco, 2006)

Where:

τ	$Shear\ stress$
K	$Consistency\ index$
n	$Power\ Law\ index$
γ	$Shear\ rate$

- ***Herschel-Bulkley model:*** Power Law model does not fully describe drilling fluids because it does not have a yield stress. This model, also called modified Power Law, is in between Bingham Plastic, which is the lowest and Power Law the highest. It can approximate more closely the true rheological behaviour of most drilling fluids, mathematical expression is:

$$\tau = \tau_0 + K\gamma^n \qquad Eq.2.4$$

Where:

τ	$Shear\ stress$
K	$Consistency\ index$
τ_0	$Yield\ stress\ or\ \ stress\ to\ intiate\ flow$
n	$Power\ Law\ index$
γ	$Shear\ rate$

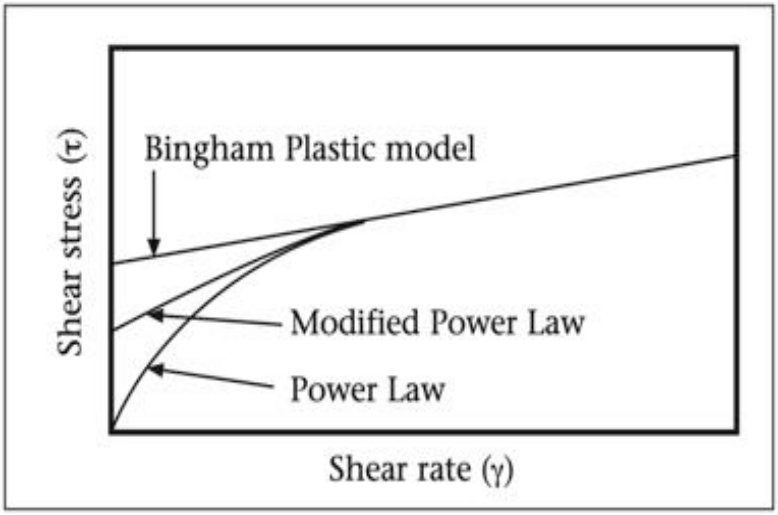

Figure 2.5 Shear stress vs shear rate graph for Herschel- Bulkley fluid (Mi-Swaco, 2006)

Drilling fluid: When a liquid (water or oil or a combination of water and oil) is treated with a clay substance, such as bentonite or polymer, the result is a drilling fluid. When the continuous liquid phase is water, the mud system is called Water Base Mud (WBM), otherwise it is an Oil Base Mud (OBM) [9]

Functions: Into the entire well system, drilling fluid performed the below listed purposes [18]:

- Remove cuttings from the well
- Control formation pressures
- Suspend and release cuttings
- Seal permeable formations
- Maintain wellbore stability
- Minimize reservoir damage
- Cool, lubricate, and support the bit and drilling assembly
- Transmit hydraulic energy to tools and bit
- Ensure adequate formation evaluation
- Control corrosion
- Facilitate cementing and completion
- Minimize impact on the environment

Drilling Circulation system

The Drill string: Defined as the union of several pipes with different lengths and diameter attached to a drilling tool. From the bottom a conventional rotary drill string consists of:

1. ***Drill Bit:*** Tool used to crush or cut rock using rotational and axial force. It must be selected depending on type of formation to be drilled and they are divided in [24]:
    a. ***Roller cone:*** Also called Rock bit, has either two or three cone-shaped cutters that roll along as the bit is turned. The drilling mechanism performed is fracturing hard rock and by gouging softer rock. Rock bits are classified conforming to the kind of teeth they have: *Milled tooth* and *Tungsten Carbide Insert (TCI).* (Figure 2.7)

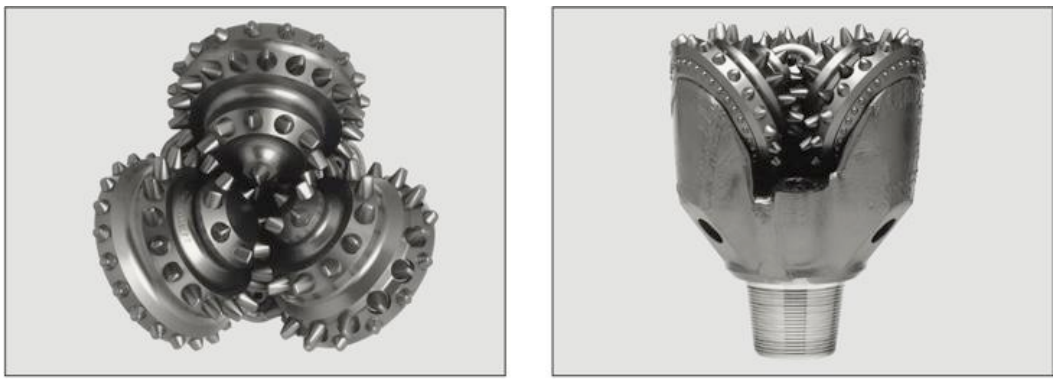

Figure 2.6 Tri-conic bit source Drilling fluids engineering Manual (Mi-Swaco, 2006)

b. ***Diamond and PDC bits:*** Fixed-cutter buts with diamond cutting surfaces, these are used for drilling medium to hard formations or special coring operations. Polycrystalline Diamond Cutters (PDC) shear the rock beneath the bit, producing large cuttings and high penetration rates. [18]

2. ***Drill Collars (DC):*** Thick-walled tubular pieces machined form solid bars of steel, that provides weight on bit for drilling, the outside diameter of the steel bars may be machined slightly to ensure roundness and, in some cases, may be machined with some sort of spiral. Usually one of the collars is made of non-magnetic metal so that a magnetic compass tool (survey tool) can be used to determine the inclination of the lower BHA and bit without magnetic metal interference.[24]

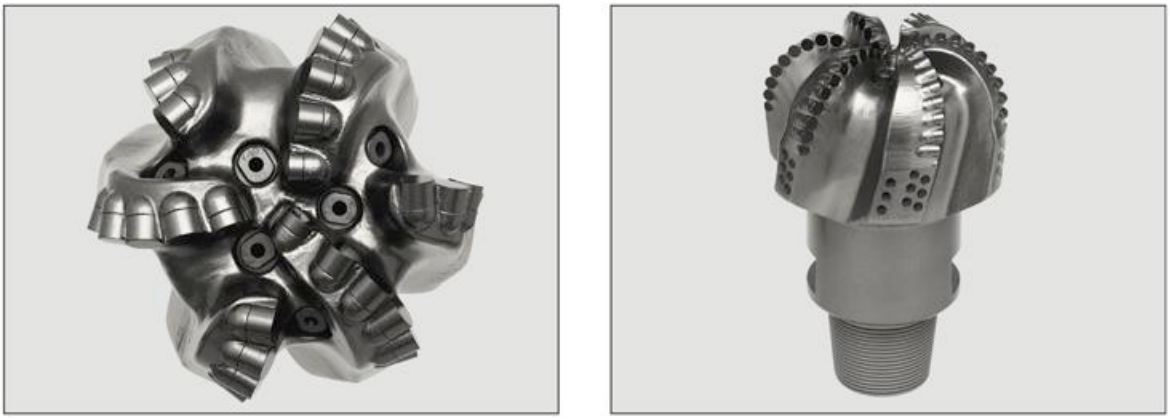

Figure 2.7 PDC bit, source Drilling fluids engineering Manual (Mi-Swaco, 2006)

3. ***Bottom Hole Assemblies (BHAs):*** Located just above the bit and includes drill collars, combined with one or more bladed stabilizers (to keep the BHA and bit concentric), possibly a reamer (to keep the hole form becoming tapered as the bit diameter wears down) and other tools.
    a. ***Measurement While Drilling (MWD)***: Provides downhole evaluation of formation parameters like gamma ray, resistivity and porosity while drilling is in progress. Mechanical parameters are also measured: *Inclination, azimuth, Rate of penetration (ROP), Weight on bit (WOB) and Torque on bit (TOB)*. MWD and mud motors are generally located low in the BHA, usually just above the bit.
    b. ***Jar***: Mechanical device used downhole to deliver an impact load to another downhole component, especially when that object is stuck. There are two primary types *Hydraulic* and *Mechanical.*

Figure 2.8 Drill Collar (www.equipoutlet.com, 2020)

4. ***Heavy Weight Drill Pipe (HWDP):*** This string section is used to make the transition between the drill collars and drill pipe. Main function is to provide a flexible transition between the Drill Collars and the Drill pipe and prevent fatigue of the drill pipe.
5. ***Drill Pipe (DP):*** Tubular steel conduit fitted with special threaded ends called tool joints. The drill pipe connects the rig surface equipment with the BHA and the bit, also provides

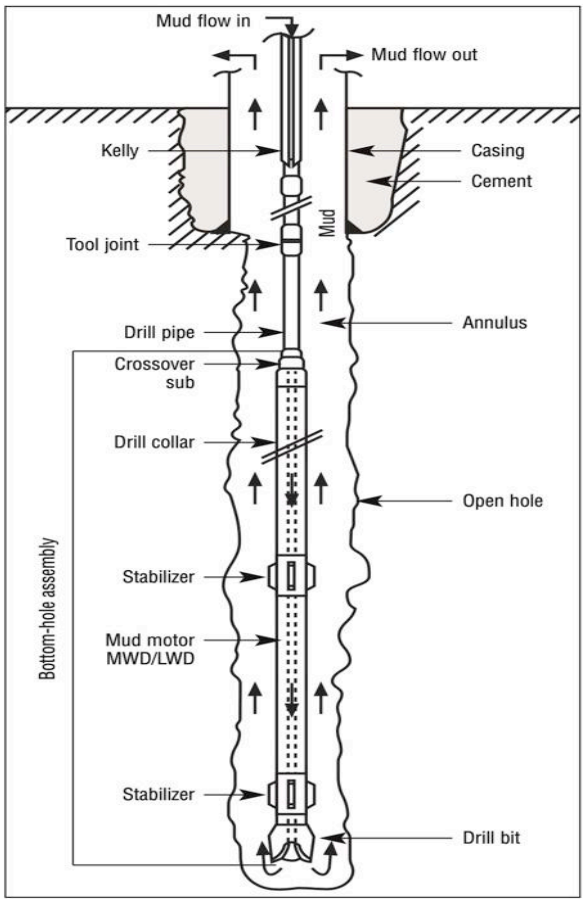

Figure 2.9 Circulation system (Mi-Swaco, 2006)

continuous circulation, each joint of drill pipe is approximately 30 ft long and has a box (female connection) welded onto one end and a pin (male connection) welded to the other. These threaded couplings (tool joints) must be strong, reliable, rugged and safe to use. Outers diameters for drill pipe range from 2 3/8 to 6 5/8.[18]

Rotary Drilling

For any vertical or directional well, different elements are needed to drill the hole successfully, including:

- ***Force***: In order to drilling through a rock a downward compression force must be applied on the bit (Weight on bit, WOB). This force is provided by slacking off tension on the drilling line that supports the total weight of the drill string. This WOB is provided by the portion of the tubular (drill string) above the bit. In a vertical well drilling, the amount of force is exerted by the weight of the length of specific types of heavier pipes such as, Heavy weight drill pipe (HWDP) and Drill Collar (DC). Normally part of the Drill Collar/HWDP go into compression. However, in directional wells DC and HWDP are normally not placed in the highly inclined portion of the hole; rather, they are placed in lesser inclination sections or near to vertical to avoid excessive frictional forces which remarkably reduce the transfer of desired WOB to the drill bit. [9]

  Since compression is not the only force experimented by all the components of a drill string. The term tension, defined as the pulling force transmitted axially by a continuous object. In a drilling rig the hoisting system is the responsible for uplifting and lowering the whole string tension

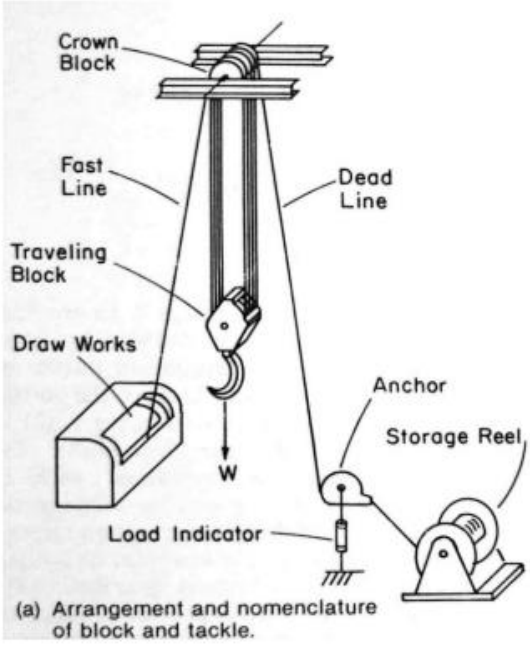

Figure 2.10 The diagram of a hoisting system (Kristensen, 2013)

***Fluid circulating systems*:** Consequence of the radiational drilling, heat and solids are produced in the hole, in the process of making a hole successful cooling and cleaning must be assured. Therefore, a fluid must be continuously circulated from the surface to the bottom. The main components of the system include [18]:

a. Mud pumps
b. High pressure surface connections
c. Drill string
d. Drill bit
e. Return annulus
f. Mud Pits
g. Mud treatment equipment

Friction

Da Vinci was the first scientific which stated about different materials creating diverse efforts due to material roughness. Amontons two centuries later came up with first consistent law: "Frictional force is directly proportional to the normal load".[10]

$$F = \mu * N \qquad Eq.2.5$$

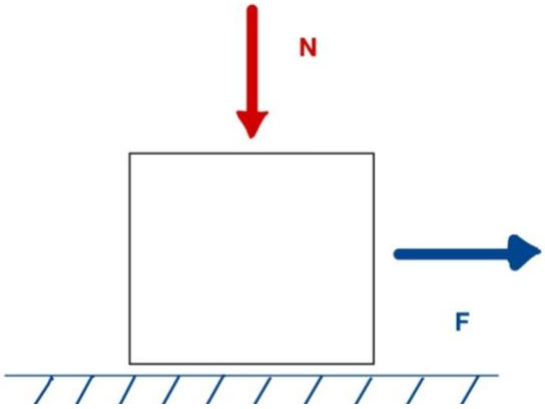

Figure 2.11 First friction law

Second law detailed that friction force is "independent of the apparent area of contact". Later Charles -Augustuin de Coulomb concluded, after experimental work, that in order to set an object in motion laying on an even surface in state of rest one need to overcome a critical force, the force of static friction, called Fs, and is roughly proportional to the normal force, N.

$$Fs = \mu_s * N \qquad Eq.2.6$$

After static friction force has been overcome, it is the resting force, F_k, kinetic friction, which act on the body. Coulomb also determined that the kinetic friction is proportional to the normal force, N.[10]

$$F_k = \mu_k * N \qquad Eq.2.7$$

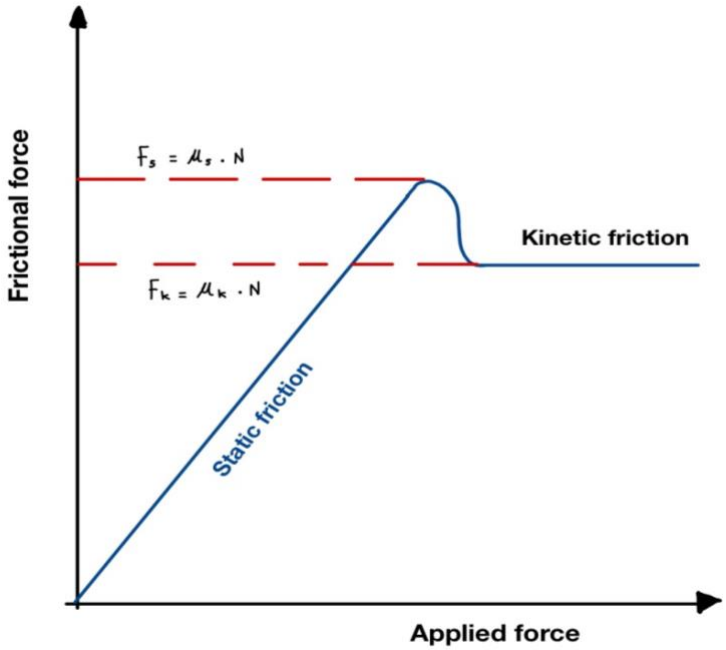

Figure 2.12 Illustration of static and kinetic friction

Where:

F	$Friction\ force\ (pound)$
F_k	$Kinetic\ friction\ force\ (pound)$
F_s	$Static\ friction\ force\ (pound)$
N	$Normal\ force\ (pound)$
μ	$Friction\ coefficient$
μ_s	$Static\ friction\ \ coefficient$
μ_k	$Dynamic\ friction\ \ coefficient$

- **Side forces:** Along the friction force, side forces include the forces that exist between the wellbore wall and any element of the drill string. Side forces also include the normal forces created by the drill string with the wellbore walls. Main factors that can cause it are:

- ***Weight of the drill string:*** Contributes to the magnitude of the normal force against the wellbore then, the heavier is the drill string the greater side forces against the wall of the hole. Therefore, this is one of the factors should be minimized within the safe limits.
- ***Tension due to dog leg severity:*** "In build sections, the direction of the pipe movement affects the direction of the side forces". When tripping in the pipe will be lying on the low side, consequently the effect of tensile load is reduced, and the resultant side force is in the direction of the weight component. For pulling out of the hole, the string will be in contact with the [25]

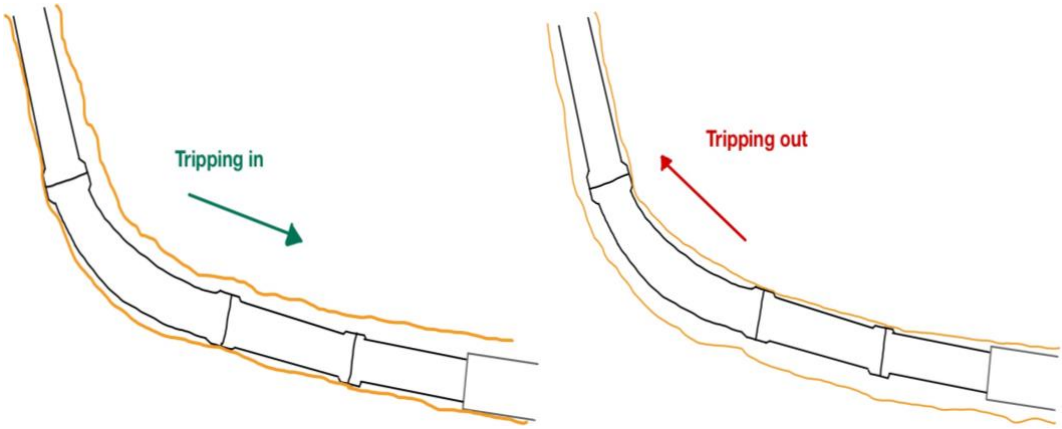

Figure 2.13 Illustration of static and kinetic friction

high side, thus the effect of tensile load is increased, and the resultant side force will be in the direction of the tensile component. The next expression calculates the side force calculation into Johancsik's mode [16]:

$$F_N = \sqrt{(F_T * \Delta\alpha * \sin(\theta))^2 + (F_T * \Delta\theta + Bw * L * \sin(\theta))^2} \qquad Eq.\,2.8$$

Where:

Bw	$Buoyant\ weight\ (pound/m)$
F_N	$Normal\ or\ side\ force\ (pound)$
F_T	$Axial\ force\ at\ bottom\ of\ section\ calculated\ using\ buoyancy\ method\ (pound)$
$\Delta\alpha$	$Change\ in\ azimuth\ over\ section\ length\ (degrees)$
θ	$Average\ inclination\ of\ the\ section\ (degrees)$
$\Delta\theta$	$Change\ in\ inclination\ over\ the\ section\ length\ (degrees)$
L	$Section\ lenght\ (m)$

Hook load

Mme et al. [12] defined this term as the "sum of vertical component of the forces acting on the drill string attached to the hook". It According to Cayeux et al.[17] hook load is determined by the forces acting on the drill string attached to the hook, including the buoyant weight, mechanical and hydraulic friction forces. Thus, hook load is sensitive to drag forces due to friction, buoyancy, inertial forces in curved string sections and fluid shear stress at pipe walls. It also controls the weight on bit and evaluate possible deteriorations of the downhole conditions such a poor hole cleaning or excessive tortuosity.

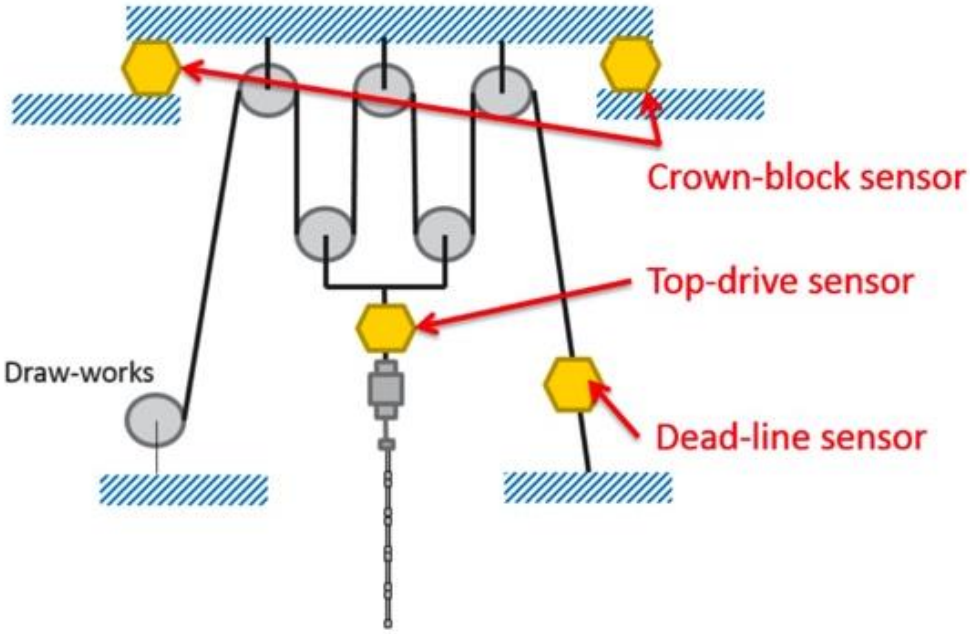

Figure 2.14 location of hook load measurements sensors (Cayeux, Skadsem, & Kluge, 2015)

The Martin-Decker diaphragm-type weight indicator has been used in most of the conventional drilling operations since 1926. Current rig hoisting system use electronic sensors located in the draw works and travelling block. [14]. Even though hook load can be measured using an instrumented IBOP (Internal Blow-out preventer) but at the present just a few portions of drilling rig units can be equipped with this type of sensor. In practice it is measured indirectly, either in the travelling equipment or as tension in the dead-line. According to [15] through a proper analysis of the Hook load is possible to be prepared for extraordinary situations in drilling such a drill line breaking and "pulling the rig in". Both

of them caused mainly to not knowing the true tension in the wire present in the block-and-tackle configuration used to support the drill string.

2.2 Previous Work

Sparks [2] related buoyancy, fluid pressure loads from axial forces in fluid columns applied to buckling forces in marine risers. Hashmi [16] studied in his master thesis the sensitivity of factors affecting torque and drag modelling, including viscous drag, hydrodynamic viscous drag and their effects on both weight on bit and torque. According to [16] viscous drag can affect up to 50% with a fix flow rate and until 25% for null circulation. Landivar [22] wrote a master thesis in 2018 giving an overview about the modern understanding of buoyancy counting the consequence on the effective tension. Aadnoy [1] introduces piston force concept in "Mechanics of drilling" where a force balance is defined through the drill string configuration also mentioning deviatoric forces in order to consider deviatoric forces in the total load applied to the pipe. Samuel et al. [7] involved the terms: hook load, true tension, effective tension and stress adding the hydrostatic effect, mostly applied to checking buckling and failure conditions in the tubular. Their study conclude that inclusion of the fluids must be accounted properly. Cayeux et al. [6] displayed some challenges about calculation and correction of drilling friction tests, and it shows in the appendix, the way to calculate reaction force generated by fluid flow in a bend, inertial force for our purposes.

2.3 Limitations of previous studies

The researches done previously showed remarkable achievements in the effect of hydrodynamic forces individually affecting the torque and drag model. Although, a deeper and more generalized approach should be made, including the impact of multiple fluid forces that in some punctual cases can even overlap themselves. However, with a proper understanding is possible quantify the influence of each one and all of the forces as a group inside the three main operations in drilling, running into the hole (RIH), circulating off the bottom and pulling out of the hole (POOH).

Chapter 3: Methodology

Chapter 3.1 Torque and Drag Model

The torque and drag model is divided in two:

Chapter 3.1.1 Straight Borehole

Inclined well model, from force balance, applying the condition of equilibrium along the axial direction, the effective force along he axial direction is calculated. Representations of the pipe segment are:

$$dF = w\Delta L(cos\emptyset \mp \mu sin\emptyset) \qquad Eq.3.01$$

Eq.3.01 is the result of a force balance along the inclined plane, the "+" applies when pulling out of the hole (POOH), and "-" when running into the hole (RIH).

$$F_{top} = F_{bottom} + w\Delta L(cos\emptyset \mp \mu sin\emptyset) \qquad Eq.3.02$$

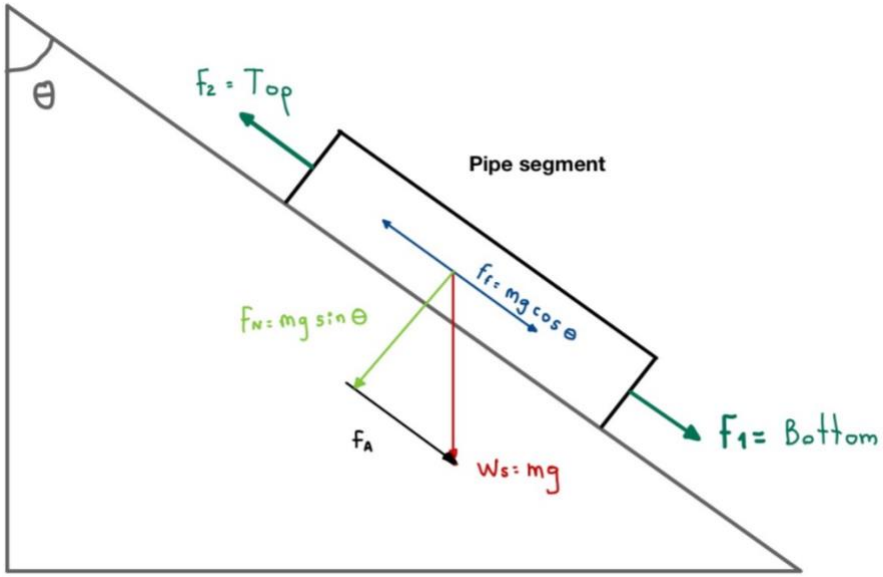

Figure 3.11 Free body diagram of a mass element

The static weight is given as:

$$w_s = w\Delta L\, cos\emptyset \qquad Eq.3.03$$

Chapter 3.1.2 Curved Borehole

Drill string segment are loaded at the top and the bottom with compressive "-"or tensile "+" loads. These loads could be thermal, hydrostatic and fluid flow shear forces, are responsible for the variation in the length of the pipe. For curved boreholes there are continuous changes in Inclination (ɵ) and Azimuth (φ) along the hole path. Following Johansick Torque and Drag model and after balancing between the net force and the vector sum of the axial component of the weight [26]:

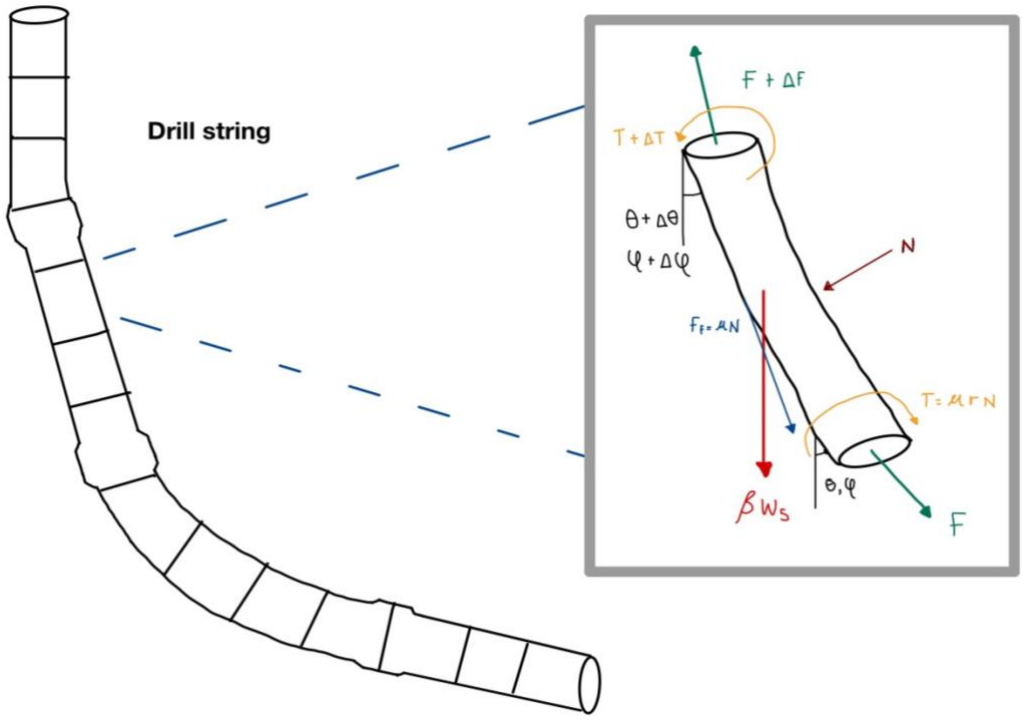

Figure 3.12 Segmented drill string and loads distribution

$$\frac{dF}{dL} = \mp\mu\left(\sqrt{\left(\beta w_s sin\emptyset + F\frac{d\emptyset}{dL}\right)^2 + \left(Fsin\emptyset\frac{d\varphi}{dL}\right)^2}\right) + \beta w_s\, cos\emptyset \qquad Eq.3.04$$

Where:

F	$Force\ in\ the\ previous\ cell\ (pound)$
$\frac{dF}{dL}$	$Change\ of\ Force\ per\ lenght\ (pound)$
$\frac{d\emptyset}{dL}$	$Change\ of\ Inclination\ per\ length\ (degree)$
$\frac{d\varphi}{dL}$	$Change\ of\ Azimuth\ per\ length\ (degree)$
F_{bottom}	$Bottom\ hydraulic\ force\ \ (pound)$
μ	$friction\ coefficient\ (dimensionless)$
ΔL	$Length\ of\ the\ pipe\ (ft)$
w	$Air\ weight\ of\ the\ segment\ (Pound/ft)$

Chapter 3.2 Effect of each of the forces acting on the Torque and Drag model

Chapter 3.2.1 Buoyancy force

The Greek scientist Archimedes (~300 B.C.) discovered that the buoyancy of a body equals the weight of the displaced fluid in which floats. For many applications this definition is enough, however, to resolve all problems a more generalized approach must be taken. [2] Goins, demonstrated that a projected area is required in order to obtain buoyancy. One of the factors that has more influence in the buoyancy calculation is the density of the fluid, which is not constant through the well profile, therefore for each datapoint of the survey mud density varies, regarding steel density, it is assumed a constant value of 64.7 ppg.

Aadnoy. B [1] stated "Buoyancy is a surface force acting on a body in the opposite direction of the gravitational force". Only pressure acting on the projected vertical area that contributes to buoyancy. The following equations are valid both for vertical and deviated boreholes:

$$Buoyacy\ factor = \beta = \left[\frac{Suspended\ weight\ in\ mud}{Weight\ in\ air}\right] = 1 - \frac{\rho_{fluid}}{\rho_{pipe}} \qquad Eq.3.10$$

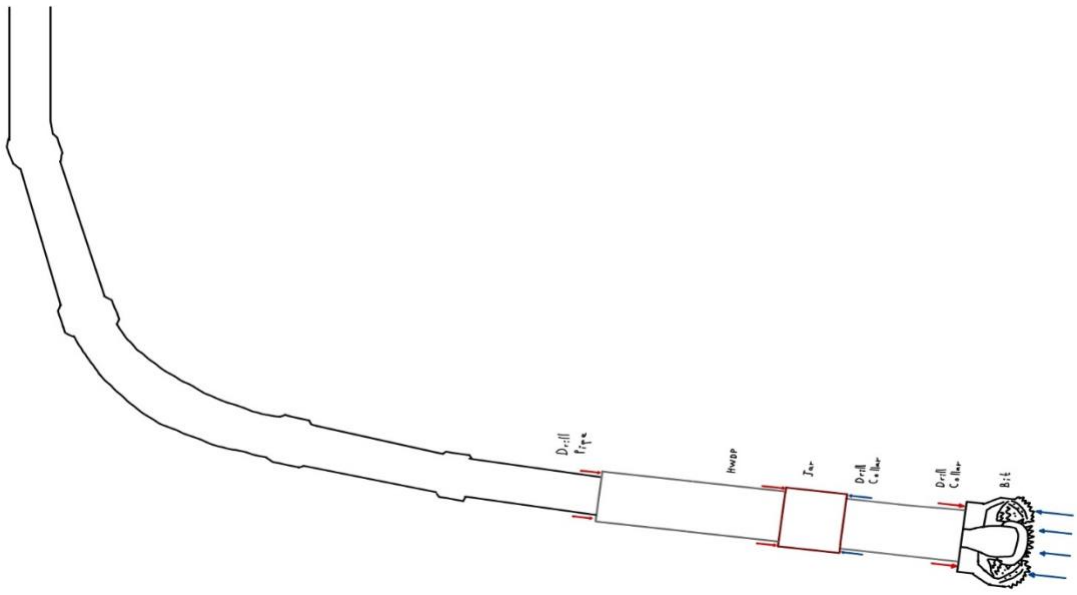

Figure 3.211 Mechanical state of the drill string

Equation 3.10 is valid only if the object is submerged in the same fluid. If there is different density both inside or outside, Eq.3.11.

$$\beta = 1 - \left[\frac{D_1(\rho_o R_1^2 - \rho_i r_1^2) + D_2(\rho_o R_2^2 - \rho_i r_2^2)}{\rho_{steel}((D_1(R_1^2 - r_1^2) + D_2(R_2^2 - r_2^2))}\right] \qquad Eq.3.11$$

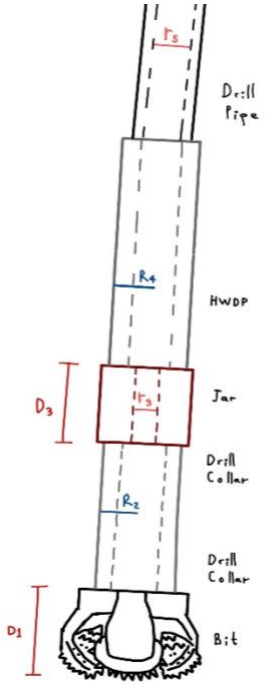

Figure 3.212 Mechanical state of the drill string

Applied to a normal case, a drill string with several diameters and lengths. Eq.3.12 shows the overall buoyancy for n elements:

$$\beta = 1 - \left[\frac{\sum_{k=1}^{n} D_k\,(\rho_o R_k^2 - \rho_i r_k^2)}{\rho_{steel}\sum_{k=1}^{n} D_k\,(R_k^2 - r_k^2)}\right] \qquad Eq.3.12$$

Therefore, buoyed weight at surface is obtained by multiplying the weight in air times total length and Buoyancy factor:

$$Buoyed\ Weight = \beta * w_{air} * h \qquad Eq.3.13$$

Where:

R_k	$Outter\ radio\ (in)$
r_k	$Inner\ radio\ (in)$
D_k	$Length\ of\ the\ section(ft)$
ρ_{steel}	$Pipe\ density\ (ppg)$
ρ_{mud}	$Mud\ Density\ at\ element\ depth\ \ (ppg)$

ρ_o	$Outer\ Mud\ Density\ at\ element\ depth\ \ (ppg)$
ρ_i	$Inner\ Mud\ Density\ at\ element\ depth\ \ (ppg)$
h	$Total\ Length\ of\ the\ string(ft)$
w_{air}	$Air\ weight\ (pound/ft)$

Chapter 3.2.2 Piston / Pressure Area force

Aadnoy. B [1] defined a force balance at every point of projected area change from the bottom to the top. This area is computed in Eq. 3.14. For this case the sign of the force change depending on the direction, downward, positive '+' and upward, negative '- '. It is assumed that body pipe is 95% and the tool joint is the remaining 5%.

$$A_e = \frac{\pi}{4}((0.95 * ODpipe)^2 + (0.05 * ODtj)^2) \qquad Eq.3.14$$

One of the main concepts for Pressure Area school is the presence of a negative upward force at the bottom (Eq.3.15).

$$F_{hb} = -0.052 * \rho_{mud} h A_{ebit} \qquad Eq.3.15$$

Then the force balance at top of the bit (Eq. 3.17) will be the hydraulic force at bottom (Eq. 3.15) plus the weight of the section. (Eq.3.16)

$$w_{bit} = \rho_{steel} L_{bit} A_{bit} * CF \qquad Eq.3.16$$

$$F_{tbit} = -0.052 * \rho_{mud} h A_{ebit} + w_{bit} \qquad Eq.3.17$$

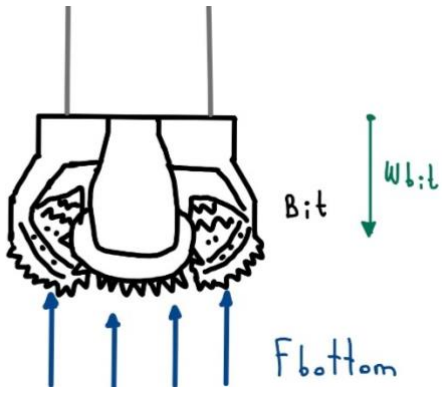

Figure 3.221 Balance force at top of the Bit

Next to the bit, the Drill Collars (DC) are placed to provide weight over the bit therefore over this point there is sudden reduction of cross-sectional area, it will cause a positive downward acting force (Eq.3.18)., the force distribution at the bottom of the Drill Collar (Eq. 3.19), will be force at the top of the bit (Eq. 3.17) plus the effect change of area effect (Eq.3.18).

$$F_{bit/DC} = 0.052 * \rho_{mud} h_{bit/DC} (A_{ebit} - A_{eDC}) \qquad Eq.3.18$$

$$F_{bDC} = -0.052 * \rho_{mud} h A_{ebit} + w_{bit} + 0.052 * \rho_{mud} h_{bit/DC} (A_{ebit} - A_{eDC}) \quad Eq. 3.19$$

Doing the same process at each change of pipe section through the whole drill string until surface these are the results.

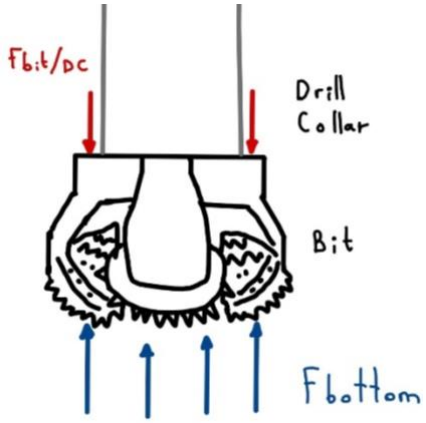

Figure 3.222 Balance force at bottom of the Drill Collar

At top of the Drill Collar (DC)

$$F_{tDC} = -0.052 * \rho_{mud} h A_{ebit} + w_{bit} + 0.052 \rho_{mud} h_{bit/DC} (A_{ebit} - A_{eDC}) + w_{DC} \quad Eq. 3.20$$

At bottom of the Jar:

$$F_{bJar} = F_{tDC} + 0.052 * \rho_{mud} h_{DC/jar} (A_{eDC} - A_{ejar}) \quad Eq. 3.21$$

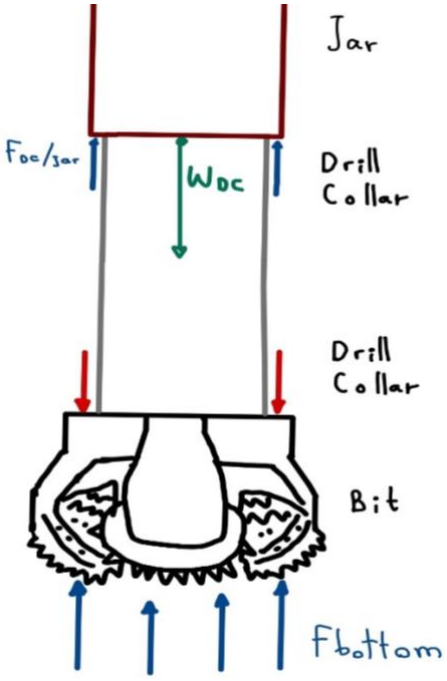

Figure 3.223 Balance force between Drill Collar and Jar

Force at top of the Jar:

$$F_{tJar} = F_{bJar} + w_{jar} \quad Eq. 3.22$$

Force at bottom of the Heavy Weight Drill Pipe (HWDP):

$$F_{bHWDP} = F_{tJar} + 0.052 * \rho_{mud} h_{\frac{jar}{HWDP}} (A_{ejar-} A_{eHWDP}) \qquad Eq. 3.23$$

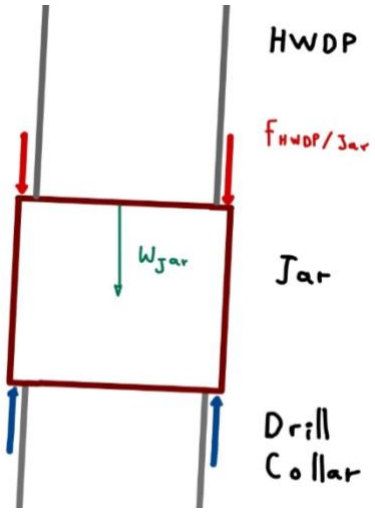

Figure 3.223 Balance force between Jar and Heavy Weight Drill Pipe

At top of the HWDP:

$$F_{tHWDP} = F_{bHWDP} + w_{HWDP} \qquad Eq. 3.24$$

At bottom of the Drill Pipe (DP)

$$F_{bDP} = F_{tHWDP} + 0.052 * \rho_{mud} h_{HWDP/DP} (A_{eHWDP-} A_{eDP}) \qquad Eq. 3.25$$

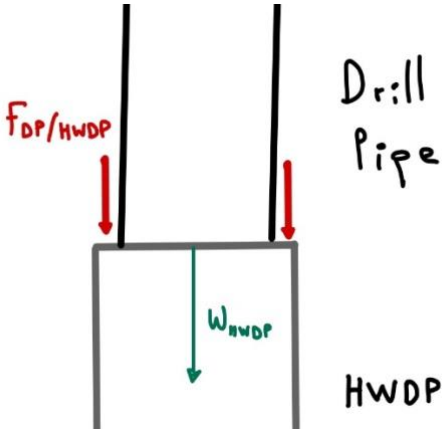

Figure 3.224 Balance force between Heavy Weight Drill Pipe and Drill Pipe

At top of the DP:

$$F_{tDP} = F_{bDP} + w_{DP} \qquad Eq. 3.26$$

In addition to the weight of the pipe, it is also necessary to add the weight of the fluid inside de pipe, which is computed as:

$$A_i = \frac{\pi}{4}((0.95 * IDpipe)^2 + (0.05 * IDtj)^2) \qquad Eq. 3.27$$

$$w_{fluid} = A_i * L_k * CF * \rho_{mud} \qquad Eq. 3.28$$

$$w_{section} = w_{steel} + w_{fluid} \qquad Eq. 3.29$$

Where:

A_e	$External\ cross\ sectional\ area\ (in^2)$
A_i	$Internal\ cross\ sectional\ area\ (in^2)$
A_{bit}	$Effective\ area\ of\ the\ bit\ (in^2)$
A_{ebit}	$External\ cross\ sectional\ area\ bit\ (in^2)$
A_{eDC}	$External\ cross\ sectional\ area\ Drill\ Collar\ (in^2)$
A_{ejar}	$External\ cross\ sectional\ area\ Jar\ (in^2)$
A_{eHWDP}	$External\ cross\ sectional\ area\ Heavy\ Weight\ Drill\ Pipe\ (in^2)$
A_{eDP}	$External\ cross\ sectional\ area\ Drill\ Pipe\ (in^2)$
CF	$Conversion\ factor\ \frac{12\ in * Gal}{1ft * 231\ in^3}$
L_{bit}	$Length\ of\ the\ bit\ (ft)$
L_k	$Length\ of\ the\ section\ (ft)$
h	$Total\ vertical\ depth\ (ft)$
$h_{bit/DC}$	$Vertical\ depth\ of\ Bit - Drill\ Collar\ \ transition(ft)$
$h_{DC/jar}$	$Vertical\ depth\ of\ Drill\ Collar - Jar\ transition\ (ft)$
$h_{jar/HWDP}$	$Vertical\ depth\ of\ Jar - HWDP\ transition\ (ft)$
$h_{HWDP/DP}$	$Vertical\ depth\ of\ HWDP - Drill\ Pipe\ transition\ (ft)$
$IDpipe$	$Inner\ diameter\ of\ the\ pipe\ (in)$
$IDtj$	$Inner\ diameter\ of\ the\ tool\ joint\ (in)$
$ODpipe$	$Outer\ diameter\ of\ the\ pipe\ (in)$
$ODtj$	$Outer\ diameter\ of\ the\ tool\ joint\ (in)$
ρ_{mud}	$Mud\ density\ (ppg)$
ρ_{steel}	$Steel\ density\ (ppg)$

w_{steel}	$Weight\ of\ the\ pipe(pound)$
w_{fluid}	$Weight\ of\ the\ Fluid\ inside\ the\ pipe\ (pound)$
w_{DC}	$Weight\ of\ the\ Drill\ Pipe\ (pound)$
w_{bit}	$Weight\ of\ the\ Bit\ (pound)$
w_{jar}	$Weight\ of\ the\ Jar\ (pound)$
w_{HWDP}	$Weight\ of\ the\ Heavy\ Weight\ Drill\ Pipe\ (pound)$
w_{DP}	$Weight\ of\ the\ Drill\ Pipe\ (pound)$

Aadnoy. B [1] states "It is interesting to observe that the two methods give different results, except at surface. For surface load calculations, both methods give correct answer". Piston force method give a proper approach of external loading on the drill string, but never should be used for failure calculations since it just considers one-dimension load and stress state is three-dimensional.

Chapter 3.2.3 Viscous friction force

With a set circulation rate in the well, normally arises a force due to the interaction among fluid and the pipe. The measure of the fluid resistance against the wall of the pipe is defined as viscous force, it is proportional to the rate at which the fluid velocity is changing in space. For mud drilling, Reynolds is the dimensionless term that relates these properties through velocity and viscosity. Consequently, it is necessary define the rheologic model in order to find an accurate pressure loss and thus find viscous force through the drill string.

Chapter 3.2.3.1 Rheological model

The chosen rheological model is Herschel-Bulkey since it emulates in a better way the behaviour of drilling fluids. Madlener et al [3] developed a generalized Reynolds number including parameters as, Yield stress (τ_y), behaviour index (n), consistency index (k) and velocity ($\bar{u}$):

$$Re_g = \frac{\rho \bar{u}^{2-n} d^n}{\left(\frac{\tau_0}{8}\right)\left(\frac{d}{\bar{u}}\right)^n + k\left(\left(\frac{3m+1}{4m}\right)\right)^n 8^{n-1}} \qquad Eq.3.30$$

with

$$m = \frac{nk\left(\frac{8\bar{u}}{d}\right)^n}{\tau_0 + k\left(\frac{8\bar{u}}{d}\right)^n} \qquad Eq.3.31$$

Since there is a set flow rate, velocity can be estimated as:

Inside the pipe

$$\bar{u} = \frac{q}{A_{pipe} * CF} \qquad Eq.3.32$$

Annuli space

$$\bar{u} = \frac{q}{A_{annuli} * CF} \qquad Eq.3.33$$

Mitchell et al [4] define turbulent flow for Reg => 4150 -1150n, laminar Reg =< 3250 - 1150n and intermediate for the remaining. After acknowledging flow regime profile of the well, computing Darcy friction factor n is needed.

Colebrook equation express Darcy friction factor f including terms Reg, f, D and ε for turbulent flow, f must be find it in an iterative:

$$\frac{1}{\sqrt{f}} = -2\log\left(\frac{\varepsilon}{3.7d} + \frac{2.51}{Reg\sqrt{f}}\right) \qquad Eq.3.34$$

For laminar flow:

$$f = \frac{64}{Reg} \qquad Eq.3.35$$

Intermediate flow:

$$f = \frac{0.3164}{Reg^{1/4}} \qquad Eq.3.36$$

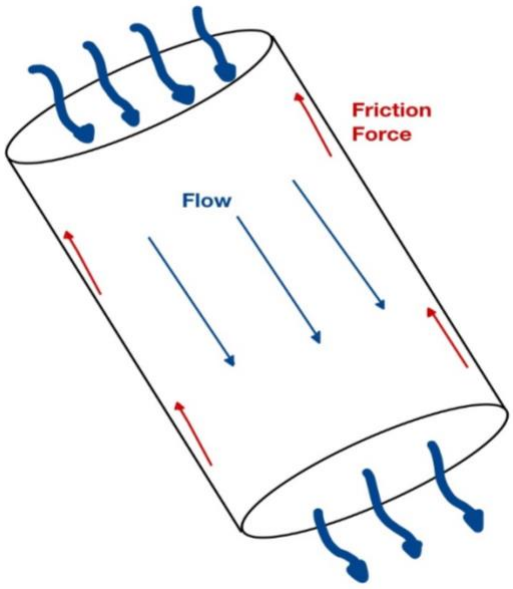

Figure 3.23 Forces in pipe with flow presence

Sui et al [5] explain that "the concept of frictional pressure losses derives from the resistance experienced by fluids flowing through pipes caused by friction against the pipe wall". Darcy-Weybach equation is expressed as:

$$\Delta P = \frac{fL\rho\bar{u}^2}{2d} * CF2 \qquad Eq.3.37$$

With

$$d = ID_{pipe} \qquad Eq.3.38$$

For flow inside the pipe.

Or

$$d = (ID_{annular} - OD_{pipe}) \qquad Eq.3.39$$

In case of annuli flow.

Aa a final step, viscous force can be calculated multiplying for the cross-sectional area of the section:

$$Viscous\ Force = \Delta P\left(\frac{\pi d^2}{4}\right) \qquad Eq.3.40$$

The additional force due to viscous drag force:

$$\Delta F_{vd} = \frac{\pi\Delta P\left(ID_{annular}{}^2 - OD_{pipe}{}^2\right) * OD_{pipe}}{4(ID_{annular} - OD_{pipe})} \qquad Eq.3.41$$

Where:

A_{pipe}	$Internal\ cross\ sectional\ area\ (in^2)$
$A_{annular}$	$Annular\ area\ (in^2)$
d	$Diameter\ (in)$
L	$Length\ of\ the\ pipe\ (ft)$
ID_{pipe}	$Inner\ diameter\ of\ the\ pipe\ (in)$
$ID_{annular}$	$Inner\ diameter\ of\ the\ annluar\ \ (in)$
OD_{pipe}	$Outer\ diameter\ of\ the\ pipe\ (in)$
f	$Darcy\ friction\ factor\ (dimensionless)$
Reg	$Generalized\ Reynolds\ number\ (dimensionless)$
q	$Flow\ rate\ (ft^3/s)$
$\bar{u}$	$Annular\ or\ pipe\ velocity\ (ft/s)$

ΔP	$Pressure\ loss\ (pounds)$
CF	$Conversion\ factor\ \frac{1ft^2}{144in^2}$
$CF2$	$Conversion\ factor\ \frac{12\ in * 7{,}481\ Gal}{1ft * ft^3}$
ρ	$Mud\ density\ in\ the\ section\ \ (ppg)$
ε	$Absolute\ roughness\ (in)$
n	$Behaviour\ index\ (dimensionless)$
k	$Consistency\ index\ (psi * s^n)$
τ_0	$Yield\ Stress\ (psi)$

Chapter 3.2.4 Inertial force

The force due to momentum of the fluid, it is usually expressed by the term ρv^2, thus inertial force would be directly proportional to density also velocity. A force that can counterbalance it is the shear stress or friction force. Cayeux et al [5] displayed some calculations regarding force generated by a flow in a bend, they consider a section of pipe with length L_i in a drill string with a DLS_i, forces from the fluid to the pipe are $\vec{F}_1$ due to pressures P_i and P_{i+1} in areas A_i and A_{i+1} respectively. Using Newton's second law, $\vec{F} = \dot{m}\vec{a}$, the wall is emitting a counterforce $-\vec{F}_2$ which can be expressed as $\vec{F}_{i,A} = -\vec{F}_2$. Then:

$$\vec{F}_1 + \vec{F}_2 = \dot{m}(\vec{v}_{i+1} - \vec{v}_i) \qquad Eq.\ 3.41$$

Is equivalent to:

$$\vec{F}_1 + (-\vec{F}_{i,A}) = \dot{m}(\vec{v}_{i+1} - \vec{v}_i) \qquad Eq.3.42$$

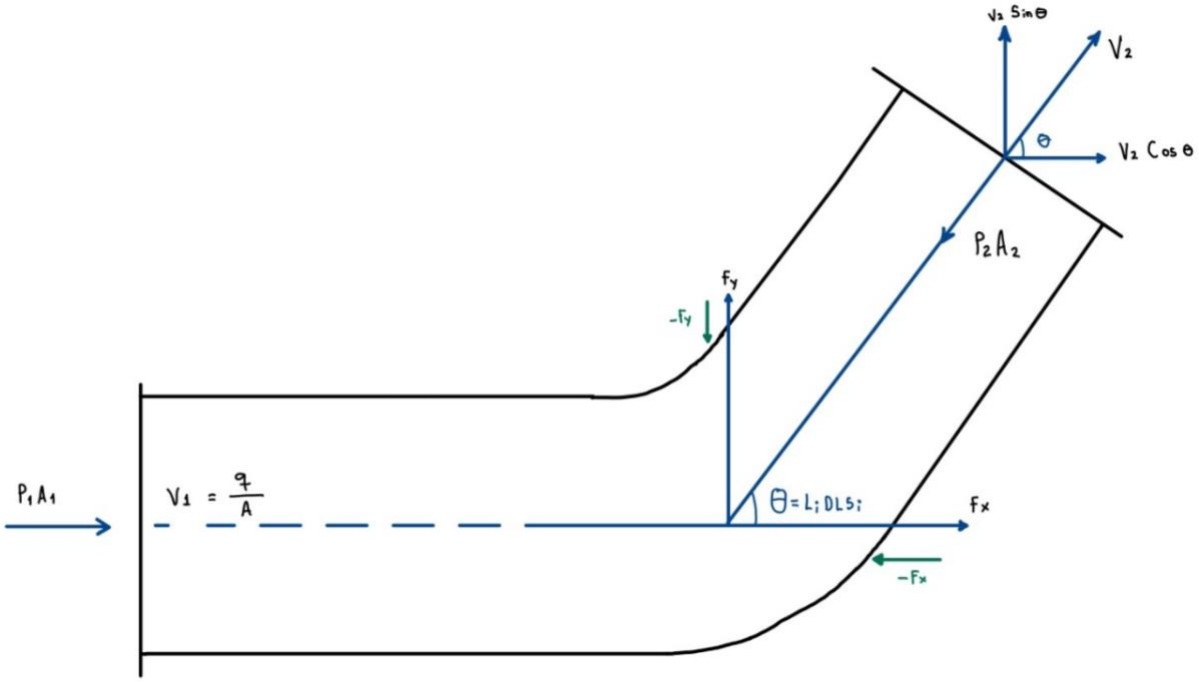

Figure 3.24 Balance force in a pipe bend

Knowing that between entrance and exit of the pipe, using DLS is possible to calculate the curvature of the arc in the tangential, $\vec{t}_i$ and normal $\vec{n}_i$ plane. Reaction force is expressed as:

$$\vec{F}_1 = (P_i A_i - P_{i+1}A_{i+1}\cos(L_i DLS_i))\vec{t}_i - (P_{i+1}A_{i+1}\sin(L_i DLS_i))\overrightarrow{n_i} \qquad Eq.3.43$$

With:

$$q * \rho_i = \dot{m}_i \qquad Eq.3.44$$

Is possible to deduce reaction force $(-\vec{F}_{i,A})$:

$$\vec{F}_{i,A} = (P_i A_i - P_{i+1}A_{i+1}\cos(L_i DLS_i) - \rho_i q(\vec{v}_{i+1}\cos(L_i DLS_i) - \vec{v}_i))\vec{t}_i - (P_{i+1}A_{i+1}\sin(L_i DLS_i) + \rho_i q(\sin(L_i DLS_i)))\overrightarrow{n_i} \qquad Eq.3.45$$

Considering that the pipe has a cross sectional area which is and circular which is constant with diameter D_i, velocity in and out should be identical an equal to $\vec{v}_{i+1} = \vec{v}_i = q/(\pi d^2/4)$. Therefore, final expression is:

$$\vec{F}_{i,A} = \frac{\pi d^2}{4}\left(P_i - P_{i+1}\cos(L_i DLS_i)) - \frac{4\rho_i q^2}{\pi D^2}(\cos(L_i DLS_i) - 1)\right)\vec{t}_i - \left(\frac{\pi D^2}{4}P_{i+1}\sin(L_i DLS_i) + \frac{4\rho_i q^2}{\pi D^2}(\sin(L_i DLS_i))\right)\overrightarrow{n_i} \qquad Eq.3.46$$

Then, the resultant force exerted by the fluid in the pipe is:

$$TIF = \sqrt{\left(\overrightarrow{Ft_i}\right)^2 + \left(\overrightarrow{Fn_i}\right)^2} \qquad Eq.3.47$$

Where:

A_i	$Internal\ cross\ sectional\ area\ of\ the\ section(in^2)$
DLS_i	$Dogleg\ severity\ of\ the\ section\ (in^2)$
d	$Diameter\ of\ the\ pipe\ (in)$
$\vec{F}_t$	$Force\ in\ tangential\ direction\ (pound)$
$\vec{F}_n$	$Force\ in\ normal\ direction\ (pound)$
L_i	$Length\ of\ the\ pipe\ (ft)$
$\dot{m}$	$Mass\ flow\ rate\ (pound/min)$
TIF	$Total\ inertial\ force\ \ (pound)$
ρ_i	$Density\ of\ the\ section\ \ (ppg)$
P_i	$Presure\ of\ the\ section\ (psi)$
q	$Flow\ rate\ (gpm)$
$\vec{v}_i$	$Flow\ velocity\ of\ the\ section\ (ft/min)$

Chapter 3.3 Combine effect of all forces in Hook Load calculations

Robello et al [6] introduce the terms "True tension" (Eq.3.47) and "Effective tension" (Eq.3.48). The first one, also called Pressure area method, is used to determine the absolute or true tension in the pipe, but the difference with the one exposed in Chapter 3.2.2 is the inclusion of triaxial pressure forces. This method is used to determine the real neutral point, at which the stress is zero, it is also used to calculate the actual effect of buoyant forces and actual stresses within a string.

$$F_t = \sum \left[W_s Cos\emptyset + F_{Drag} + \Delta F_{area}\right] - F_{bottom} - WOB \qquad Eq.3.47$$

On the other side Buoyancy method assumed that the force exerted by the fluid in the bottom is distributed along the entire string. This method is used to determine where the buckling first occurs and is given by:

$$F_e = \sum \left[W_s Cos\emptyset + F_{Drag} + \Delta F_{area}\right] - F_{bottom} - WOB + (P_o + \rho_o u_o^2)A_o - (P_i + \rho_i u_i^2)A_i \qquad Eq.3.48$$

Clearly previous two equations presented have influence of circulation flow rate, the rate of change of momentum (ρAv) entering and leaving the pipe section should also be included in the effective tension equation.

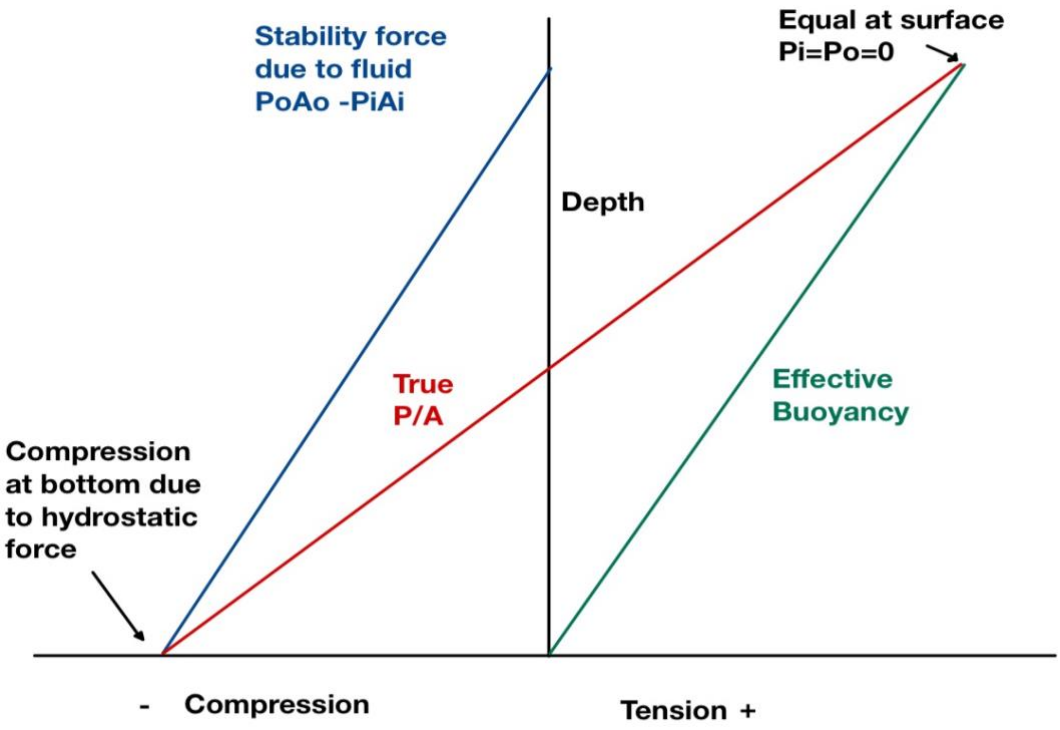

Figure 3.3 Effective and true tension

F_{Drag} is the drag force, sign might change from +1 for tripping out, -1 for tripping in and sliding assembly drilling and 0 for rotating on and off bottom.

Where:

A_i	$Internal\ cross\ sectional\ area\ of\ the\ section(in^2)$
A_o	$External\ cross\ sectional\ area\ of\ the\ section(in^2)$
DLS_i	$Dogleg\ severity\ of\ the\ section\ (in^2)$
D	$Diameter\ of\ the\ pipe\ (in)$
F_{drag}	$Drag\ force\ (Lb)$
$\dot{m}$	$Mass\ flow\ rate\ (Lb/min)$
ρ_i	$Inner\ density\ of\ the\ section\ \ (ppg)$
ρ_o	$Outer\ density\ of\ the\ section\ \ (ppg)$
F_{bottom}	$Bottom\ hydraulic\ force\ \ (Lb)$
P_i	$Outer\ pressure\ (psi)$

P_o	$Inner\ pressure\ (psi)$
ΔF_{area}	$Force\ due\ to\ change\ of\ area\ (pound)$
WOB	$Weight\ on\ Bit(pound)$
W_s	$Air\ weight\ of\ the\ segment\ [L * wair]\ (ft/min)$

Chapter 4: Results and discussions

Chapter 4.1 Source of data

The data used as an input for the fluid force calculations was taken from "Mariner 9.5 Real trajectory and BHA" a project property of MHWirth. The data is visualized through DHS simulator program, where the input is divided into the categories with detailed information regarding downhole parameters.

Chapter 4.2 Introduction of the data

Chapter 4.2.1 Drilling parameters involved

Into DHT downhole simulator, it is possible to find the next categories:

- ***Trajectory:*** Well details are displayed, starting with simple aspects such a "*Well name", "Well ID"* until trajectory parameters. Therefore each 10 m measured depth (MD) the next data is shown:
    - Measured Depth [m]
    - Inclination [degrees]
    - Azimuth[degrees]
    - Total Vertical Depth [m]
    - North [m]
    - East [m]
    - Dogleg [degree]
    - Dogleg Severity [degree/100m]

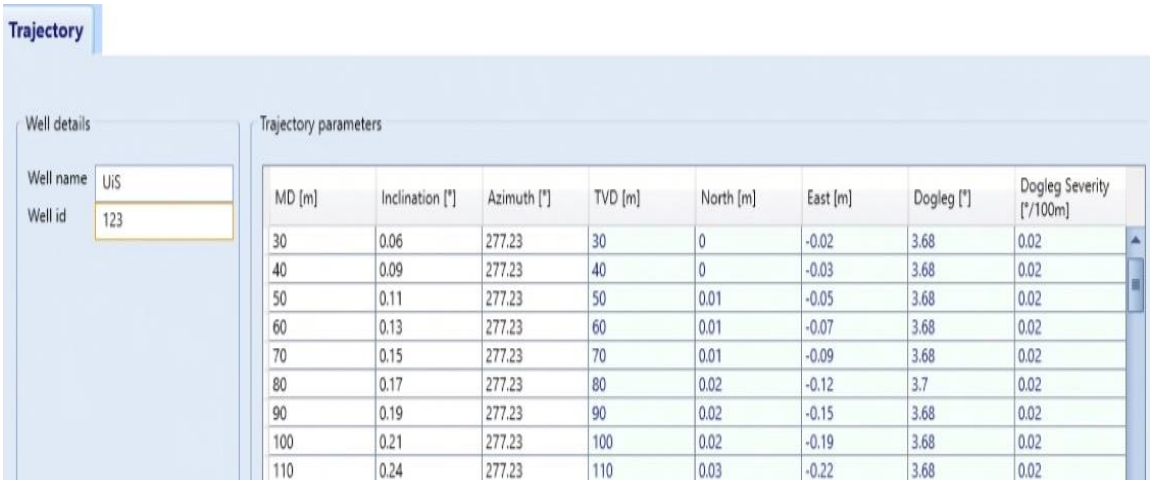

MD [m]	Inclination [°]	Azimuth [°]	TVD [m]	North [m]	East [m]	Dogleg [°]	Dogleg Severity [°/100m]
30	0.06	277.23	30	0	-0.02	3.68	0.02
40	0.09	277.23	40	0	-0.03	3.68	0.02
50	0.11	277.23	50	0.01	-0.05	3.68	0.02
60	0.13	277.23	60	0.01	-0.07	3.68	0.02
70	0.15	277.23	70	0.01	-0.09	3.68	0.02
80	0.17	277.23	80	0.02	-0.12	3.7	0.02
90	0.19	277.23	90	0.02	-0.15	3.68	0.02
100	0.21	277.23	100	0.02	-0.19	3.68	0.02
110	0.24	277.23	110	0.03	-0.22	3.68	0.02

Figure 4.1 Trajectory parameters

The data go from surface (Measured Depth=0 [m]) until final depth of 4238,5 [m], therefore we have 425 cells with detailed information about well trajectory.

- ***Tubular / Open hole:*** Details about each element of the Drill string, casing and bit as *Length [m], Outer diameter [m], Inner diameter [m], Linear mass [kg/m], Mass[kg], Casing suspension [m], Casing shoe depth [m]*. Moreover, open hole information, *Total Length [m], Diameter [in], Reamed section length[m], Reamed section diameter [m], Initial bit depth [m], Initial hole depth [m]*. Dimensions of the riser such a *Body OD [in], Body ID [in]* and *Length [m]* and friction factor for rotational, sliding, open hole and cased-hole.

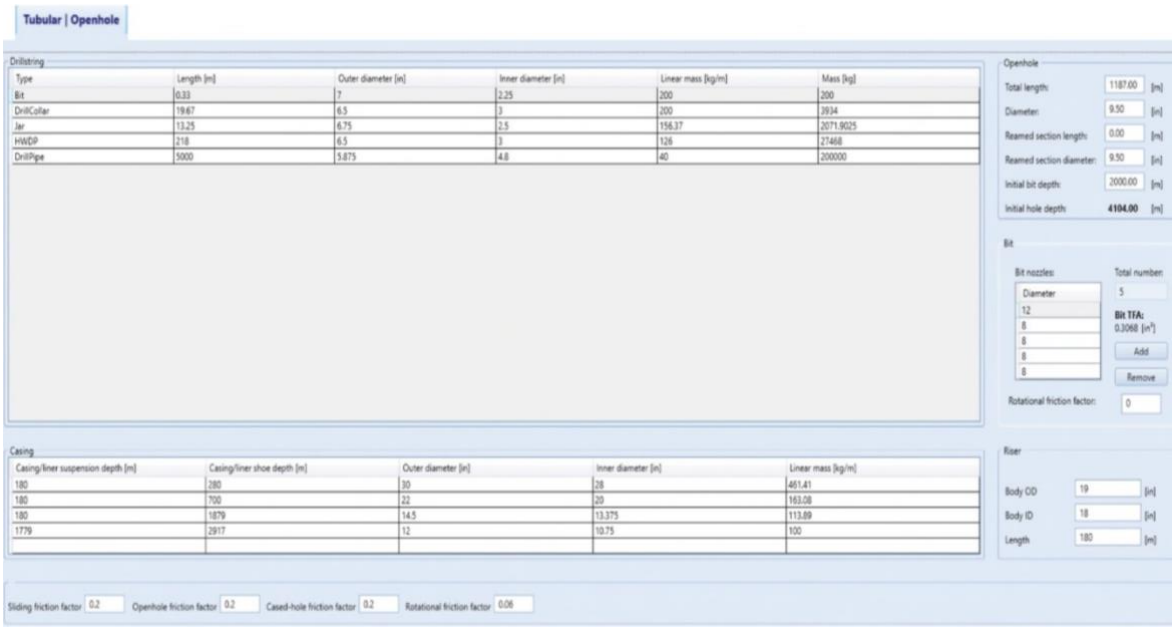

Figure 4.2 Tubular / open hole parameters

- ***Geology:*** Formations characteristics regarding to a specific *Total vertical depth [m]* like *Uniaxial compressive strength [MPa], Specific heat coefficient [J/kgK], Geothermal gradient [ºC/100m] Heat conductivity [W/mk]* and *Ambient temperature [ºC]*.

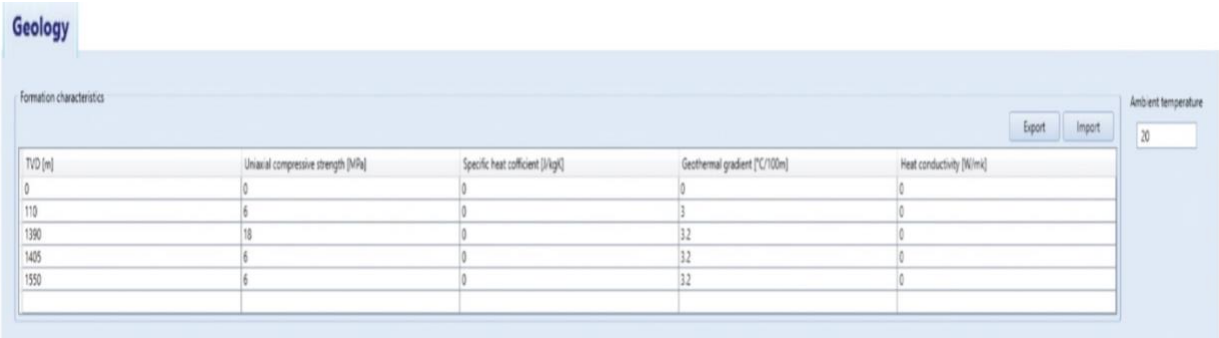

Figure 4.3 Geology parameters

- ***Fluid:*** Reference density of water, solid and oil inside the wellbore, *solid fraction*, *oil water ratio*. In the mud section, *Reference density [sg], specific heat [J/kgK],* reading of *Gel [Pa]* for 10 seconds and 10 min. Hershel-Bulkley rheology parameters, *Yield stress* τ_y *[Pa], Behaviour index 'n', Consistency index 'k' [Pa*s^n]*. Finally, Rheometer readings (Fann data) with *Reference temperature [ºC], Pressure atmosphere [bar], stress [pound/100ft^2] for 3 rpm, 6 rpm, 100 rpm, 200 rpm, 300 rpm, 600 rpm.*

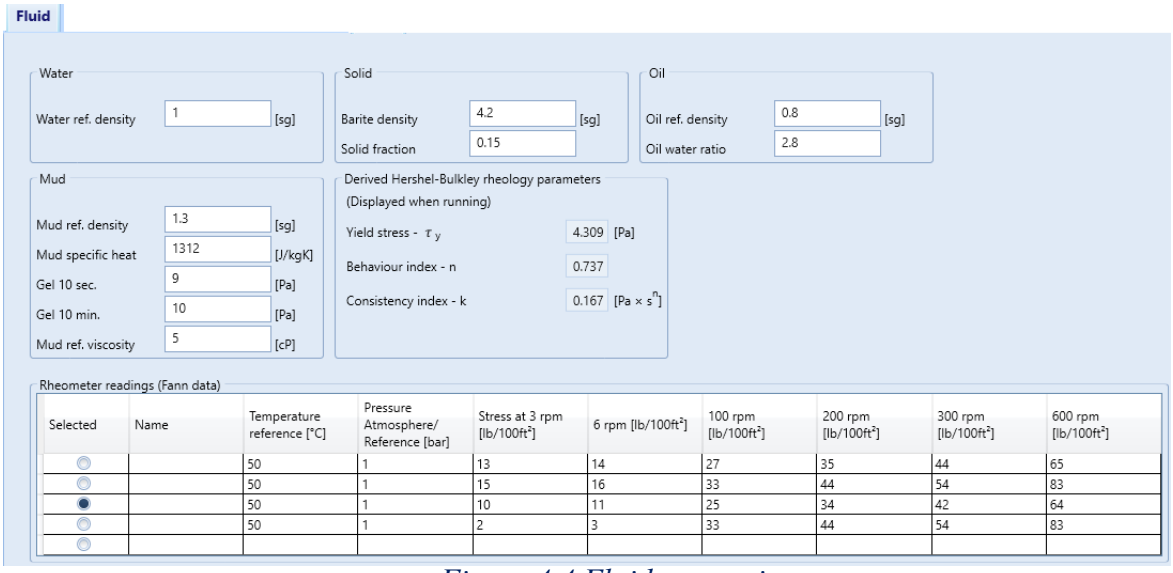

Figure 4.4 Fluid properties

Chapter 4.2.2 Problems regarding data

One of the main obstacles found from this information was the lack of data regarding both rock formations and pore pressure, since there is an open hole section, the ideal condition would have been to know the formation pressure in order to calculate operational density of the drilling fluid

Chapter 4.2.2.1 Pressure and density profile

A method to find Pressure and density in each point of the point of the survey was used knowing initials properties of the mud at surface and using boundary condition of atmospheric pressure as 14.7 psi. Kutasov [4] developed an empirical equation to model the behaviour of drilling fluids. The equation is:

$$\rho = \rho_0 * \exp[\alpha P + \beta(T - T_s) + \gamma(T - T_s) \qquad Eq.4.1$$

The coefficients α, β, ϒ are defined from each type of drilling mud, for this case we assume water-based mud (WBM). The initial input includes information about geothermal gradient, which is 0,896 $[F/m]$, the values for T_s and ρ_0 are 68 [F] and 10,829 [ppg] respectively.

Where:

α	$2{,}7384 * 10^{-6}$	$[1/psig]$
β	$-0{,}00015353$	$[1/F]$
γ	$-7{,}469 * 10^{-7}$	$[1/F]^2$

ρ_0	$Reference\ mud\ density$	ppg
T_s	$Reference\ temperature$	$[F]$

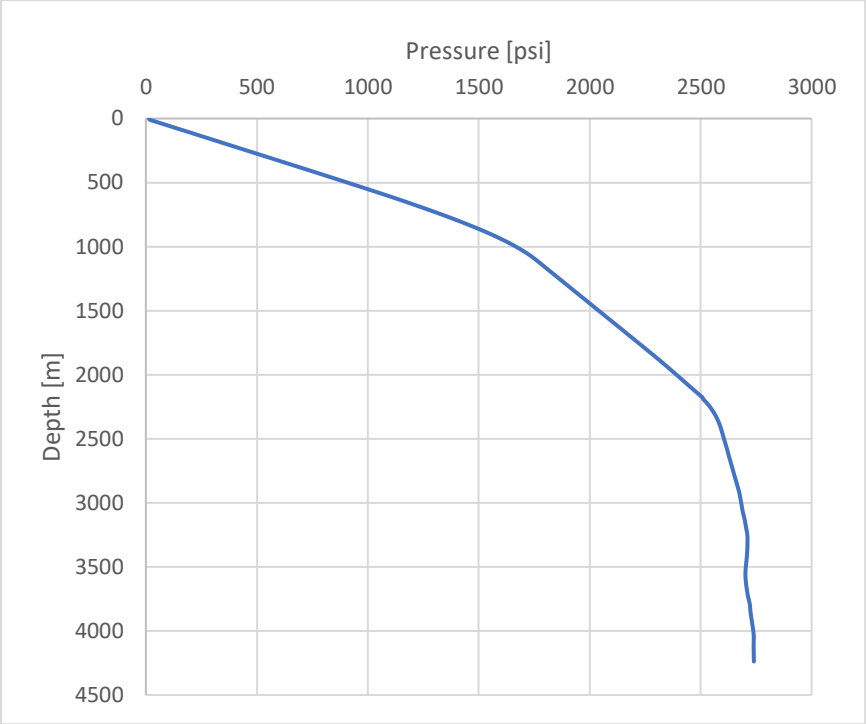

Figure 4.5 Pressure through the well

Using an iterative method in Matlab, see appendix 2, is possible to correct the current cell hydrostatic pressure, $P = 0{,}052 * \rho * TVD$, using the previous cell density, repeating the same process for the other 424 cells, is possible to get a smooth and physically consistent curves of density and pressure through

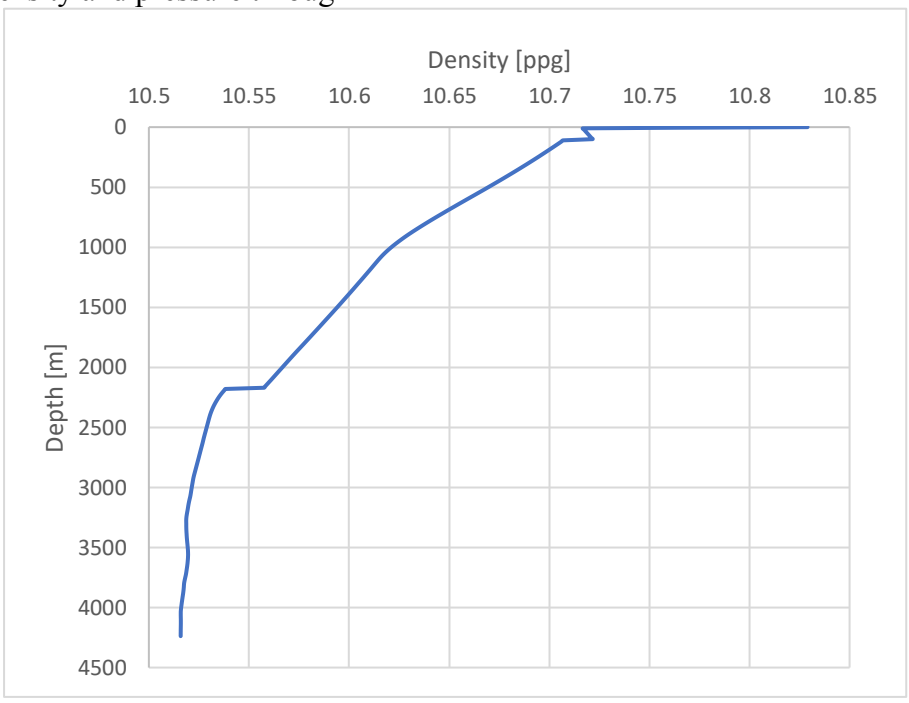

Figure 4.6 Density through the well

the well. The behaviour of the pressure is directly proportional to the depth, while the drilling fluid density present and inverse conduct as it is shown in the Figure 4.23.

Chapter 4.2.2.2 Projected weight

In previous chapters the concept of weight is mentioned but for most of the cases, applies in vertical wells. Nowadays is more common face directional than vertical wells, for the first group the component of weight is divided into "Axial" and "Normal", as shown in Fig 3.11. Thus, axial component of weight can be described as:

$$Wa = mg * \cos(\theta) \qquad Eq.\ 4.2$$

Where:

m	$Mass\ of\ the\ pipe$	$pound$
g	$Gravity$	ft/s^2
θ	$Inclination$	$degrees$

Chapter 4.3 Data interpretation

Based in the information given as input it is possible to draft the geometry of the well, drill string mechanics and type of rig.

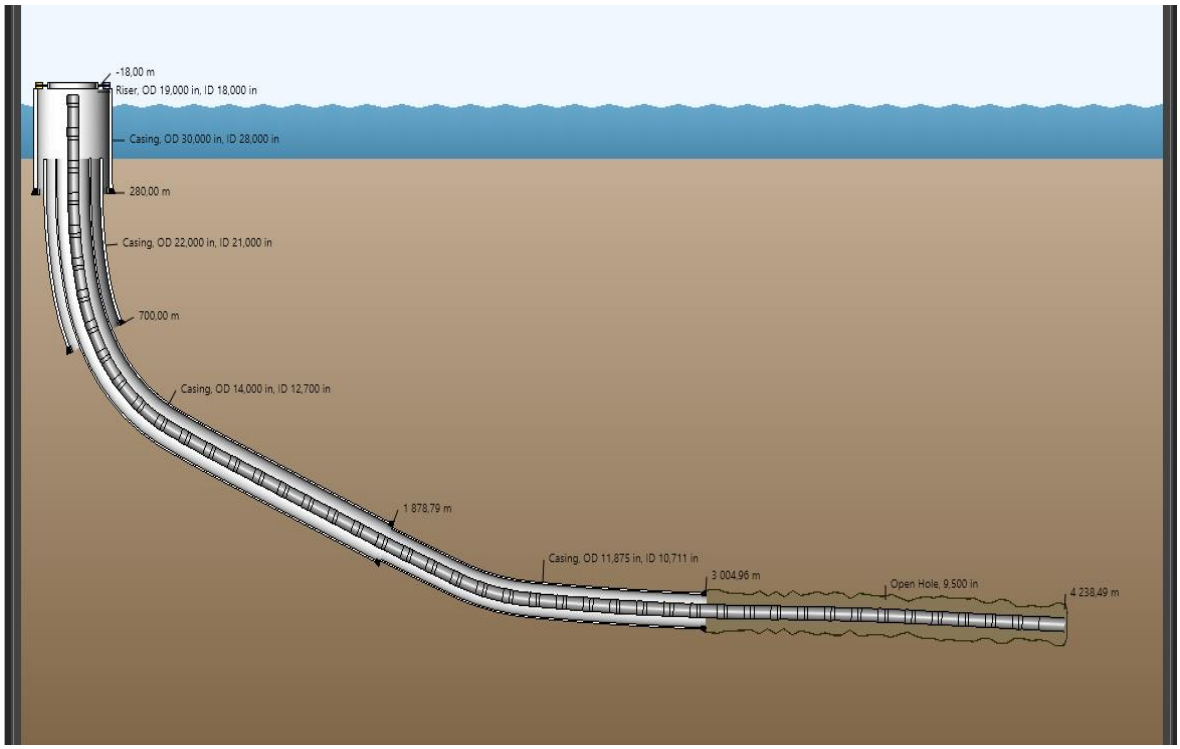

Figure 4.7 Well Mechanics. Source: WellPlan™

Drill string:

Type	Length [m]	OD [in]	ID [in]	Linear Mass [pound/m]
Bit	0,33	7	2,25	440,925
Drill Collar	19,67	6,5	3	440,925
Jar	13,25	6,75	2,5	344,736
HWDP	218	6,5	3	277,782
Drill Pipe	3987,25	5,875	4,8	88,18

Table 4.1 String mechanical specifications

Casing

Casing/liner suspension depth [m]	Casing/liner shoe depth [m]	Outer Diameter [in]	Inner Diameter [in]	Linear Mass [pound/m]
180	280	30	28	1017,23
180	700	22	20	359,529
180	1879	14,5	13,375	251,084
1779	2917	12	10,75	220,462

Table 4.2 Casing mechanical specifications

Open-hole section:

Total Length [m]	1187
Diameter [in]	9,5
Reamed section diameter [in]	9,5

Table 4.3 Open hole specifications

Riser:

Body OD[in]	19
Body ID [in]	18
Length[m]	180

Table 4.4 Risers specifications

Based in the length of the riser clearly, we are talking about an offshore rig, with the inclination (See Appendix 1) is possible to imply that the well is a "L" type since the angle starts at 0 degrees, then build the well around 66 degrees and later becomes completely horizontal 89,8 degrees. Fig. 4.3.

Geology:

Total Vertical Depth [m]	Geothermal gradient [F/100 m]
0	0
110	37,4
1390	89,6
1405	89,6
1550	89,6

Table 4.5 Geothermal gradient

Fluid:

Mud:

Mud ref. density ρ_0	10,829	$[\boldsymbol{ppg}]$
Mud ref. viscosity	5	[cP]

Table 4.6 Drilling fluid properties

Derived Herschel-Bulkley rheology parameters

Yield stress τ_0	9,0	$[\boldsymbol{pound/100ft^2}]$
Behaviour index, n	0,737	
Consistency index, K	0,00349	$[[lb * s^n]/ft^2$

Table 4.7 Derived Herschel-Bulkley parameters

Chapter 4.4 Calculations performed

Chapter 4.4.1 Step by step of each force

With the data gotten as input, and the extra calculation performed, the next step is calculating each one of the forces, analyse the effect in the Hook load and finally combine them all.

Chapter 4.4.1.1 Buoyancy force

Assumptions: Density of the steel = 64,7 [ppg], inside density equal to outside density.

As displayed in the chapter 3, Buoyancy, from a volumetric point of view, will depend directly from the density of the mud and the pipe. Consequently, first step is finding the Buoyancy factor, applying Eq. 3.12:

$$\beta = 1 - \left[\frac{\sum_{k=1}^{n} D_k \left(\rho_o R_k^2 - \rho_i r_k^2\right)}{\rho_{steel} \sum_{k=1}^{n} D_k \left(R_k^2 - r_k^2\right)}\right] \qquad Eq.3.12$$

Taking in account assumptions previous explained Eq. 3.12 reduces itself to a shorter form (Eq.4.2). As it was mentioned in chapter 4.2.2.1 density varies through the depth, for this reason there will be a different Buoyancy factor for each 10 [m] as Fig 4.4 displays.

$$\beta = 1 - \left[\frac{\sum_{k=1}^{n} \rho_k}{\rho_{steel}}\right] \qquad Eq.4.3$$

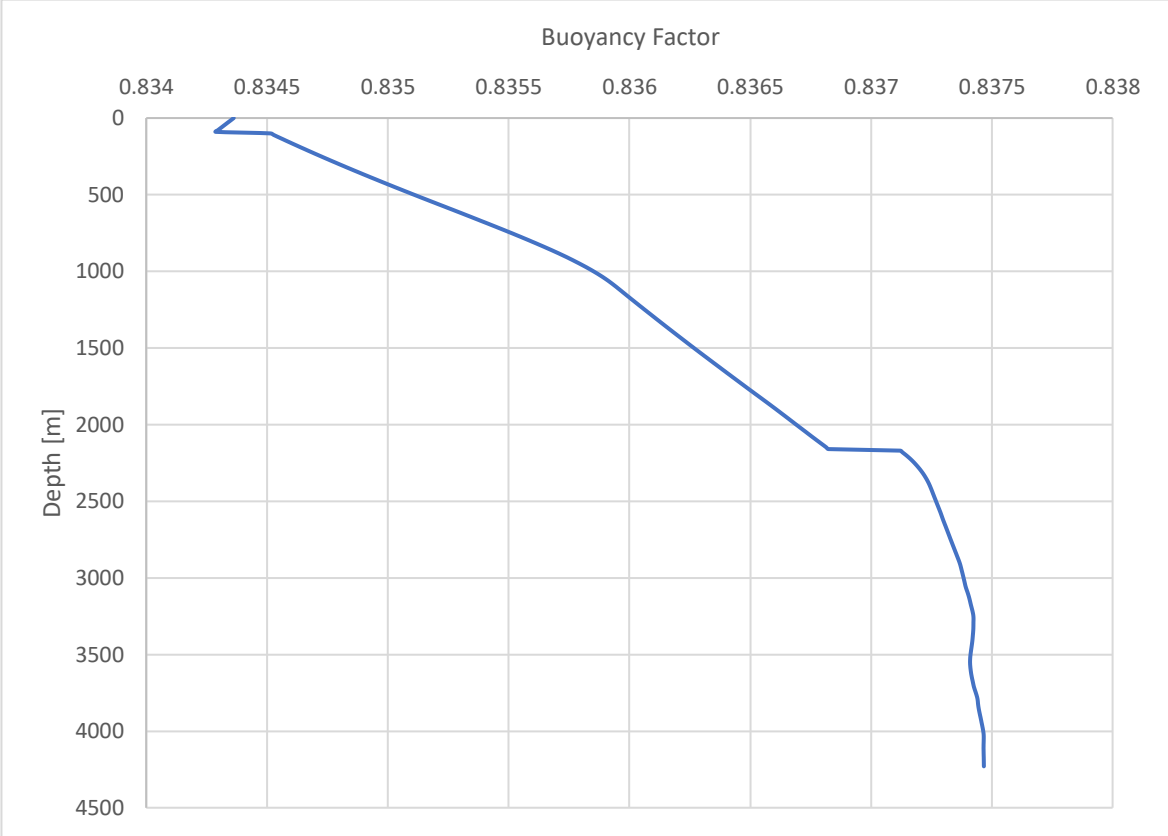

Figure 4.8 Buoyancy factor through the well static conditions

Applying Eq. 4.2. to our situation and following parameters of Johancsik torque and drag model which reveal the increment of axial weight it is possible to find the projected weight of each pipe section following:

$$Pw = \sum_{k=2}^{n} Wair_k * D_k * cos\left(\frac{\theta_k + \theta_{k-1}}{2}\right) \qquad Eq.4.4$$

As can be seen, after Buoyancy factor and Projected weight are calculated, the Buoyant weight is just Buoyancy factor times Projected weight as is shown in Eq.4.5:

$$Bw = \beta * Pw - SF \qquad Eq.4.5$$

Making an average of all the Buoyancy factors through the well, the overall Buoyancy factor will be, $\beta = 0{,}8366$.

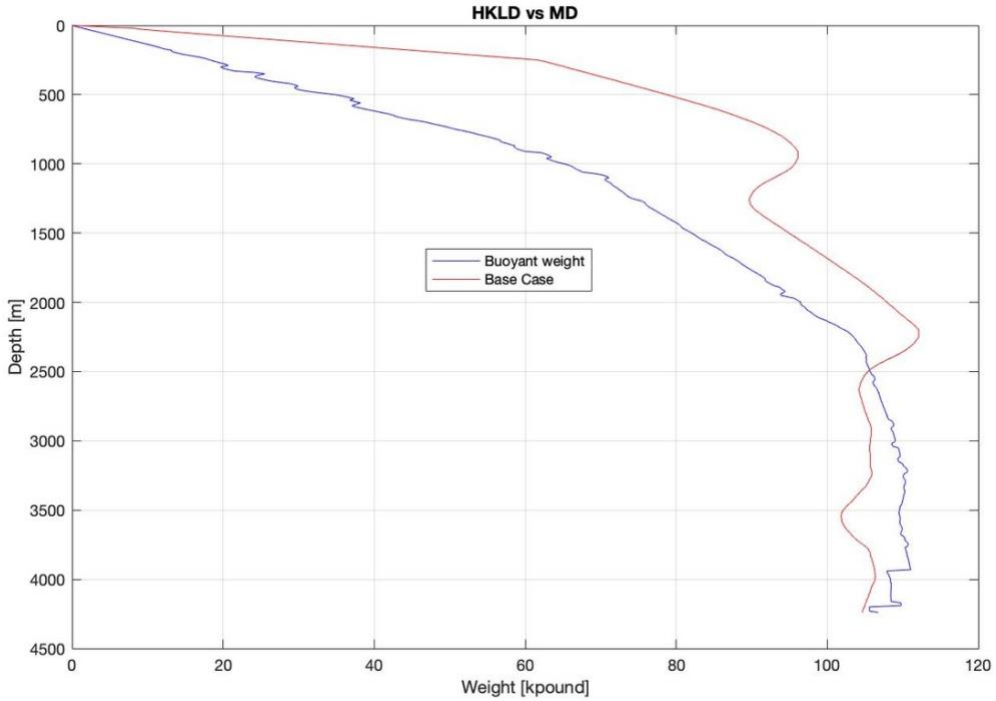

Figure 4.9 Buoyancy weight vs base case

The Hook load at the end of the pipe, considering the effect of the buoyancy will be 106,72 [Klb], having a difference respect to the base case of: 2,12 [Klb].

Where:

Bw	$Buoyant\ weight\ (pound)$
R_k	$Outer\ radio\ (in)$
r_k	$Inner\ radio\ (in)$
D_k	$Length\ of\ the\ section(ft)$
SF	$Side\ force\ (pound)$
Pw	$Projected\ weight\ (ft)$
ρ_{steel}	$Pipe\ density\ (ppg)$
ρ_k	$Mud\ Density\ at\ element\ depth\ \ (ppg)$
ρ_o	$Outer\ Mud\ Density\ at\ element\ depth\ \ (ppg)$
ρ_i	$Inner\ Mud\ Density\ at\ element\ depth\ \ (ppg)$

w_{air}	$Air\ weight\ (pound/ft)$
θ_k	$Inclination\ of\ the\ current\ section\ (degrees)$
θ_{k-1}	$Inclination\ of\ the\ previous\ section\ (degrees)$

Chapter 4.4.1.2 Pressure Area force

Assumptions: Just consider changes in outer diameters, inside density equal to outside density. Pump rate: 792,5 [gpm].

In order to summarize what is explained in the chapter 3, at each change of area, a hydraulic force will act, either downward (positive) or upward (negative), affecting the total weight of the drill string, which in this case will include also the projected weight of the mud (Eq. 4.7):

$$TPw = Pw + Pwm \qquad Eq.4.6$$

$$Pwm = \sum_{k=2}^{n} Ai_k * D_k * \rho_k * cos\left(\frac{\theta_k + \theta_{k-1}}{2}\right) \qquad Eq.4.7$$

Hence, for static conditions, at each change of area the corresponding hydrostatic pressure times the change of area is equal to the hydraulic force acting on this point. (Eq. 4.8):

$$HyF_k = (A_1 - A_2) * P_{hydr} \qquad Eq.4.8$$

The corresponding force balance from bottom (compression) to the top has a couple of changes when there is a presence of pump rate. Consequently, for dynamic circumstances is necessary to find pump pressure, as below:

$$PP = P_{hydr} + \Delta P_{pipe} + \Delta P_{ann} \qquad Eq.4.9$$

In the case of ΔP_{pipe}, pressure loss in the bit nozzles and due to the reductions in the tool joints. For ΔP_{ann}, additional force due to viscous drag force (Eq.3.41) should be take it in account. Given the above procedure, next step is to compute Bottom Hole Pressure (BHP) (Eq. 4.9) and finally the new dynamic pressure in the annular (Eq.4.11) will be BHP plus ΔP_{ann}.

$$BHP = PP + P_{Hydr} - \Delta P_{pipe} \qquad Eq.4.10$$

$$P_{Dyn} = BHP + \Delta P_{ann} \qquad Eq.4.11$$

Since the main purpose of this chapter is to analyse the effect of each force without any kind of overlapping, the hydrostatic pressure should be subtracted from Eq. 4.11 to realize the outcome of the flow rate in the pressure area force, and use P_{DynPA} Eq. 4.8 to find Hydraulic forces under dynamic circumstances.

$$P_{DynPA} = BHP + \Delta P_{ann} - P_{Hydr} \qquad Eq.4.12$$

$$\Delta F_{areaD} = (A_k - A_{k+1}) * P_{DynPA} \qquad Eq.4.12b$$

With this new annular dynamic pressure and with the already known area changes there is a new force balance from the bottom to the top of the well (Fig 4.6)

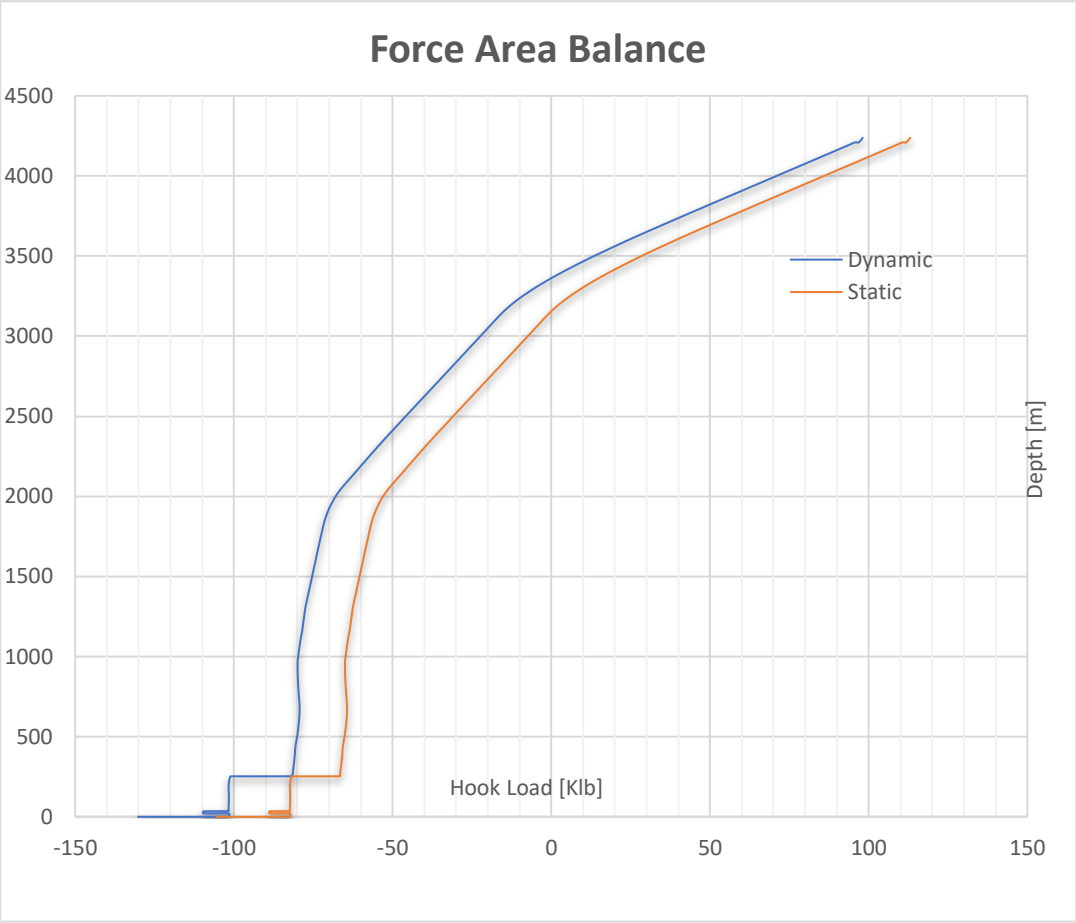

Figure 4.10 Force balance comparison

The force balance starts from the bottom; 0 [m], with the drill string in compression, going through each different section adding weight and considering forces in area transitions, thus the Hook load can be read at surface with values of 113,069 [Klb] and 91,81 [Klb] for static and dynamic conditions respectively. Details about changes in hydraulic forces are displayed in the following table:

Area changes	Static	Dynamic	Units
Hydraulic force at HWDP/Drill Pipe	15,127	19,482	[Klb]
Hydraulic force at Jar/HWDP	6,288	7,818	[Klb]
Hydraulic force at DC/Jar	-6,450	-8,006	[Klb]
Hydraulic force at Bit/Drill Collar	23,161	28,644	[Klb]
Hydraulic force at bottom	-105,438	-134,194	[Klb]

Table 4.8 Hydraulic forces due to change of area

On previous chapters was mentioned the fact that Pressure area force method shows that the lower part of the drill string is in compression, but it cannot be used as failure criteria, therefore the proper way to visualize the effect of this force is just recording the weight over the string, from the top 0 [m], and sum the additional hydraulic forces due to change of area.

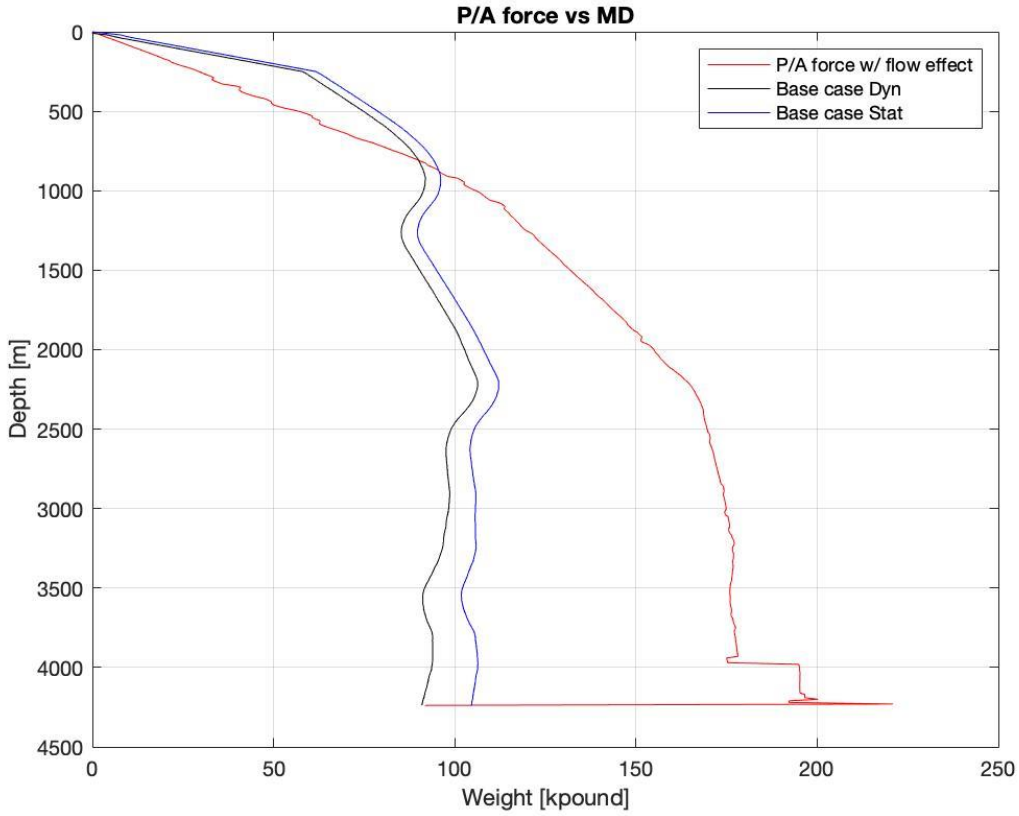

Figure 4.11 Effect of Piston force under dynamic state

Given the above graph the curves and compared the calculation performed with the base case the difference is 0,91 [Klb]. The gap between WellPlan™ data for static, 104,6 [Klb] and dynamic, 90,9 [Klb] is 13,7 [Klb].

Where:

Ai_k	$Inner\ area\ of\ the\ section\ (in^2)$
A_1	$Outer\ area\ of\ the\ section\ (in^2)$
A_2	$Outer\ area\ of\ the\ next\ section\ (in^2)$
HyF_k	$Hydraulic\ force\ of\ the\ section\ (pound)$
$HyFD_k$	$Hydraulic\ dynamic\ force\ of\ the\ section\ (pound)$
BHP	$Bottom\ Hole\ Pressure\ (BHP)$
D_k	$Length\ of\ the\ section(ft)$
Pw	$Projected\ weight\ (ft)$
PP	$Pump\ pressure\ (psi)$

Pw	$Projected\ weight\ of\ the\ pipe\ (pound)$
Pwm	$Projected\ weight\ of\ the\ mud\ (pound)$
P_{hydr}	$Hydrostatic\ Pressure\ (psi)$
P_{Dyn}	$Dynamic\ Pressure\ (psi)$
P_{DynPA}	$Dynamic\ Pressure\ used\ for\ pressure\ area\ method\ (psi)$
TPw	$Total\ projected\ weight\ (pound)$
ρ_k	$Density\ at\ element\ depth\ \ (ppg)$
ΔP_{pipe}	$Pressure\ losses\ inside\ the\ pipe\ (pound/ft)$
ΔP_{ann}	$Pressure\ losses\ in\ the\ annular\ (pound/ft)$
θ_k	$Inclination\ of\ the\ current\ section\ (degrees)$
θ_{k-1}	$Inclination\ of\ the\ previous\ section\ (degrees)$

Chapter 4.4.1.3 Inertial force

After doing the force analyse inside a curved pipe in the chapter 3 and adopting Eq.346 and Eq. 3.47 it is possible to find the resultant force exerted by the fluid to the pipe wall.

$$\vec{F}_{i,A} = \frac{\pi d^2}{4}\left(P_i - P_{i+1}\cos(L_i DLS_i)) - \frac{4\rho_i q^2}{\pi d^2}(\cos(L_i DLS_i) - 1)\right)\vec{t}_i - \left(\frac{\pi d^2}{4}P_{i+1}\sin(L_i DLS_i) + \frac{4\rho_i q^2}{\pi d^2}(\sin(L_i DLS_i))\right)\overrightarrow{n_i} \qquad Eq.3.46$$

Total inertial force vector is calculated by [13]:

$$TIF = \sqrt{\left(\overrightarrow{Ft_i}\right)^2 + \left(\overrightarrow{Fn_i}\right)^2} \qquad Eq.3.47$$

For inertial force dynamic pressure is imperative to use the dynamic pressure, which was figured out in the previous chapter (Eq. 4.11)

$$P_{Dyn} = BHP + \Delta P_{ann} \qquad Eq.4.11$$

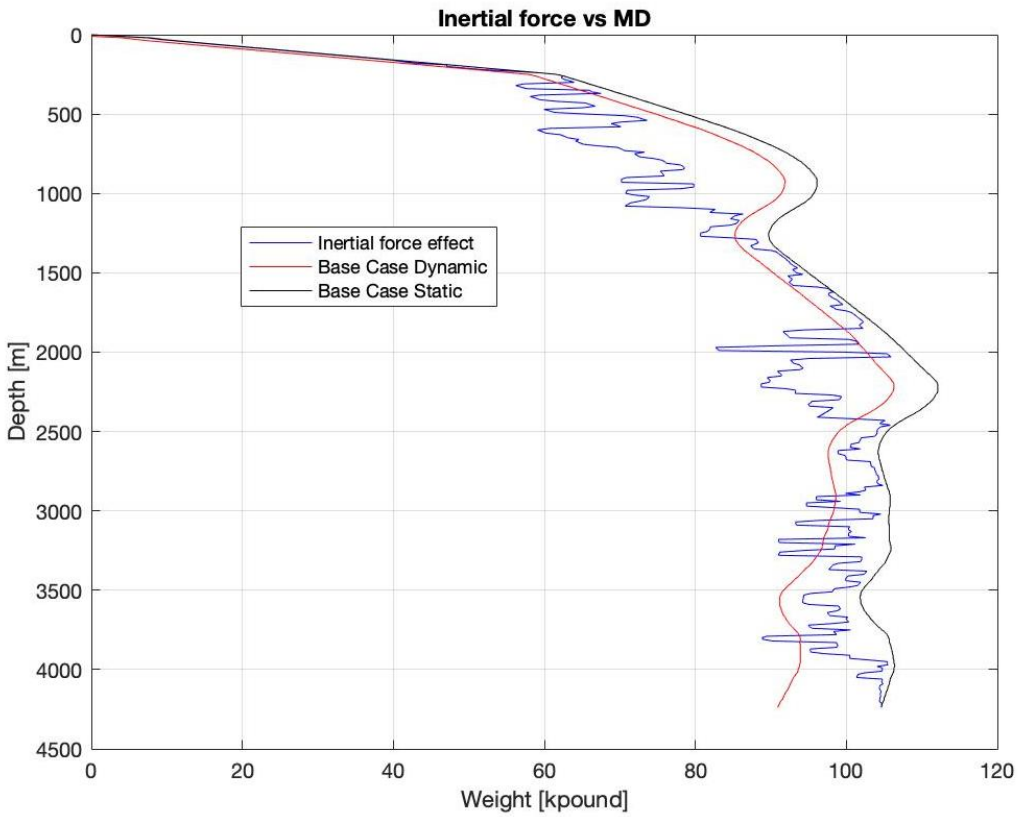

Figure 4.12 Effect of Inertial force under dynamic state

As described in the plot, the blue curve shows the effect of the inertial force, the biggest difference on Hook load can be found when the well is building up curve, around 40-50 degrees and near to 1,2 degrees / 100 m of DLS. Approximately from 900m to 1000m the repercussion of inertial force under the Buoyant weight is 26 [Klb] approximately. It can be concluded that the closer to the horizontal (90 degrees) or vertical (0 degrees), the less impact of the fluid in the pipe walls and therefore in the hook load measurement.

Chapter 4.4.1.4 Viscous force

Using the Rheological model chosen, Herschel Bulkey, exposed in chapter 3 and after finding Reg, f and ΔP, the viscous force both in the pipe and annulus can be calculated. Regarding Inside pressure loss, pressure loss in the bit nozzles must be included also losses in the tool joints.

$$\Delta P_{inside} = \Delta P_{pipe} + \Delta P_{tj} + \Delta P_{bit} \qquad Eq.4.13$$

WellPlan™ use the following expression to quantify this value:

$$\Delta P_{tj} = \frac{\rho K_{tj} v_f^2}{2} \qquad Eq.4.14$$

If

$$Reg < 1000$$

Then,

$$K_{tj} = 0$$

K_{tj} is the tool joint loss coefficient which is in function of the Reynold number inside the pipe section.

If

$$1000 < Reg < 3000$$

Then

$$K_{tj} = 1{,}91 * \log(Reg) - 5{,}64$$

If

$$3000 < Reg < 13000$$

Then

$$K_{tj} = 4{,}66 - (1{,}05 * \log(Reg))$$

If

$$Reg > 13000$$

Then

$$K_{tj} = 0{,}33$$

The Pressure drop across the Bit Nozzles was studied by Azar and Robello [8] , concluding the subsequent expression:

$$\Delta P_{bit} = \frac{(8{,}3 * 10^{-5})\rho Q^2}{C_d^2 A_t^2} \qquad Eq.\,4.15$$

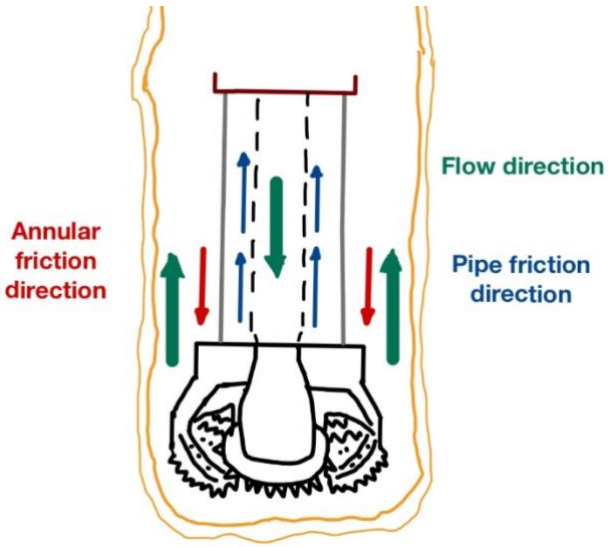

Figure 4.13 Flow and friction direction

With respect to pressure losses, the assignment made by the programmed Matlab code which has included different works regarding Reynolds number, Herschel Bulkley rheological model and Darcy friction factor displayed the following results:

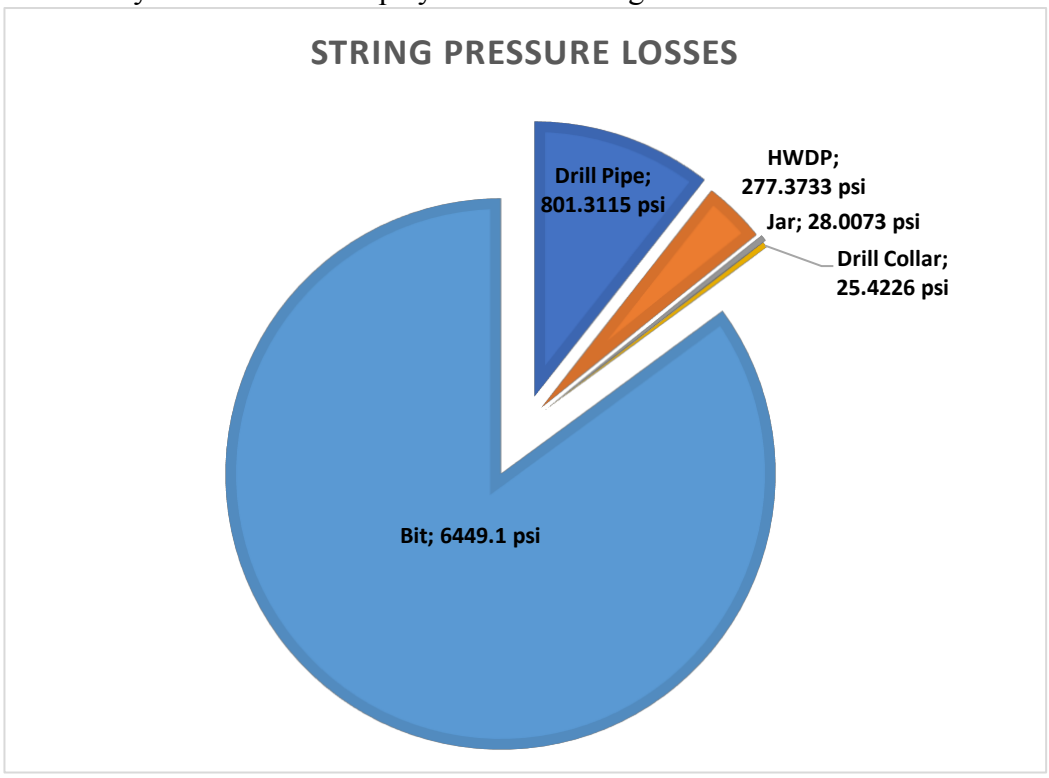

Figure 4.14 String Pressure drop distribution

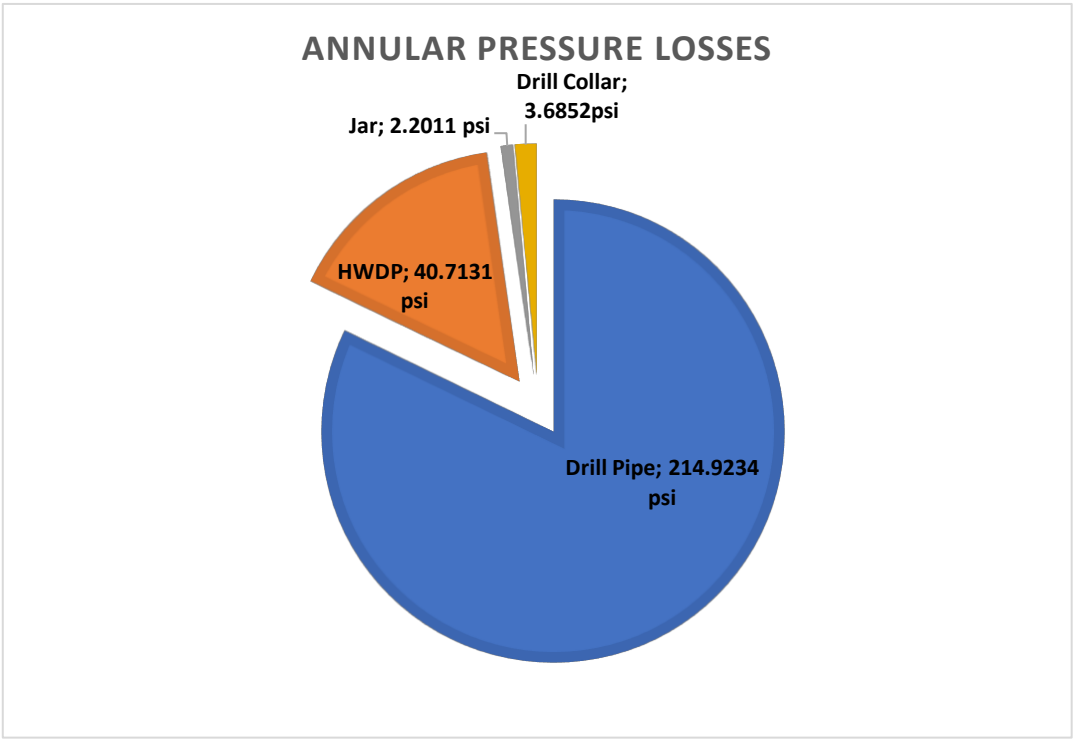

Figure 4.15 Annular Pressure drop distribution

Consequently, using the definition of viscous force given in the chapter 3, this magnitude for each section of the well would be defined as:

$$VF_k = VF_{ann} - VF_{pipe} \qquad Eq.4.16$$

$$WDVF = BC + VF_{pipe} \qquad Eq.4.17$$

Eq. 4.17 clarifies the effect only of the viscous force in the hook load from the base case measured at surface by a force balance

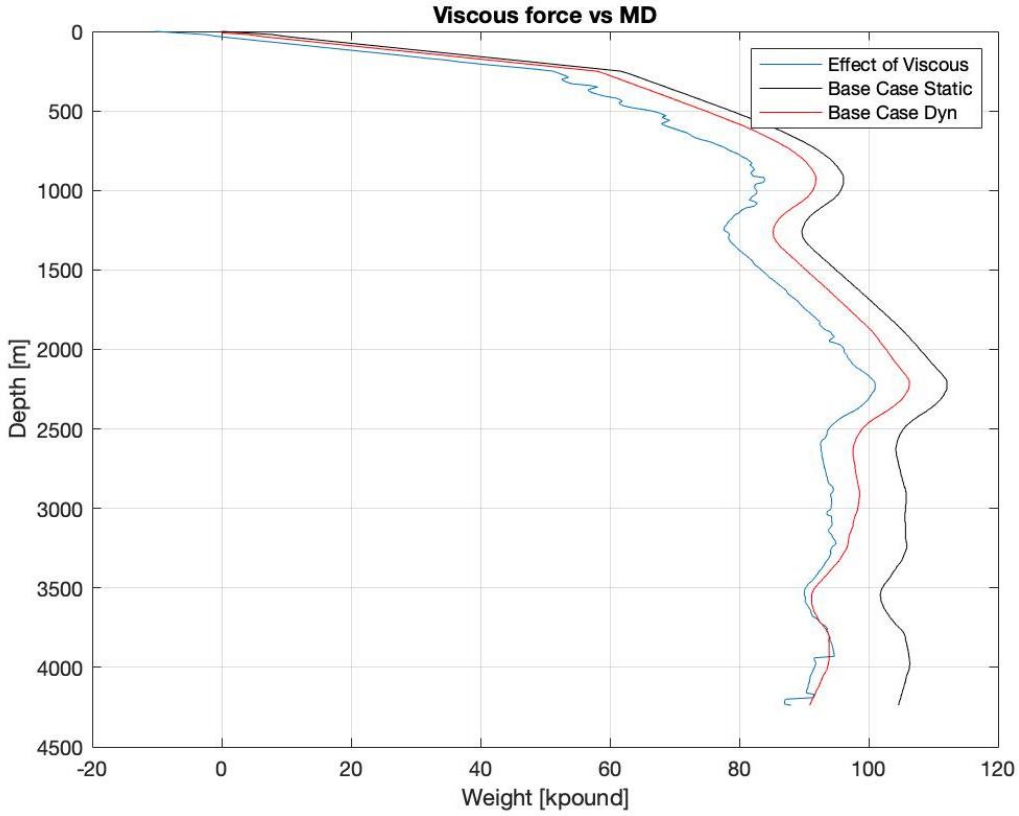

Figure 4.16 Effect of viscous force in the hook load

Based in the information that can be taken from the plot Hook load of the whole drill string considering viscous force is 102,78 [Klb], which means 10,25 [Klb] of response respect to the base case.

Where:

BC	$Hook\ load\ from\ base\ case\ (pound)$
A_t	$Total\ flow\ area\ (in^2)$
C_d	$Nozzle\ coefficient = 0{,}95$
Pw	$Projected\ weight\ (ft)$
K_{tj}	$Tool\ joint\ loss\ coefficient$

Q	$Pump\ rate\ (gpm)$
Reg	$Reynolds\ number$
VF_k	$Viscous\ force\ at\ element\ depth\ (pound)$
VF_{ann}	$Annular\ viscous\ force\ at\ element\ depth\ (pound)$
VF_{pipe}	$Pipe\ viscous\ force\ at\ element\ depth\ (pound)$
$WDVF$	$Weight\ due\ to\ viscos\ force\ (pound)$
ρ	$Mud\ Density\ at\ element\ depth\ \ (ppg)$
ΔP_{tj}	$Pressure\ loss\ in\ the\ tool\ joint\ \ (psi)$
ΔP_{bit}	$Pressure\ loss\ in\ the\ bit\ nozzles\ \ (psi)$

Chapter 4.4.2 Combine all forces into T&D model

Assumptions: Friction force coefficient: 0.2, same density inside and outside the pipe [pound/in^3], pressure inside equal to pressure inside [psi], Weight On Bit: 0 [Klb]

After analysing each force for separate, it is moment to blend them all together and see a more realistic impact into the Hook load. For the first case, just rotating off the bottom, the string is still but there is a pump rate of 792,5 [gpm]. With respect to the basic case is clearly a variation of 22,87 [Klb]

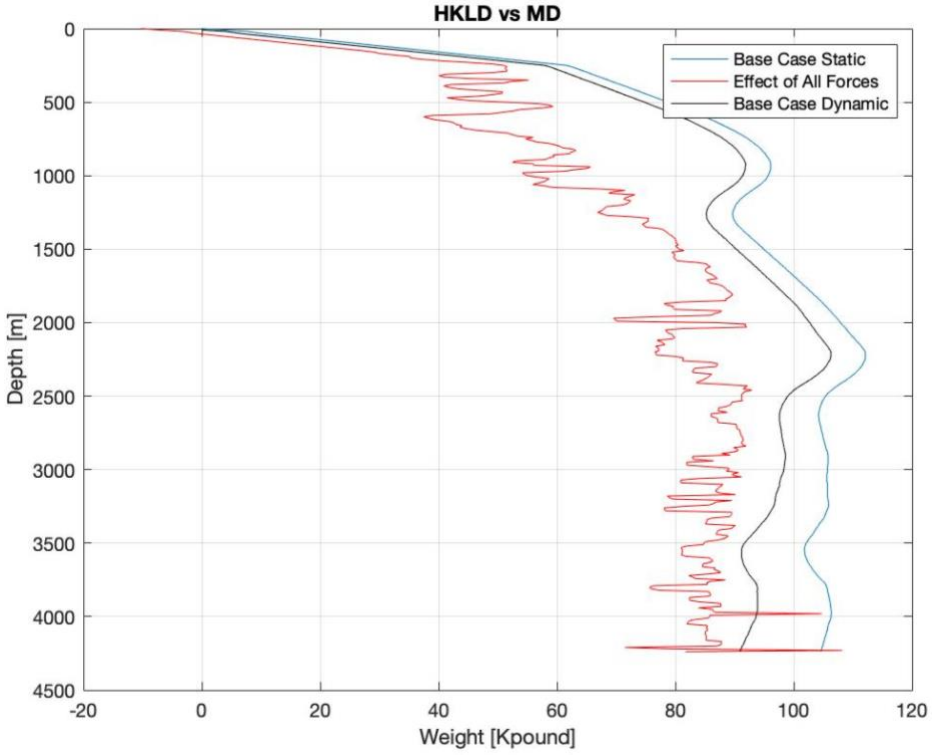

Figure 4.17 Effect of all the forces in the hook load

To summarise and define how this result was found, it is required a basic force balance. It is necessary to bring up equations 3.47, 4.5, 4.8, 4.12b,4.16:

$$HKLD_{NC} = \beta * Pw + F_{Drag} + \Delta F_{areaD} - TIF + VF_{ann} - VF_{pipe} \qquad Eq.4.18$$

Rotating off the bottom is a procedure developed to mainly to circulate viscous pill and clean the hole. But trip in and trip out are procedures required when there is a change in the BHA. Since a displacement of the string is seen, the drag force then must be considered, Robello et al [6] exposed it as:

$$F_{Drag} = SF * L_k * \mu_f * sign \qquad Eq.4.19$$

The sign might change from +1 for pulling out of the hole (POOH), -1 for running into the hole (RIH) and 0 for rotating on and off bottom. Doing some changes in Effective Tension expression (Eq.3.4), then it becomes:

$$F_e = \sum [HKLD_{NC} + F_{Drag}] - F_{bottom} + (P + \rho u_o^2)A_o - (P + \rho u_i^2)A_i \qquad Eq.4.20$$

In relation to F_{bottom} is computed by the fluid Pressure applied over the cross-sectional area of the bottom component.

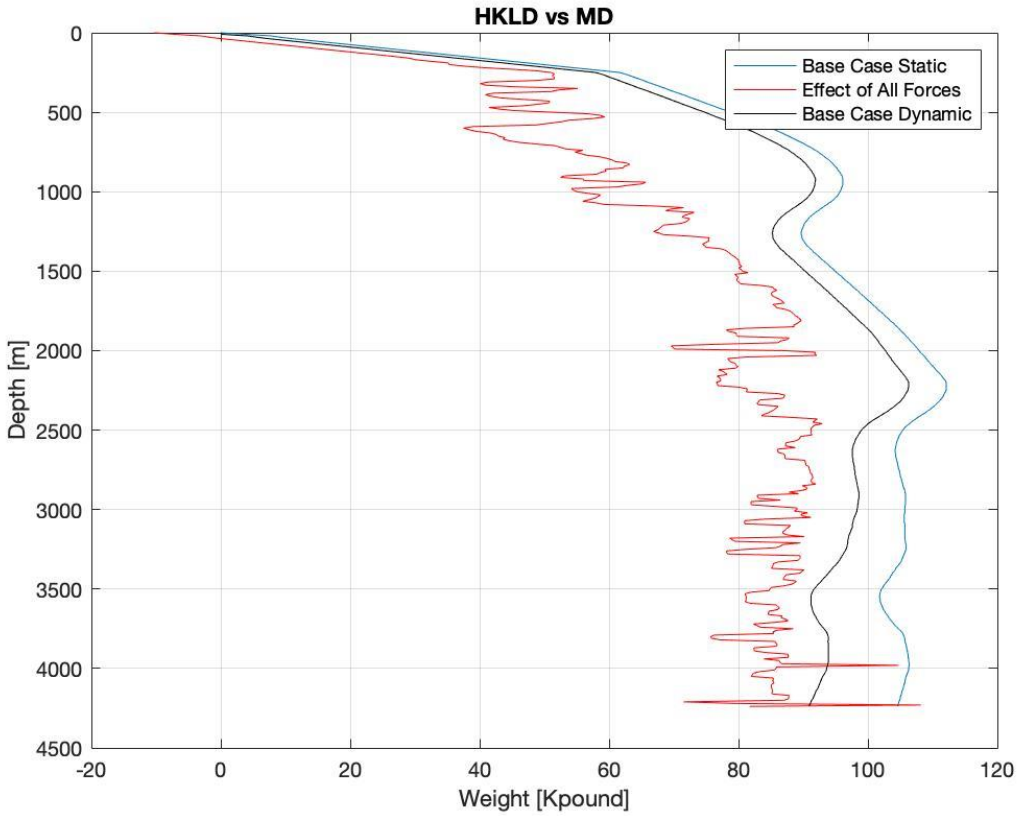

Figure 4.18 Effect of all the forces in the Torque and drag model

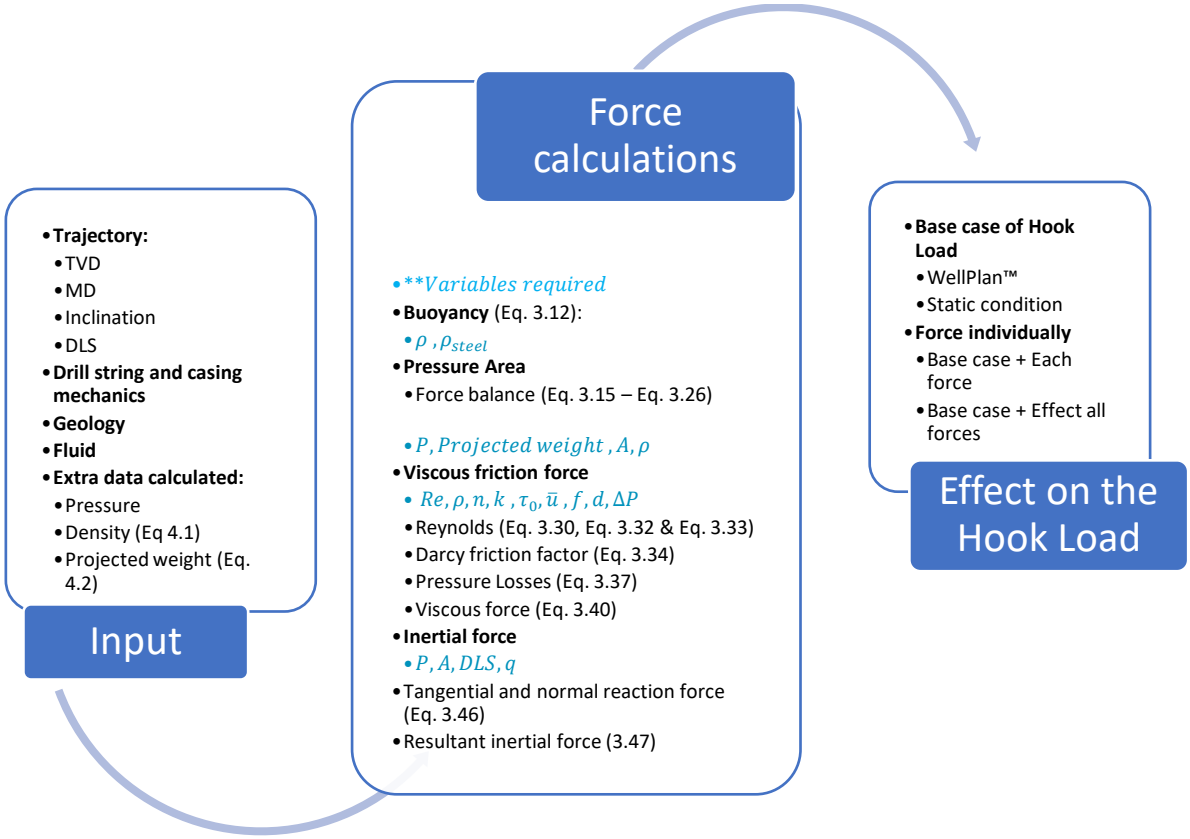

Figure 4.19 Calculation process

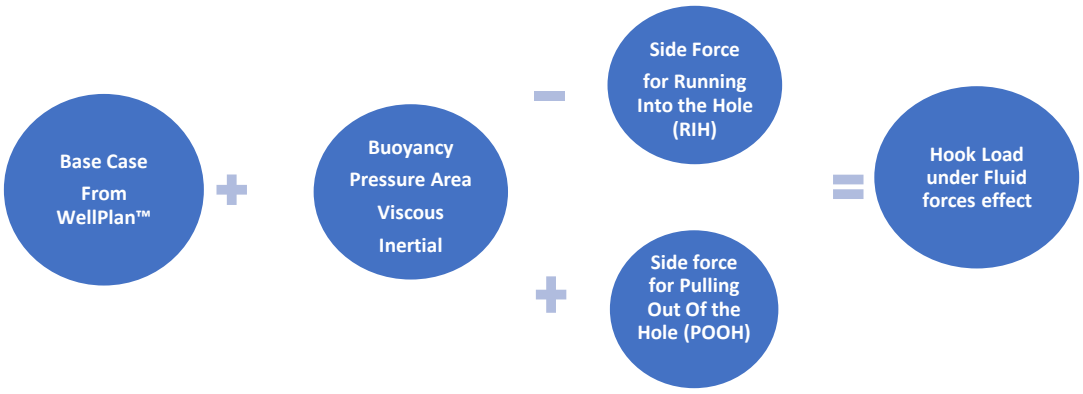

Figure 4.20 Calculation process for torque and drag

Where:

A_i	$Inside\ cross-sectional\ area\ (in^2)$
A_o	$Outside\ cross-sectional\ area\ (in^2)$
$HKLD_{NC}$	$Hook\ load\ under\ new\ conditions\ (pound)$
F_{Drag}	$Drag\ force\ (pound)$
F_{bottom}	$Bottom\ pressure\ force\ (pound)$
L_k	$Length\ of\ the\ pipe\ section\ (pound)$
Pw	$Projected\ weight\ (pound)$
P	$Pressure\ (psi)$
SF	$Side\ force\ (pound/m)$
u_i^2	$Inside\ velocity\ (in/s)$
u_o^2	$Outside\ velocity\ (in/s)$
VF_{ann}	$Annular\ viscous\ force\ at\ element\ depth\ (pound)$
VF_{pipe}	$Pipe\ viscous\ force\ at\ element\ depth\ (pound)$
ρ	$Mud\ Density\ at\ element\ depth\ \ (ppg)$
β	$Buoyancy\ factor$
μ_f	$Friction\ coefficient$
ΔF_{areaD}	$Hydraulic\ force\ due\ to\ change\ of\ area\ at\ dynamic\ conditions\ (pound)$

Chapter 4.5 Impact of the results

After displaying graphically, the effects of the forces in the Hook load and torque and drag model both individually and grouped, it is the moment for a more analytical approach. The base case used to validate result is the one ran into WellPlan™ with zero flow rate and in static condition with a value of 104,6 [Klb]. The static base case also includes data of Hook Load in case of tripping in (RIH) or Tripping out of the hole (POOH). In some previous plots, the term "Base case Dynamic" is also presented, this also comes from WellPlan™ but under the influence of flow rate, which will be use

Force	Total Hook load measured [Klb]	Base case [Klb]	Impact [%]
Buoyancy	106,727	104,6	2,03
Buoyancy RIH	100,41	40,5	147,92
Buoyancy POOH	113,035	186,7	39,45

Table 4.9 Hook load at bottom of the string for each operation under Buoyancy force

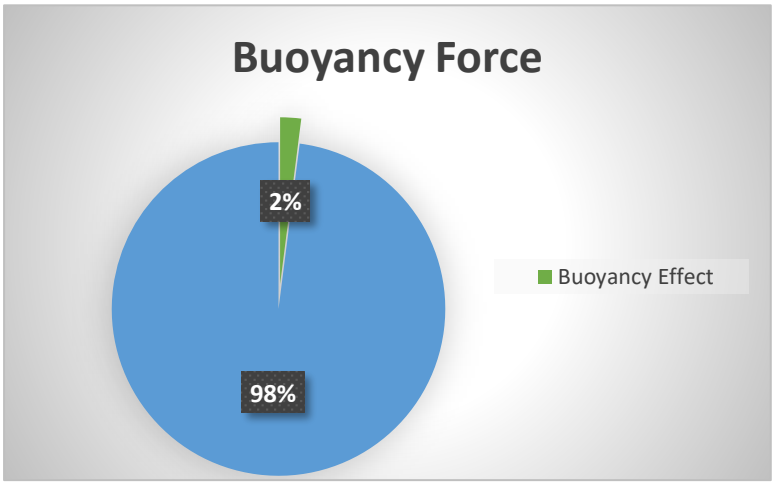

Figure 4.21 Effect of Buoyancy in Hook load

Depending the type of operation at which the string is being subdued, the drag force between de pipe and the wellbore will change for running into the hole (RIH) or pulling out of the hole (POOH)

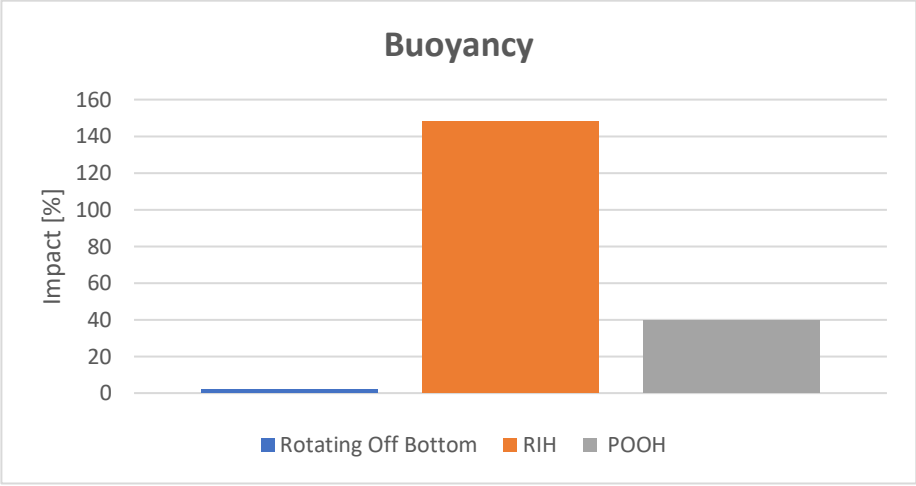

Figure 4.22 Effect of Buoyancy by operation

Figure 4.17 exposed the hook load and effective tension for the bottom of the string, therefore a continuous calculation of these two parameters, RIH and POOH, through the depth of the well is needed as the following regarding to buoyancy.

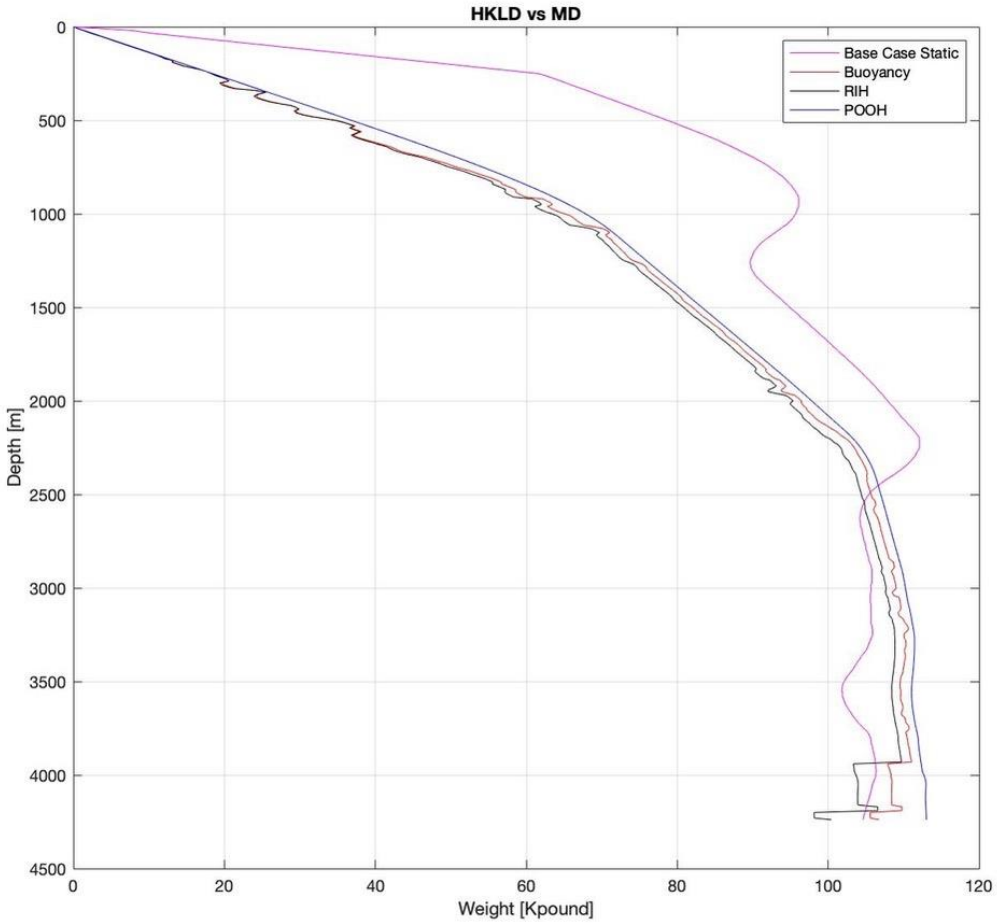

Figure 4.23 Effect buoyancy by operation

According to table 4.9 the impact of the buoyancy comparing with the base case is quite small with respect to static condition, 2,03 [%], and large when RIH and POOH.

The consecutive table explained the result applied to pressure area force:

Force	Total Hook load measured [Klb]	Base case [Klb]	Impact [%]
Pressure Area	91,818	104,6	12,22
Pressure Area RIH	85,80	40,5	111,85
Pressure Area POOH	98,126	186,7	47,44

Table 4.10 Hook load at bottom of the string for each operation under Pressure Area force

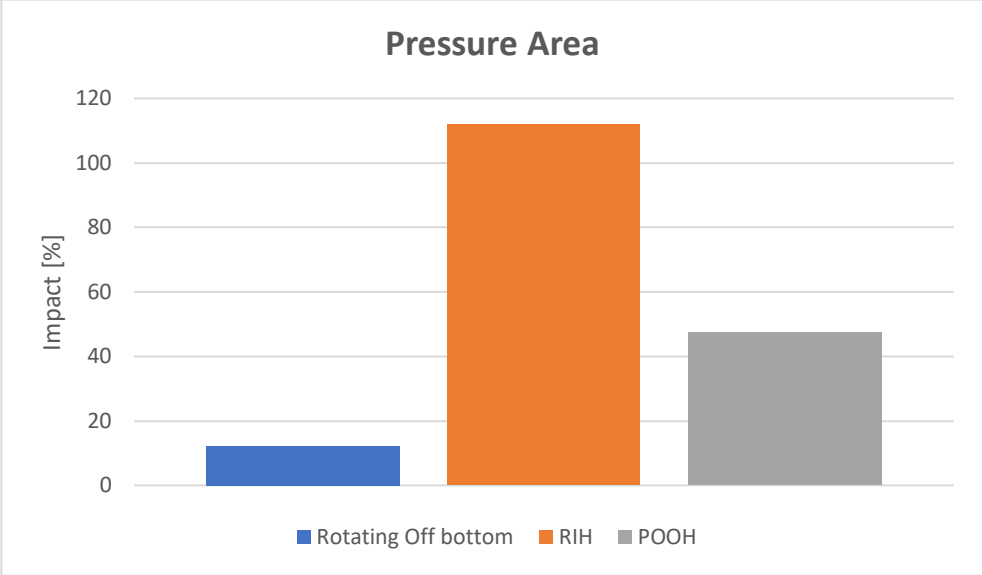

Figure 4.24 Effect of pressure area

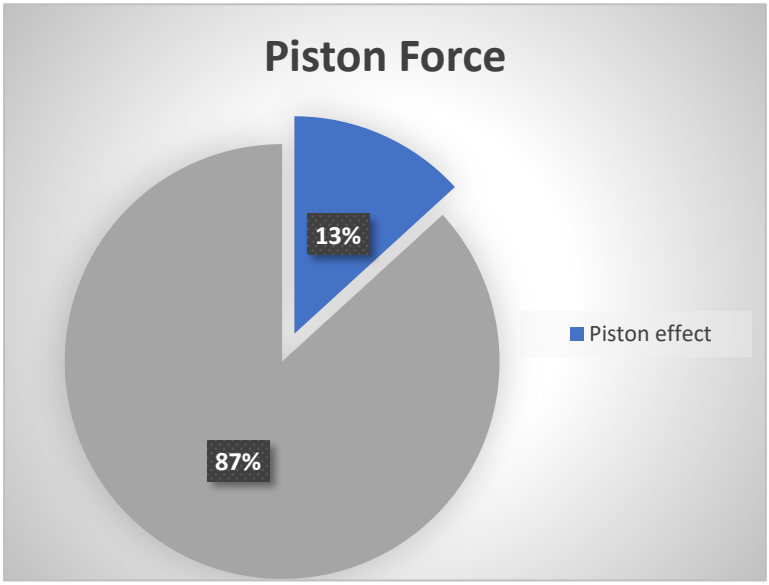

Figure 4.25 Effect of pressure area by operation

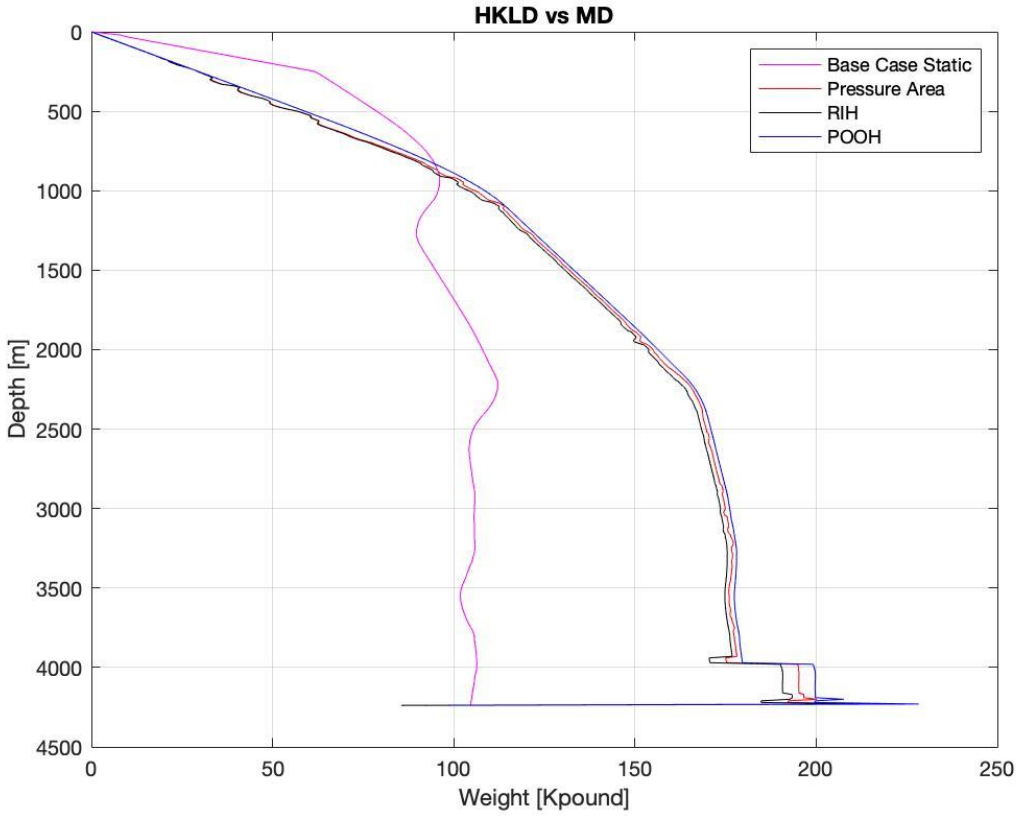

Figure 4.26 Effect buoyancy by operation through the well

Since inertial force is in function of dog leg severity (DLS) and at total depth the well is completely horizontal; inclination = 89,9 [degrees] and DLS = 0, which indicates that inertial force effect will become 0 [%]

Force	Total Hook load measured [Klb]	Base case [Klb]	Impact [%]
Inertial	104,6	104,6	0
Inertial at 600 m	59,089	85,6	30,97
Inertial RIH	98,291	40,5	142,69
Inertial POOH	110,908	186,7	40,59

Table 4.11 Hook load at bottom of the string for each operation under Inertial force

For this reason, Figure 4.25 displays the effect of inertial force through the measured depth and the highest impact is seen at 600 [m] depth. This value is included in the above table

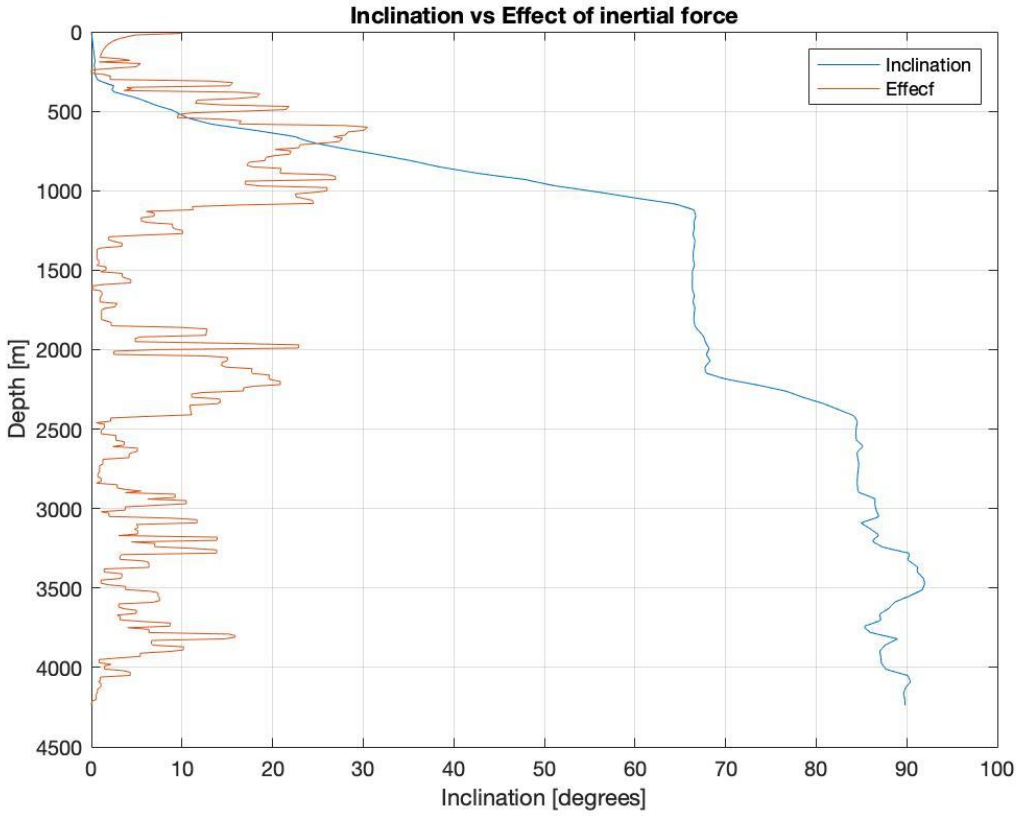

Figure 4.27 Effect of inertial force by operation through the well

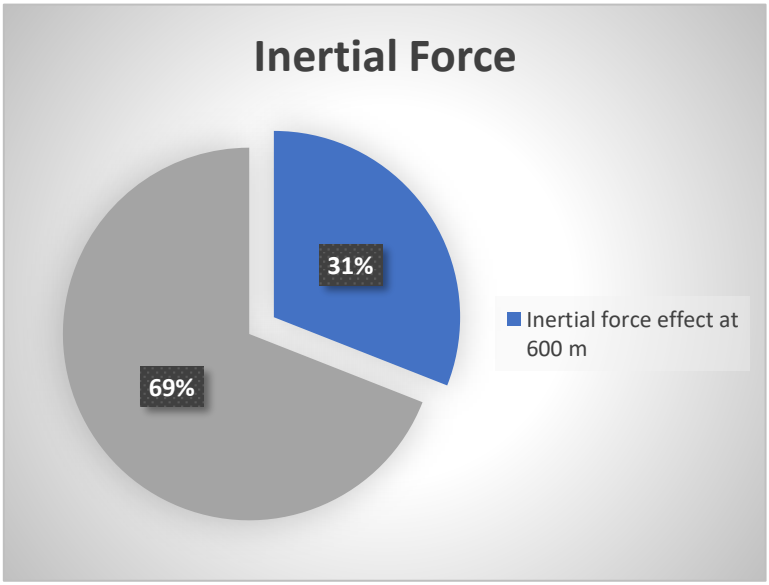

Figure 4.28 Effect of inertial force at 600 m

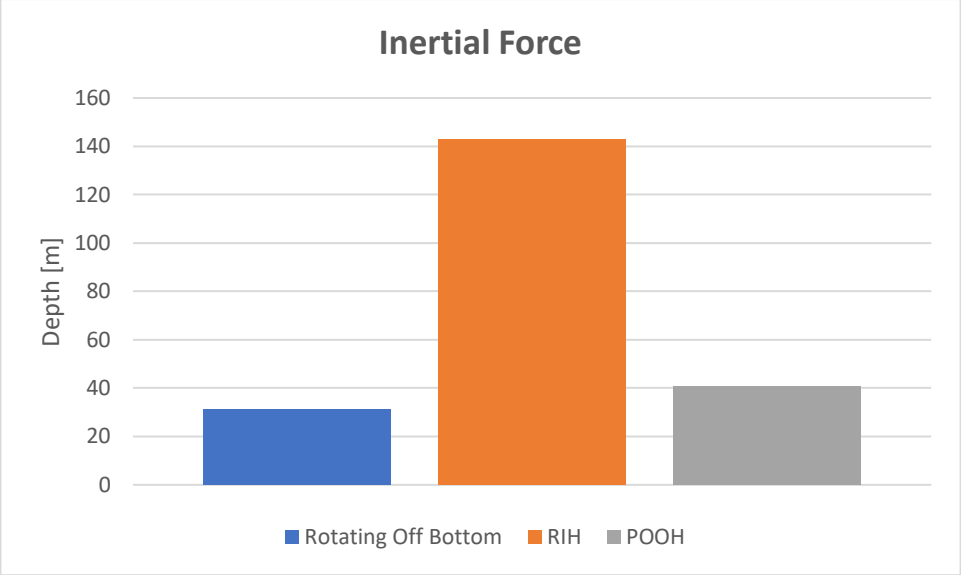

Figure 4.29 Inertial force in drag scenario

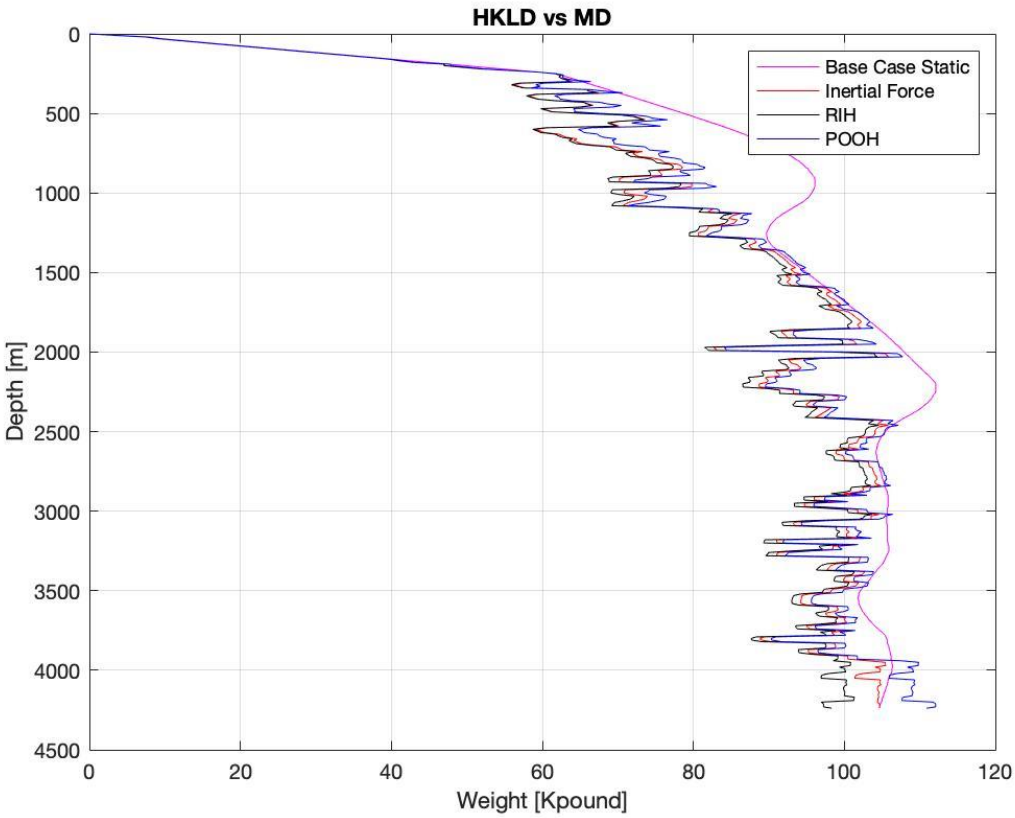

Figure 4.30 Effect of inertial force profile

Viscous force is directly proportional to pressure drop, then in order to find pressure drop, and flow regime, flow velocity is a key part of the process. Therefore, while tripping in the effective velocities through the annuli. Since the fluid is moving upward in the annulus and for running into the hole (RIH), string is moving downwards the friction is higher. When

pulling out of the hole drilling fluid is motioning in the same direction as the pipe, then the change in hook load would be lesser considering small friction [8]

Force	Total Hook load measured [Klb]	Base case [Klb]	Impact [%]
Viscous	88,034	104,6	15,83
Viscous RIH	81,725	40,5	101,79
Viscous POOH	94,343	186,7	49,47

Table 4.12 Hook load at bottom of the string for each operation under viscous force

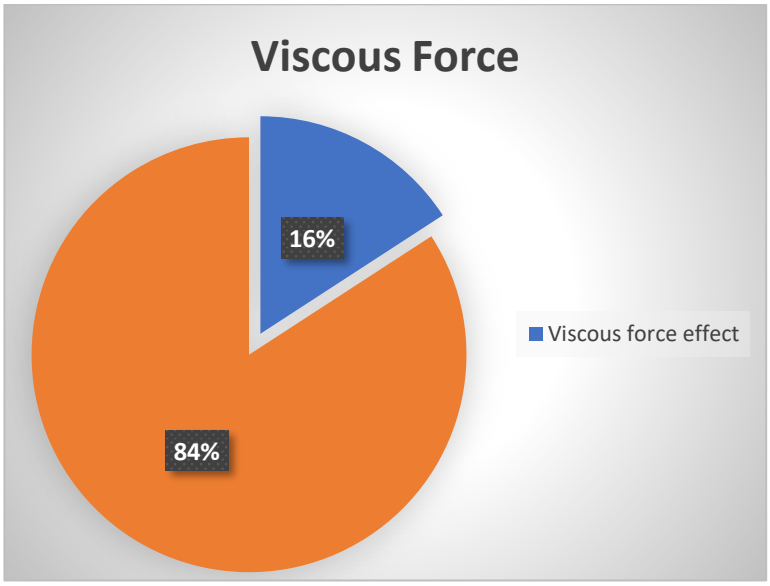

Figure 4.31 Effect of viscous force in percentage

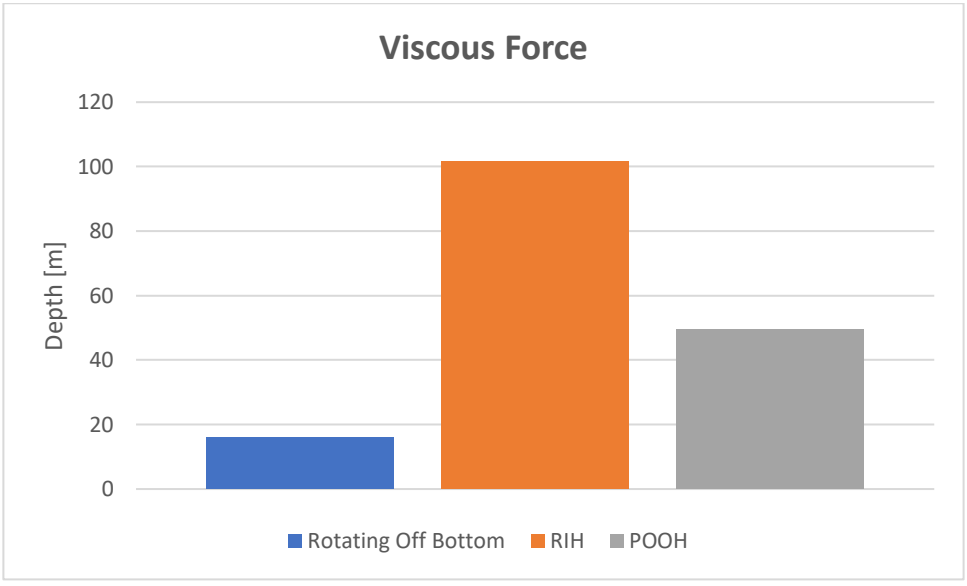

Figure 4.32 Effect of viscous force by operation

At surface a negative hook load is registered which means an excessive weight loss since the effect of travel block weight is neglected.

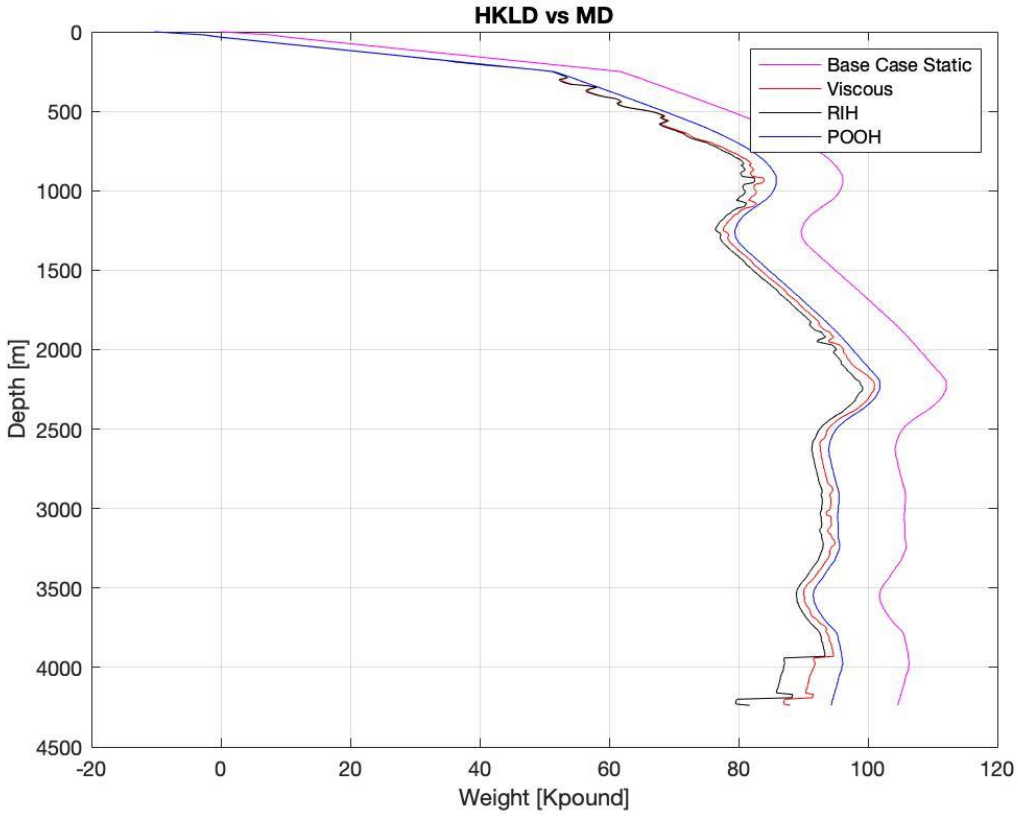

Figure 4.33 Viscous force through measured depth

Force	Total Hook load measured [Klb]	Base case [Klb]	Impact [%]
Combined	81,725	104,6	21,86
Combined RIH	75,417	40,5	86,21
Combined POOH	88,034	186,7	52,84

Table 4.13 Hook load at bottom of the string for each operation with forces combined

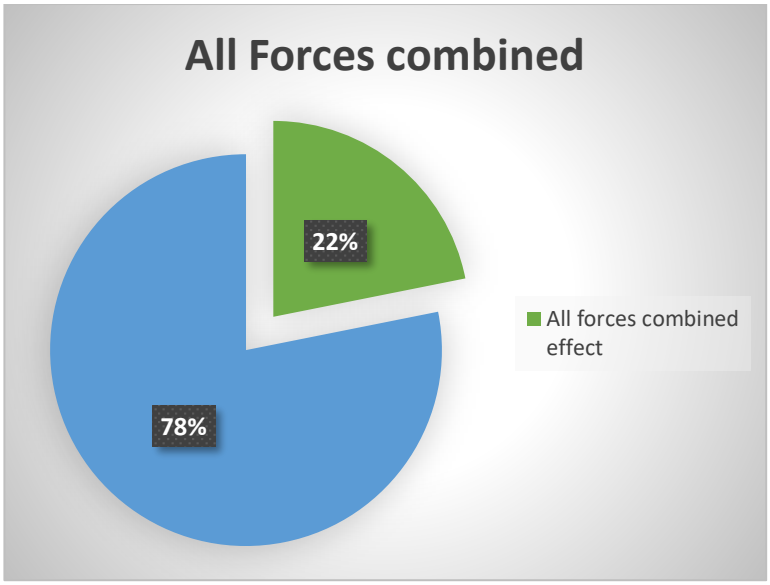

Figure 4.34 Effect of all forces combined as percentage

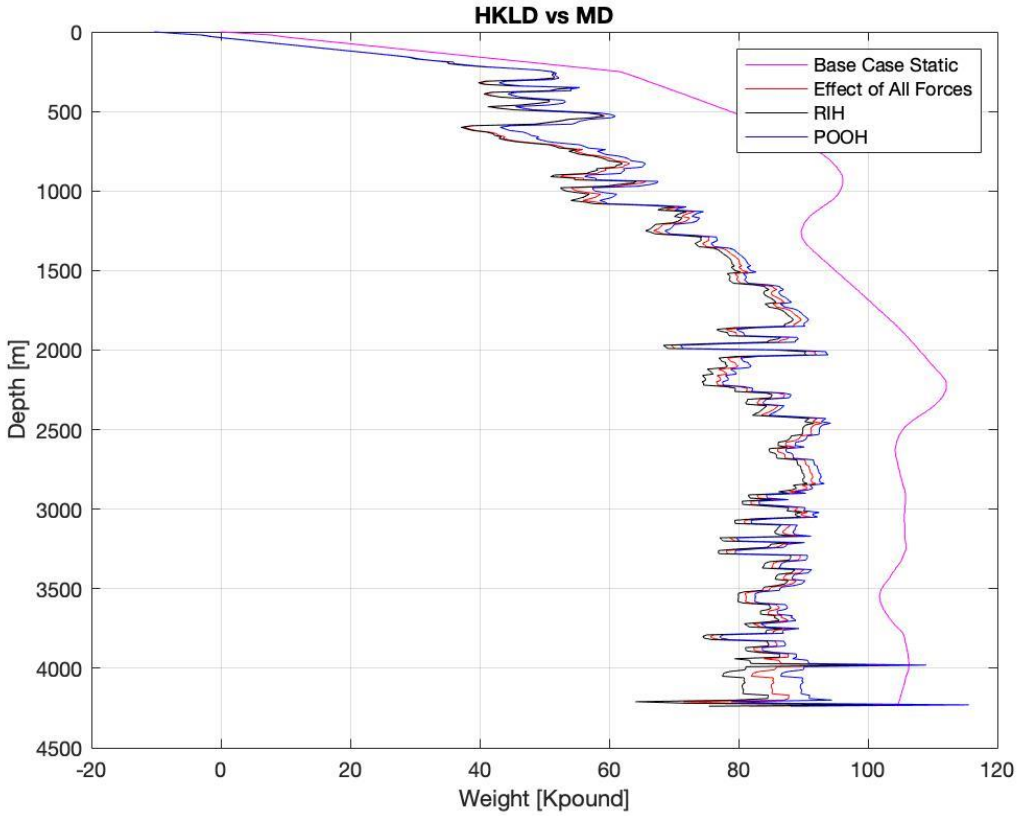

Figure 4.35 Effect of all forces in the hook load combined through measured depth

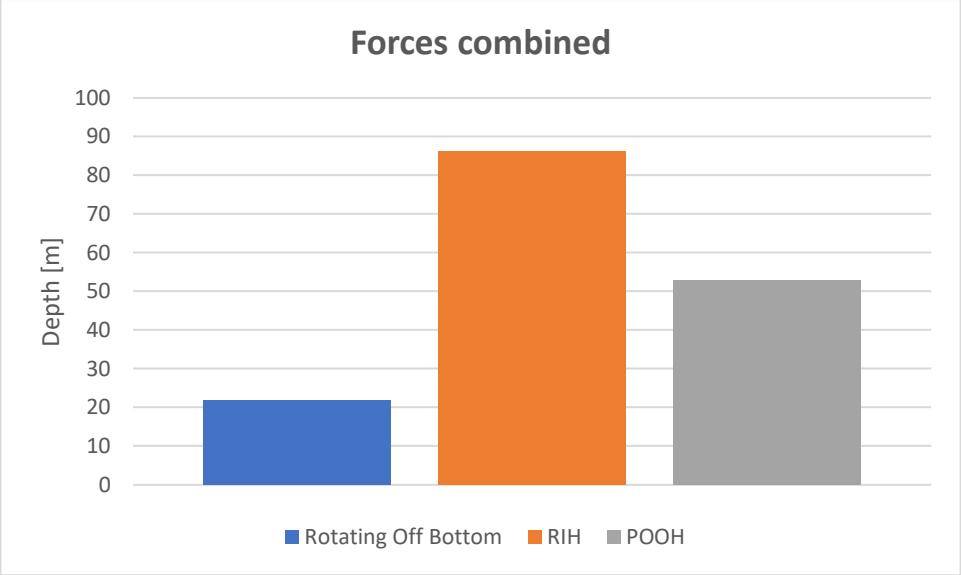

Figure 4.36 Effect of viscous force by operation

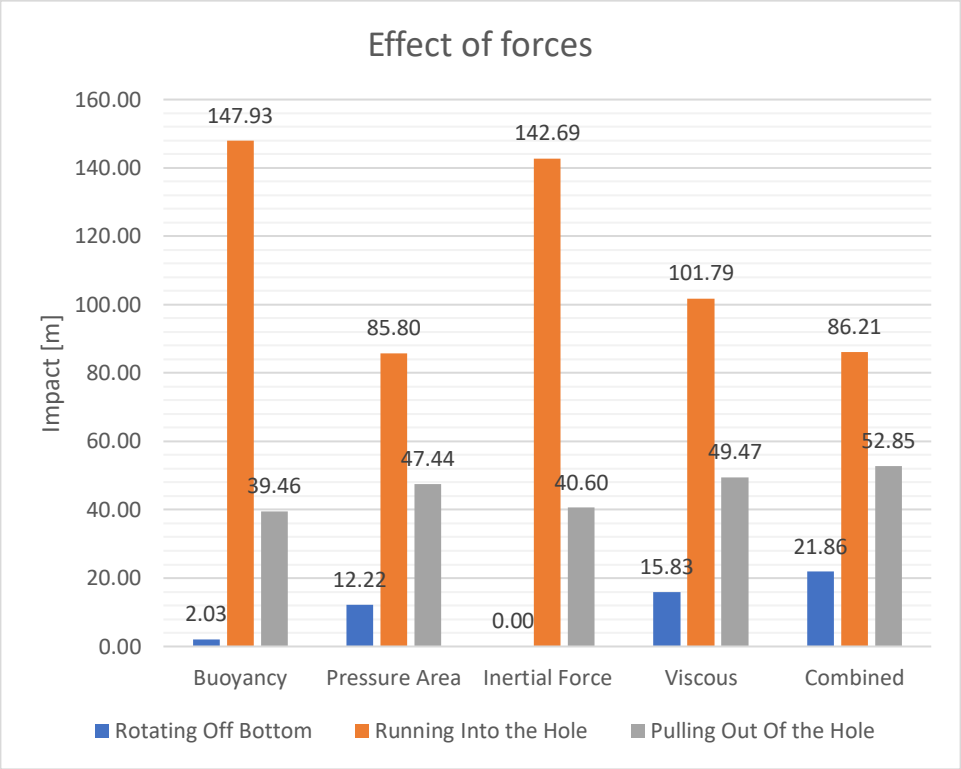

Figure 4.37 Overview of the action of all forces by operation

The differences beyond that 100 [%] specially in Running into the hole can be attributed to not considering the effect of additional side force due to increased contact between the wellbore and the string.

Chapter 4.5.1 Validation of the model

In order to have some scientific support and calibrate the accuracy of the Matlab code programmed within this master thesis project. The true reference of hook load both for static and dynamic is the value find it in WellPlan™.

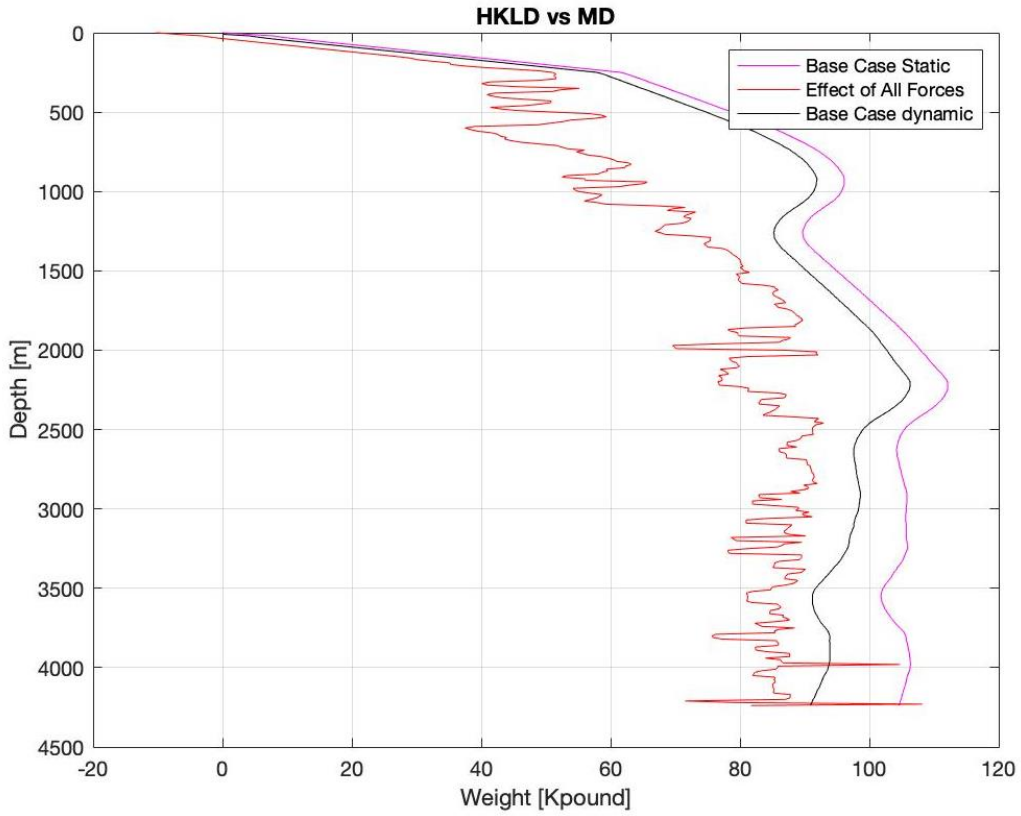

Figure 4.38 Action of all forces respect to Dynamic base case

Force	Total Hook load measured [Klb]	Base case dynamic [Klb]	Error [%]
Combined all forces	81,725	90,9	10,01
Viscous	88,034	90,9	3,15

Table 4.14 Error from Matlab with WellPlan™

Comparing values of hook load obtained from the Matlab code with WellPlan™ is possible to conclude that results from the code are quite accurate also that base case for dynamic condition is mostly governed by the action of viscous forces.

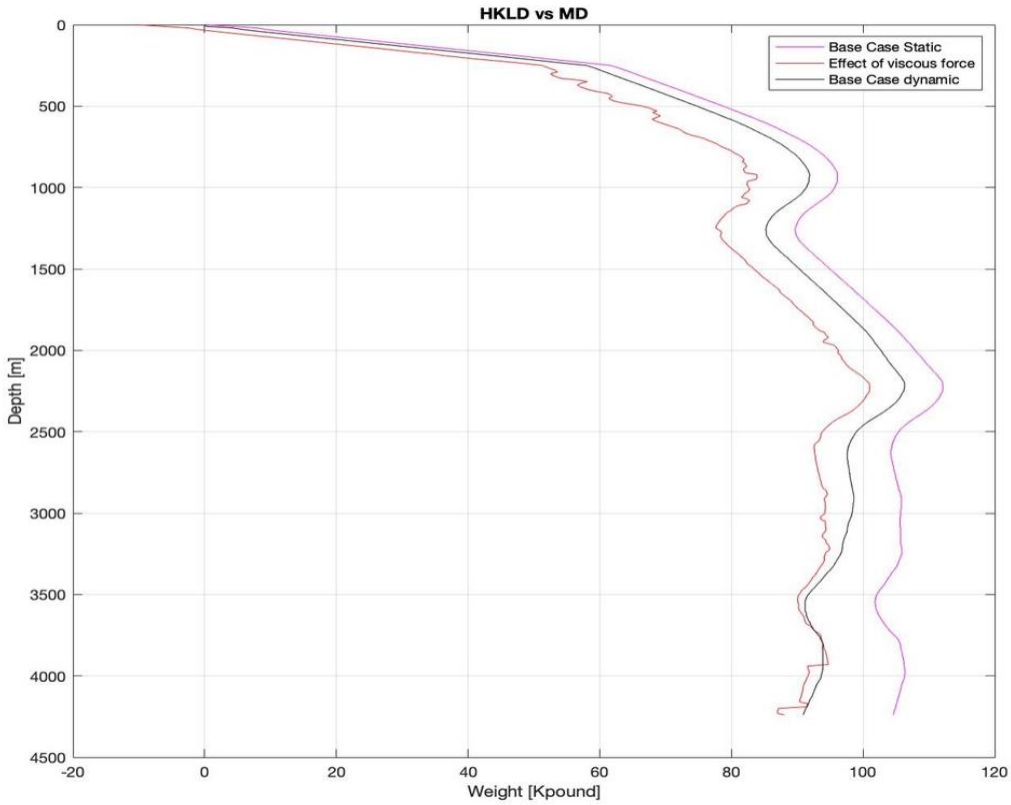

Figure 4.39 Action of viscous forces respect to Dynamic base case

Chapter 4.6 Sensitivity analysis

In a normal drilling operation, some parameter might be dynamic. Pump rate for example will vary depending on the necessity of the process and for controlling undesirable inflow conditions. The base case at which all the calculations were performed had a constant pump rate of 792,5 [gpm] / 3000 [lpm].

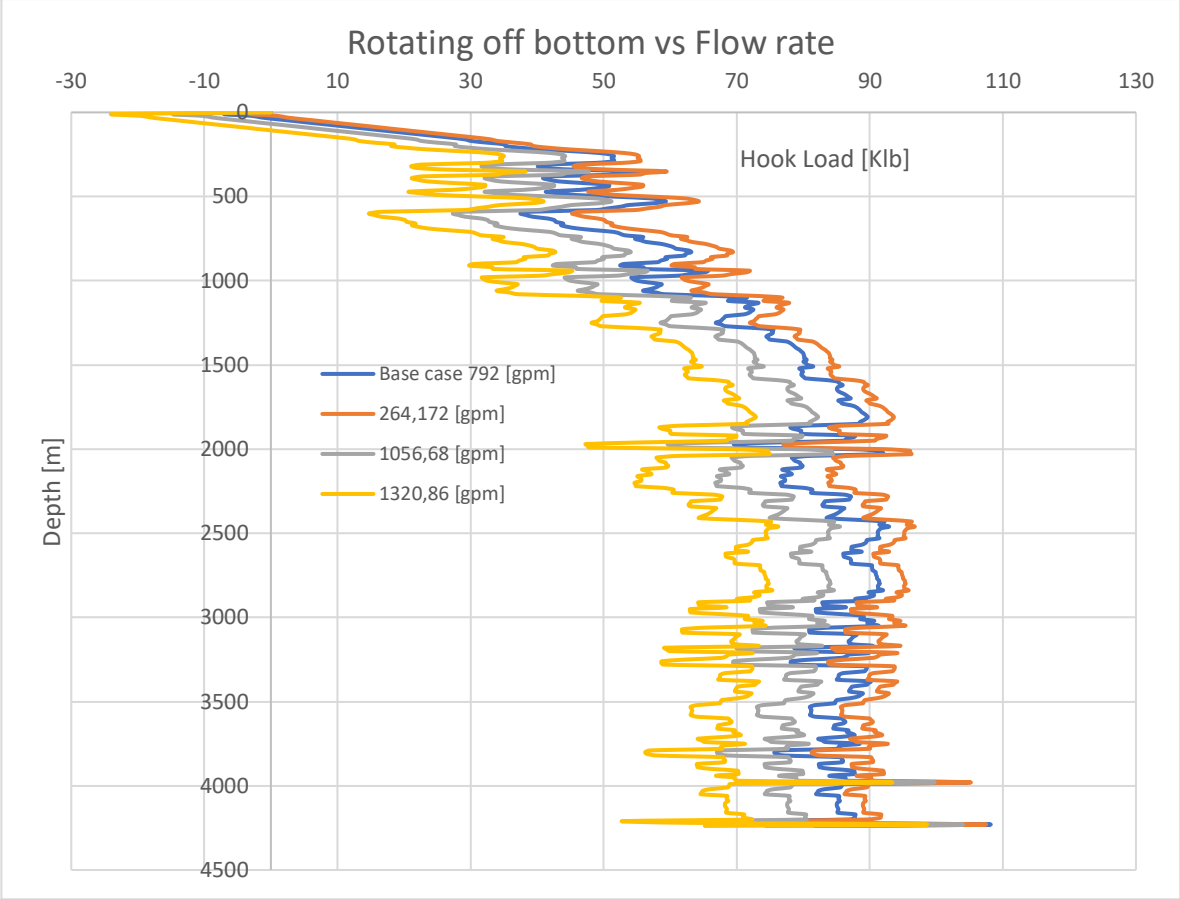

Figure 4.40 Hook load with flow rate variation

As can be seen there is an inverse proportionality among pump rate and hook load, can be denoted that the more flow rate the more velocity both pipe and annulus, which lead to an increase in the wall shear stress and thus in the viscous force as well in the pressure area force. According to $Eq.\,3.45$ Inertial force has also a contrary connection with flow velocity, the effect of increasing flow rate will cause a diminish in the hook load.

Flow rate [gpm]	Total Hook load measured [Klb]	Buoyant weight [Klb]	Impact [%]
264,17 / 1000 [lpm]	85,48	104,6	18,27
1056,69 / 4000 [lpm]	65,21	104,6	37,65
1320,86 / 5000 [lpm]	86,267	104,6	17,53

Table 4.15 Hook load at bottom of the string with flow rate variation

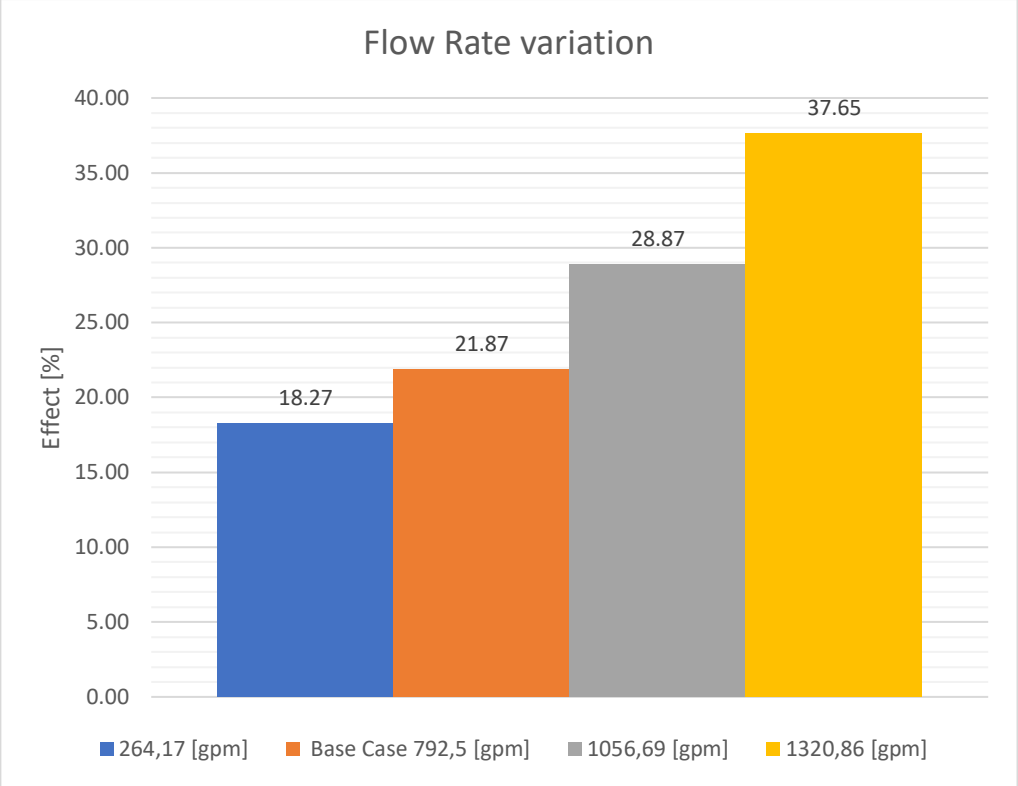

Figure 4.41 Effect of the flow rate in Hook load

Mud weight is another of the properties that usually are modified lean on the formations the well is going through or in case of any type of kick. Having a fixed pump rate of 792,5 [gpm]. For that case, if a gas bubble is going inside the borehole drilling fluid density will decrease, therefore Buoyancy factor will be closer to 1, density is directly related to Reynolds number, which provokes more turbulent fluid in the hole then more pressure drops.

Density [ppg]	Total Hook load measured [Klb]	Buoyant weight [Klb]	Impact [%]
9,8	82,598	104,6	21,03
12,495	80,320	104,6	23,21
13	79,895	104,6	23,62

Table 4.16 Hook load at bottom of the string with flow rate variation

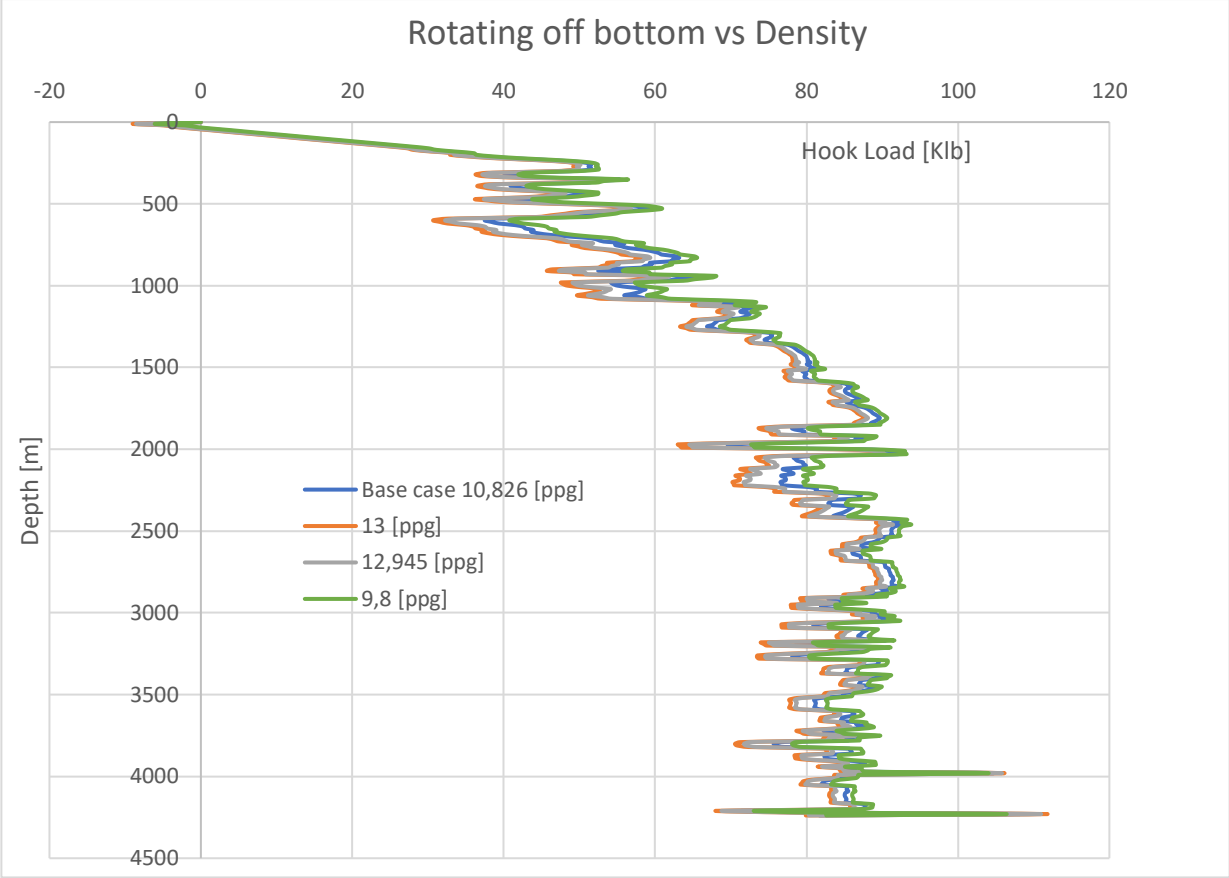

Figure 4.42 Hook load with density variation

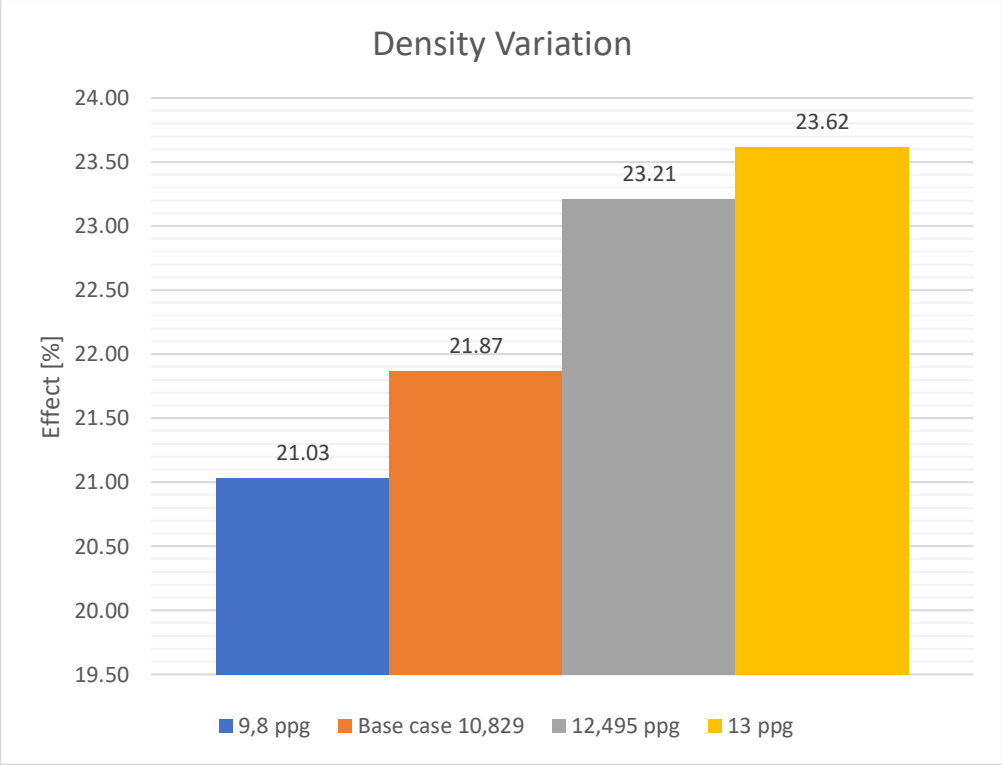

Figure 4.43 Effect of the density in Hook load

Chapter 5: Conclusion and Recommendations

Chapter 5.1 Conclusions

The main scope of this work was bringing into the spotlight the importance of considering fluid forces into the measurement of hook load in surface within drilling operations. The work developed in this master thesis was supervised by MHWirth. The company always was source of support in case of uncertainties and help to improve the process.

- Inertial effects should be neglected, for cases where the well land into the formation with a 90 degrees angle of inclination. However, when the build-up section is drilled, inertial force has a large impact and should be accounted for hook load corrections.
- The combined effect of the four forces is about 21,86 [%] but those that have more effect on the hook load are pressure area and viscous force, therefore as a result, when sensibility examination was presented, flow rate and density have a direct proportion influence in the impact of the hook load. Since these two parameters are mostly variable in the drilling lifecycle, it is crucial to include them in correction factors.
- One of the main purposes of the master thesis was develop a code that was able to accurately predict the behaviour of the drilling fluid regarding flow regime and pressure losses both inside and in the annuli space. Merging Herschel-Bulkley rheological model with other authors frictional Darcy factor. For this reason, the results gotten from the code are validated by WellPlan™ showing significant outcomes.
- The maximum impact into the torque and drag model is seen when running into the hole since the direction of the string is creating more differences in effective velocity, which will increase, pressure losses, the hydraulic force in the change of area also shear wall stress and therefore viscous drag force effect.
- The application of this study can be focused in optimizing of BHA design in order to avoid abruptly changes of diameter which can exceed high pull capacities of the drilling rig.

Chapter 5.2 Recommendations for future work

The concepts developed in this master thesis represent an enhancement for torque and drag knowledge, more precisely in hook load calculation, which still represents an uncertainty aspect to measure in well operations. Consequently, the contribution made in this work would help to relief the uncertainty in the hook load indirect measurement and leave doors open for future assemblies with torque and drag models that want to have an integral inspection of the forces in the wellbore during drilling, cleaning and tripping scenarios.

Possible improvements can be handled e.g. developing a more complex drilling fluid density model that includes cutting transport and redefine how it would affect the hook load. In addition, the settlement of possible undesired scenarios such a reservoir kicks, differential sticking and fluid losses.

Bibliography

[1] Aadnoy, B.S. (2006): *Mechanics of Drilling,* Shaker Verlag. Aachen, 2006, ISBN 3-8322-4861-7

[2] Aadnoy, B. S., Kaarstad, E., et al. (2006). *Theory and application of buoyancy in wells.* In IADC/SPE Asia Pacific Drilling Technology Conference and

[3] Sparks, C. P. "*Fundamentals of marine riser mechanics basic principles and simplified analyses*", PennWell Corporation, 2004. ProQuest Central, http//ebookcentral.proquest.com/lib/uisbib/detail.action?docID=3385148.

[4] Kutasov, I.M.: "*Empirical Correlation Determines Downhole Mud Density*" *Oil & Gas J.* (Dec. 22, 1988) Pag 61-63

[5]Sui, D., & Martinez Viadur, J. C. Automated Characterizacion of Non Newtonian Fluids Using Laboratory Setup . *Walter de Grutyer and Journals*.

[6] Cayeux, E., Skadsem, H. J., Daireaux, B., & Holand, R. (2017, March 14). "*Challenges and Solutions to the Correct Interpretation of Drilling Friction Tests"*. Society of Petroleum Engineers. doi:10.2118/184657-MS

[7] Samuel, R., & Kumar, A. (2012, January 1). "*Effective Force and True Force: What are They?"* Society of Petroleum Engineers. doi:10.2118/151407-MS

[8]. Babu, D. R. (1993, January 1). "*Effects Of P-p-T Behaviour Of Muds On Static Pressures During Deep Well Drilling - Part 1: P-p-7 Behaviour*". Society of Petroleum Engineers.

[9] Azar, J. J., & Samuel, G. R. (2007). *Drilling Engineering.* Tulsa: PennWell Corporation

[10] Busterud, J., *"Slipforming – Materials effect on friction",* Master Thesis, Stavanger, University of Stavanger, 2016.

[11] Douglas, J. F., Gasiorek, J. M., Swaffield, J. A., & Jack, L. B. (2005). *Fluid Mechanics* (5th ed.), Pages 115-130, Harlow: Pearson Education Limited.

[12]. Mme, U., Skalle, P., Johansen, S.T. et al. 2012. *Analysis and modeling of normal hook load response during tripping operations*. Technical report, Norwegian University of Science and Technology (NTNU), Norway (unpublished).

[13]. Kristensen, Edvin, *Model of Hook Load During Tripping Operation, Norwegian University of Science and Technology*, Master Thesis. Norwegian University of Science and Technology, Department of Petroleum Engineering and Applied Geophysics.

[14] Adzokpe, J., "*Hook-load Measurements made with a Draw-works as a function of sensor placement and Dynamic Conditions"* Master Thesis, Stavanger, University of Stavanger, 2014.

[15] Determination of True Hook Load and Line Tension Under Dynamic Conditions by G.R. Luke, SPE, and H.C. Juvkam-Wold, SPE, Texas A&M U.

[16] Hashmi, M., *"Sensitivity analysis of factors affecting torque"* Master Thesis, Stavanger, University of Stavanger, 2014.

[17] Gao Baokui , Ren Jingwei, The Analysis of fluid pressure impact on string force and deformation in oil and gas wells.

[18] Mi-Swaco (2006). Introduction & Rheology and Hydraulics. In Mi-Swaco, "*Drilling Fluids Engineering Manal"* (Vol 2.1, pp. 1.12-1.13). United States of America, United States of America: Mi-Swaco.

[19]. Eric, C., Skadsem, H. J., & Kluge, R. (2015, March 17). *Accuracy and Correction of Hook Load Measurements During Drilling Operations*. Society of Petroleum Engineers. doi:10.2118/173035-MS

[20] Mirhaj, A., *"Torque and Drag Modeling in Long-Reach Wellbores"* Doctorate Thesis, Stavanger, University of Stavanger, 2019.

[21]. Bourgoyne , A. T., Millheim, K., Chenevert, E. M., & Young, J. F. (1991). *Applied Drilling Engineering.* Richardson, Texas, United States Of America.

[22] Landivar M., "*The Physics of Buoyancy, Effective Tension and Pinching-off Effect"* Master Thesis, Stavanger, University of Stavanger, 2018.

23. Madlener. K, Frey. B. & Ciezki H.K. "*Generalized Reynolds number for non-newtonian fluids"*

[24]. Schlumberger, *Schlumberger Glossary,* 2020. Available https://www.glossary.oilfield.slb.com/. Accessed on: 24 May 2020.

[25] Romero, S. (2020, 05 24). *LinkedIn*. Retrieved from https://www.linkedin.com/pulse/understanding-torque-drag-concepts-analysis-sixto-romero

[26] Taboada, J., "*Well Engineering Simulation (WellPlan™) Challenges and uncertainties in Drilling Engineering",* Master Thesis, Stavanger; University of Stavanger, 2014.

Appendix

Appendix 1: Input data

MD (m)	Inclination (Degree)	Azimuth (Degree)	TVD (m)	DLS [degree/100m]
0	0	0	0	0
10	0,02	277,23	10	0,02
20	0,04	277,23	20	0,02
30	0,06	277,23	30	0,02
40	0,09	277,23	40	0,02
50	0,11	277,23	50	0,02
60	0,13	277,23	60	0,02
70	0,15	277,23	70	0,02
80	0,17	277,23	80	0,02
90	0,19	277,23	90	0,02
100	0,21	277,23	100	0,02
110	0,24	277,23	110	0,02
120	0,26	277,23	120	0,02
130	0,28	277,23	130	0,02
140	0,3	277,23	140	0,02
150	0,32	277,23	150	0,02
160	0,34	277,23	160	0,02
170	0,36	267,08	170	0,07
180	0,4	253,49	180	0,1
190	0,41	251,28	190	0,02
200	0,34	269,44	200	0,14
210	0,31	293,29	210	0,14
220	0,35	316,41	220	0,14
230	0,38	325,43	230	0,07
240	0,38	325,43	240	0
250	0,38	325,43	250	0
260	0,38	325,43	260	0
270	0,43	327,25	270	0,05
280	0,5	329,59	280	0,07
290	0,57	331,35	290	0,07
300	0,64	332,73	300	0,07
310	0,96	355,67	309,99	0,45
320	1,43	8,21	319,99	0,54
330	1,95	14,34	329,99	0,54
340	2,47	17,9	339,98	0,54
350	2,4	15,06	349,97	0,14
360	2,3	11,74	359,96	0,16
370	2,3	14,85	369,96	0,13

380	2,58	26,97	379,95	0,59
390	3,24	31,03	389,93	0,69
400	3,91	33,71	399,91	0,69
410	4,59	35,61	409,89	0,69
420	5,19	36,7	419,85	0,61
430	5,64	36,96	429,8	0,45
440	6,1	37,18	439,75	0,45
450	6,55	37,37	449,69	0,45
460	7,01	40,14	459,62	0,57
470	7,55	45,61	469,54	0,87
480	8,14	50,33	479,45	0,87
490	8,78	54,38	489,34	0,87
500	9,17	57,97	499,22	0,68
510	9,47	60,17	509,08	0,46
520	9,83	61,22	518,94	0,4
530	10,19	62,2	528,79	0,4
540	10,55	63,11	538,63	0,4
550	11,13	64,17	548,45	0,61
560	11,8	65,21	558,25	0,71
570	12,49	66,14	568,03	0,71
580	13,17	66,98	577,78	0,71
590	14,29	69,12	587,49	1,23
600	15,53	71,22	597,15	1,35
610	16,78	73,03	606,76	1,35
620	18,05	74,58	616,3	1,35
630	19,16	76,62	625,78	1,28
640	20,28	78,44	635,19	1,28
650	21,42	80,07	644,54	1,28
660	22,47	81,81	653,81	1,23
670	22,93	84,91	663,04	1,28
680	23,44	87,89	672,23	1,28
690	24,02	90,73	681,39	1,28
700	24,7	93,17	690,5	1,21
710	25,57	94,7	699,55	1,09
720	26,46	96,13	708,54	1,09
730	27,36	97,48	717,45	1,09
740	28,32	97,85	726,3	0,97
750	29,33	97,23	735,06	1,06
760	30,35	96,65	743,73	1,06
770	31,37	96,1	752,31	1,06
780	32,35	95,85	760,81	0,98
790	33,29	95,78	769,21	0,94
800	34,23	95,72	777,52	0,94
810	35,17	95,66	785,75	0,94
820	35,99	96,1	793,88	0,86

830	36,78	96,66	801,93	0,85
840	37,57	97,2	809,9	0,85
850	38,4	97,64	817,78	0,88
860	39,45	97,69	825,56	1,04
870	40,49	97,74	833,22	1,04
880	41,53	97,79	840,77	1,04
890	42,58	97,83	848,19	1,04
900	43,88	98,05	855,48	1,31
910	45,21	98,28	862,61	1,35
920	46,55	98,49	869,57	1,35
930	47,89	98,7	876,36	1,35
940	48,71	99	883,01	0,85
950	49,53	99,28	889,56	0,85
960	50,35	99,57	895,99	0,85
970	51,24	99,9	902,31	0,93
980	52,46	100,47	908,49	1,3
990	53,68	101,03	914,5	1,3
1000	54,89	101,57	920,34	1,3
1010	56,08	101,99	926	1,23
1020	57,18	102,22	931,5	1,12
1030	58,28	102,44	936,84	1,12
1040	59,38	102,65	942,02	1,12
1050	60,52	102,89	947,03	1,16
1060	61,7	103,16	951,86	1,2
1070	62,88	103,42	956,51	1,2
1080	64,06	103,68	960,97	1,2
1090	64,84	103,8	965,29	0,79
1100	65,38	103,84	969,49	0,54
1110	65,92	103,87	973,62	0,54
1120	66,45	103,9	977,65	0,54
1130	66,58	103,62	981,64	0,29
1140	66,62	103,26	985,61	0,33
1150	66,67	102,9	989,57	0,33
1160	66,71	102,54	993,53	0,33
1170	66,66	102,82	997,49	0,26
1180	66,6	103,1	1001,46	0,26
1190	66,55	103,38	1005,43	0,26
1200	66,5	103,69	1009,42	0,29
1210	66,52	104,15	1013,4	0,42
1220	66,53	104,6	1017,39	0,42
1230	66,55	105,06	1021,37	0,42
1240	66,55	105,53	1025,35	0,43
1250	66,5	106,04	1029,33	0,47
1260	66,45	106,55	1033,32	0,47
1270	66,41	107,06	1037,32	0,47

1280	66,41	107,34	1041,32	0,26
1290	66,47	107,28	1045,32	0,09
1300	66,54	107,21	1049,31	0,09
1310	66,61	107,14	1053,28	0,09
1320	66,62	107,01	1057,25	0,12
1330	66,59	106,83	1061,22	0,16
1340	66,57	106,65	1065,2	0,16
1350	66,54	106,48	1069,18	0,16
1360	66,51	106,43	1073,16	0,05
1370	66,48	106,43	1077,15	0,03
1380	66,46	106,44	1081,14	0,03
1390	66,43	106,44	1085,13	0,03
1400	66,43	106,41	1089,13	0,03
1410	66,43	106,38	1093,13	0,03
1420	66,43	106,34	1097,13	0,03
1430	66,43	106,31	1101,13	0,03
1440	66,47	106,33	1105,12	0,04
1450	66,51	106,34	1109,11	0,04
1460	66,55	106,36	1113,1	0,04
1470	66,57	106,38	1117,07	0,03
1480	66,5	106,44	1121,06	0,08
1490	66,44	106,5	1125,05	0,08
1500	66,37	106,56	1129,05	0,08
1510	66,33	106,54	1133,06	0,05
1520	66,33	106,36	1137,08	0,17
1530	66,34	106,17	1141,09	0,17
1540	66,34	105,99	1145,1	0,17
1550	66,34	105,78	1149,12	0,19
1560	66,34	105,55	1153,13	0,22
1570	66,33	105,31	1157,15	0,22
1580	66,33	105,08	1161,16	0,22
1590	66,33	105	1165,17	0,07
1600	66,33	105	1169,19	0
1610	66,33	105,01	1173,2	0,01
1620	66,33	105,01	1177,22	0
1630	66,38	105,01	1181,23	0,05
1640	66,44	105	1185,23	0,06
1650	66,5	105	1189,22	0,06
1660	66,56	104,99	1193,21	0,06
1670	66,52	104,96	1197,19	0,05
1680	66,48	104,93	1201,18	0,05
1690	66,44	104,9	1205,17	0,05
1700	66,41	104,85	1209,17	0,05
1710	66,46	104,71	1213,17	0,15
1720	66,52	104,56	1217,16	0,14

1730	66,58	104,42	1221,14	0,14
1740	66,61	104,34	1225,11	0,08
1750	66,59	104,41	1229,08	0,06
1760	66,57	104,47	1233,05	0,06
1770	66,54	104,53	1237,03	0,06
1780	66,53	104,6	1241,01	0,06
1790	66,52	104,66	1245	0,06
1800	66,51	104,72	1248,98	0,06
1810	66,5	104,78	1252,97	0,06
1820	66,52	104,88	1256,96	0,09
1830	66,55	105,01	1260,94	0,12
1840	66,58	105,13	1264,91	0,12
1850	66,61	105,26	1268,89	0,12
1860	66,73	104,68	1272,85	0,54
1870	66,87	103,93	1276,79	0,7
1880	67,02	103,19	1280,7	0,7
1890	67,17	102,44	1284,59	0,7
1900	67,32	101,7	1288,46	0,7
1910	67,48	100,96	1292,3	0,7
1920	67,6	100,66	1296,12	0,3
1930	67,65	100,94	1299,93	0,27
1940	67,71	101,22	1303,73	0,27
1950	67,77	101,5	1307,52	0,27
1960	67,85	102,41	1311,29	0,85
1970	67,94	103,79	1315,06	1,29
1980	68,05	105,18	1318,8	1,29
1990	68,17	106,55	1322,53	1,29
2000	68,14	107,01	1326,25	0,42
2010	68,06	107,13	1329,98	0,14
2020	67,97	107,26	1333,73	0,14
2030	67,89	107,38	1337,48	0,14
2040	67,97	106,61	1341,24	0,72
2050	68,08	105,69	1344,98	0,86
2060	68,19	104,77	1348,71	0,86
2070	68,31	103,85	1352,41	0,86
2080	68,16	102,98	1356,12	0,83
2090	68,01	102,1	1359,85	0,83
2100	67,86	101,22	1363,61	0,83
2110	67,74	100,31	1367,39	0,86
2120	67,75	99,19	1371,18	1,03
2130	67,76	98,08	1374,96	1,03
2140	67,78	96,97	1378,75	1,03
2150	67,98	95,87	1382,51	1,04
2160	68,54	94,79	1386,22	1,15
2170	69,1	93,71	1389,83	1,15

2180	69,68	92,64	1393,35	1,15
2190	70,44	91,7	1396,76	1,17
2200	71,38	90,87	1400,03	1,23
2210	72,33	90,05	1403,14	1,23
2220	73,29	89,24	1406,1	1,23
2230	74,14	88,57	1408,9	1,06
2240	74,94	87,98	1411,57	0,99
2250	75,75	87,39	1414,1	0,99
2260	76,55	86,81	1416,49	0,99
2270	77,1	86,32	1418,77	0,72
2280	77,58	85,88	1420,96	0,65
2290	78,05	85,43	1423,08	0,65
2300	78,53	84,98	1425,11	0,65
2310	79,1	84,38	1427,05	0,83
2320	79,68	83,76	1428,89	0,83
2330	80,26	83,16	1430,63	0,83
2340	80,82	82,57	1432,27	0,81
2350	81,26	82,12	1433,83	0,63
2360	81,7	81,67	1435,31	0,63
2370	82,15	81,22	1436,72	0,63
2380	82,59	80,77	1438,04	0,63
2390	83,03	80,32	1439,3	0,63
2400	83,48	79,88	1440,47	0,63
2410	83,92	79,43	1441,57	0,63
2420	84,21	79,22	1442,6	0,36
2430	84,31	79,28	1443,6	0,12
2440	84,42	79,35	1444,58	0,12
2450	84,52	79,41	1445,55	0,12
2460	84,54	79,39	1446,5	0,03
2470	84,5	79,32	1447,46	0,08
2480	84,47	79,24	1448,42	0,08
2490	84,43	79,17	1449,39	0,08
2500	84,41	79,1	1450,36	0,07
2510	84,41	79,04	1451,33	0,06
2520	84,4	78,98	1452,31	0,06
2530	84,39	78,91	1453,28	0,06
2540	84,4	78,77	1454,26	0,15
2550	84,41	78,61	1455,24	0,15
2560	84,43	78,46	1456,21	0,15
2570	84,45	78,31	1457,18	0,15
2580	84,65	78,29	1458,13	0,2
2590	84,84	78,26	1459,04	0,2
2600	85,04	78,24	1459,92	0,2
2610	85,15	78,17	1460,78	0,13
2620	84,97	77,95	1461,64	0,28

2630	84,79	77,73	1462,53	0,28
2640	84,61	77,51	1463,46	0,28
2650	84,51	77,29	1464,41	0,24
2660	84,53	77,06	1465,36	0,23
2670	84,56	76,83	1466,31	0,23
2680	84,58	76,6	1467,26	0,23
2690	84,61	76,54	1468,2	0,07
2700	84,64	76,6	1469,14	0,07
2710	84,67	76,66	1470,07	0,07
2720	84,7	76,72	1471	0,07
2730	84,69	76,77	1471,92	0,05
2740	84,67	76,82	1472,85	0,05
2750	84,65	76,87	1473,78	0,05
2760	84,62	76,91	1474,71	0,05
2770	84,61	76,95	1475,65	0,05
2780	84,59	77	1476,59	0,04
2790	84,58	77,04	1477,54	0,04
2800	84,56	77,08	1478,48	0,04
2810	84,55	77,14	1479,43	0,06
2820	84,54	77,19	1480,38	0,06
2830	84,54	77,25	1481,33	0,06
2840	84,53	77,28	1482,28	0,03
2850	84,55	77,12	1483,24	0,16
2860	84,56	76,96	1484,19	0,16
2870	84,58	76,79	1485,13	0,16
2880	84,59	76,59	1486,07	0,21
2890	84,61	76,28	1487,02	0,31
2900	84,77	76,15	1487,94	0,21
2910	85,24	76,4	1488,81	0,52
2920	85,7	76,65	1489,6	0,52
2930	86,16	76,89	1490,31	0,52
2940	86,51	76,94	1490,95	0,35
2950	86,5	76,35	1491,56	0,59
2960	86,49	75,77	1492,17	0,59
2970	86,48	75,18	1492,79	0,59
2980	86,5	74,79	1493,4	0,39
2990	86,55	74,58	1494	0,21
3000	86,59	74,37	1494,6	0,21
3010	86,64	74,16	1495,19	0,21
3020	86,7	74,16	1495,77	0,06
3030	86,78	74,24	1496,34	0,11
3040	86,85	74,33	1496,9	0,11
3050	86,92	74,41	1497,44	0,11
3060	86,54	74,72	1498,01	0,49
3070	86	75,11	1498,66	0,66

3080	85,47	75,5	1499,41	0,66
3090	84,94	75,89	1500,24	0,66
3100	85,21	75,82	1501,1	0,28
3110	85,48	75,75	1501,91	0,29
3120	85,76	75,67	1502,67	0,29
3130	86,04	75,64	1503,39	0,27
3140	86,28	75,8	1504,06	0,29
3150	86,53	75,96	1504,69	0,29
3160	86,77	76,12	1505,27	0,29
3170	86,88	75,99	1505,83	0,17
3180	86,67	75,23	1506,39	0,79
3190	86,46	74,47	1506,99	0,79
3200	86,26	73,7	1507,62	0,79
3210	86,32	73,46	1508,27	0,25
3220	86,63	73,71	1508,88	0,4
3230	86,94	73,96	1509,44	0,4
3240	87,25	74,21	1509,95	0,4
3250	87,86	74,37	1510,38	0,63
3260	88,64	74,48	1510,68	0,79
3270	89,42	74,59	1510,85	0,79
3280	90,2	74,71	1510,89	0,79
3290	90,31	74,86	1510,84	0,19
3300	90,24	75,02	1510,79	0,18
3310	90,16	75,19	1510,76	0,18
3320	90,09	75,35	1510,74	0,18
3330	90,29	75,61	1510,7	0,33
3340	90,52	75,88	1510,63	0,36
3350	90,76	76,16	1510,52	0,36
3360	91	76,43	1510,37	0,36
3370	91,23	76,7	1510,17	0,36
3380	91,18	76,63	1509,96	0,08
3390	91,14	76,56	1509,76	0,08
3400	91,18	76,49	1509,56	0,08
3410	91,35	76,4	1509,34	0,19
3420	91,52	76,31	1509,09	0,19
3430	91,69	76,22	1508,81	0,19
3440	91,85	76,14	1508,5	0,18
3450	91,89	76,09	1508,17	0,06
3460	91,93	76,04	1507,84	0,06
3470	91,97	75,99	1507,49	0,06
3480	91,94	76,09	1507,15	0,11
3490	91,87	76,29	1506,82	0,21
3500	91,8	76,48	1506,5	0,21
3510	91,72	76,68	1506,19	0,21
3520	91,41	76,86	1505,92	0,36

3530	91,04	77,03	1505,7	0,41
3540	90,67	77,2	1505,55	0,41
3550	90,3	77,37	1505,47	0,41
3560	89,88	77,43	1505,45	0,42
3570	89,46	77,48	1505,51	0,42
3580	89,04	77,54	1505,64	0,42
3590	88,66	77,57	1505,84	0,38
3600	88,5	77,52	1506,09	0,17
3610	88,33	77,47	1506,37	0,17
3620	88,16	77,42	1506,67	0,17
3630	87,97	77,37	1507,01	0,2
3640	87,69	77,34	1507,39	0,28
3650	87,41	77,31	1507,82	0,28
3660	87,13	77,28	1508,29	0,28
3670	87	77,17	1508,81	0,16
3680	87,05	76,99	1509,33	0,18
3690	87,09	76,82	1509,84	0,18
3700	87,13	76,64	1510,34	0,18
3710	86,84	76,55	1510,87	0,31
3720	86,34	76,52	1511,46	0,5
3730	85,84	76,48	1512,15	0,5
3740	85,34	76,45	1512,92	0,5
3750	85,37	76,68	1513,72	0,23
3760	85,57	76,99	1514,51	0,37
3770	85,77	77,31	1515,27	0,37
3780	85,98	77,62	1515,99	0,37
3790	86,71	78,11	1516,63	0,89
3800	87,49	78,62	1517,13	0,93
3810	88,26	79,13	1517,5	0,93
3820	88,98	79,6	1517,74	0,86
3830	88,63	79,44	1517,95	0,39
3840	88,27	79,28	1518,22	0,39
3850	87,92	79,11	1518,55	0,39
3860	87,6	78,88	1518,94	0,4
3870	87,44	78,3	1519,38	0,6
3880	87,28	77,73	1519,84	0,6
3890	87,12	77,15	1520,32	0,6
3900	87,03	76,66	1520,83	0,5
3910	87,06	76,34	1521,35	0,32
3920	87,09	76,02	1521,86	0,32
3930	87,12	75,7	1522,36	0,32
3940	87,15	75,52	1522,86	0,18
3950	87,16	75,47	1523,36	0,05
3960	87,18	75,43	1523,85	0,05
3970	87,19	75,39	1524,34	0,05

3980	87,29	75,48	1524,82	0,13
3990	87,42	75,65	1525,29	0,22
4000	87,55	75,82	1525,73	0,22
4010	87,68	76	1526,14	0,22
4020	88,21	75,9	1526,5	0,53
4030	88,84	75,74	1526,76	0,65
4040	89,46	75,58	1526,91	0,65
4050	90,09	75,43	1526,95	0,65
4060	90,19	75,54	1526,92	0,15
4070	90,27	75,67	1526,88	0,15
4080	90,36	75,79	1526,83	0,15
4090	90,41	75,89	1526,76	0,12
4100	90,27	75,82	1526,7	0,16
4110	90,12	75,75	1526,67	0,16
4120	89,97	75,68	1526,66	0,16
4130	89,85	75,64	1526,67	0,13
4140	89,78	75,72	1526,71	0,1
4150	89,72	75,79	1526,75	0,1
4160	89,66	75,87	1526,8	0,1
4170	89,65	75,94	1526,86	0,08
4180	89,7	76,02	1526,92	0,08
4190	89,74	76,09	1526,97	0,08
4200	89,79	76,16	1527,01	0,08
4210	89,8	76,18	1527,05	0,03
4220	89,8	76,18	1527,08	0
4230	89,8	76,18	1527,12	0
4238,5	89,8	76,18	1527,15	0

Appendix 2: Matlab code used for calculations

The code also can find it on:

https://github.com/diegopinto93/Fluid-forces-calculation

For calibration of density the Matlab code is the following:

```
function rhol = roliq(pressure,T)

% A simple liquid dens model wich takes into pressure varations vs.
pressure
% is implemented. P0 is the atmosperic pressure. D0 is density at
surface
% conditions

  rou0 = 10.829;%
  T0 = 68;

  beta=-0.0001535;
  alpha=2.7384e-06;
  gamma=-7.469e-07;
```

```
rhol = rou0*exp(alpha*pressure + beta*(T-T0)+gamma*(T-T0)^2 );
```

The code for the force calculations, use inputs from an excel file.

```
clear;
clc;
TVDm= xlsread('BPF.xlsx', 'E4:E428');%Total vertical Depth [m]
TVDft= xlsread('BPF.xlsx', 'F4:F428');%Total vertical Depth [ft]
tgrad= xlsread('BPF.xlsx','J4:J8');%Temperature gradient
md=xlsread('BPF.xlsx', 'A4:A428');%Measured depth [m]
mdft=xlsread('BPF.xlsx', 'B4:B428');%Measured depth [ft]
Inclin=xlsread('BPF.xlsx', 'C4:C428');%Inclination
DLS=xlsread('BPF.xlsx', 'G4:G428');%Dog Leg Severity
z=size(md);
temp=zeros(z);%Temperature vector
tref= 50;% Temperature of reference [C]
Ts=122;%Temperature of reference [F]
Rhopipe= 64.7;
mwref= xlsread('BPF.xlsx','N4:N4');%MW reference
Pref=14.7; %Pressure reference [psi]
IDpipe=xlsread('BPF.xlsx','V4:V10'); %Inner pipe diameter [in]
IDann=xlsread('BPF.xlsx','AE4:AE11');%Inner annuli diameter [in]
ODpipe= xlsread('BPF.xlsx','T4:T10'); %Outer pipe diameter [in]
ODp1= xlsread('BPF.xlsx','AF4:AF11');
Ai=xlsread('BPF.xlsx','AH4:AH10');%[m2]
Ao=xlsread('BPF.xlsx','AG4:AG11');%[m2]
Lpipe= xlsread('BPF.xlsx','R28:R32');
Lpipe2=xlsread('BPF.xlsx','AD4:AD10');%Pipe Length  [m]
Lpipe1=xlsread('BPF.xlsx','R4:R8');% Pipe Length 1 [m]
Aipipe=xlsread('BPF.xlsx','X4:X10'); % Inner Cross sectional area
pipe[in2]
wair=xlsread('BPF.xlsx','Y4:Y8');
IDtj=xlsread('BPF.xlsx','P4:P8');
BC=xlsread('BPF.xlsx','AL4:AL428');%Base case Static
BC2=xlsread('BPF.xlsx','AO4:AO428');%Base Case Dynamic
SFR=xlsread('BPF.xlsx','AR4:AR428');%Side Force RIH
SFP=xlsread('BPF.xlsx','AS4:AS428');%Side Force POOH
SFS=xlsread('BPF.xlsx','AS4:AS428');%Side Force Rotating off Bottom
Aoann=(pi.*((IDann.*0.0254).^2)./4)-Ao; % Annuli cross sectional area
[m2]
AIH=zeros(z); %Area annular
Abn=0.3069;%Bit nozzles area[in2]
Ty= 6.703;% Yield stress [Pa]
n= 0.787; % Behaviour index
k= 0.149; % Consistency index [Pa*s^n]
m= 1/n;
R= zeros(z);
R1=zeros(z);
N=size(IDpipe);
N1=size(IDann);
n1=size(Lpipe1);
na=size(z);
D=(0.0254.*IDann)-(0.0254.*ODp1);%annular diameter [m]
D1=(0.0254.*IDpipe); %inside diameter [m]
Dtj=(0.0254.*IDtj);%inside diameter tool joint [m]
q=3000/(60000); %flow [m3/s] 3000 l/min CAMBIOOOOOS
Q=3000*0.264172; % flow [gpm]CAMBIOSSSS
v=q./(0.0254^2.*Aipipe);% velocity [m/s]
vpipe=zeros(z);%velocity inside pipe
vann=zeros(z); %velocity annular
e=4.6E-05; %Pipe roughness
```

```
b=426;
Rho= zeros(z);%Density [ppg]
Rho1=zeros(z);
P=zeros(z);% Pressure [psi]
Rho(1)= mwref;%Density
P(1)=Pref;% Pressure at cell 1
Recp1=zeros(z);%Re pipe
Reca1=zeros(z);%Re ann
Retj=zeros(z);%Re tool joint
deltaP=zeros(z);% Change of pressure [psi]
P2=zeros(z);
P3=zeros(z);
P4=zeros(z);
fp1=zeros(z);%Darcy friction factor pipe
DpDlp1=zeros(z);%dpdl inside pipe [Pa/m]
Dpp1=zeros(z);%pressure loss inside pipe [Pa]
fa1=zeros(z);%Darcy friction factor annular
DpDlann=zeros(z);%dpdl annular [Pa/m]
Dpa1=zeros(z);%pressure loss inside pipe [Pa]
VFp1=zeros(z);%Viscous Force inside pipe
VFa1=zeros(z);%Viscous Force annular
tol=0.001;% tolerance
dfvd=zeros(z); %Additional force due to viscous drag
dptj=zeros(z);
ktj=zeros(z);
atj=zeros(z);%Area of the Tool Joint
Ao1=zeros(z);
Ai1=zeros(z);
Atj=(pi.*((IDtj).^2)./4);%CAMBIEEEE de m2 para in2
Pwem=zeros(z);%Projected weight of the mud
Pwei=zeros(z);
Pw=zeros(z);
FdeltaA= xlsread('BPF.xlsx', 'AJ4:AJ428');%HYDROSTATIC FORCES DUE TO
CHANGE IN AREA
Dfpv=zeros(z); %
BHP1=zeros(z);%Effective tension Dynamic
cf=12/231; %Conversion Factor
Ptp=zeros(z); %Total pressure pipe
Pta=zeros(z); %Total pressure annular
PAF=zeros(z); %Pressure area force
Dpa=zeros(z);
BFn=zeros(z);
BFd=zeros(z);
Ao1=([Ao1;0]);
IDH=zeros(z);%Inner diameter hole
PAFD=zeros(z);
IF=zeros(z);
IFt=zeros(z);
IFn=zeros(z);
l=zeros(z);
IFSt=zeros(z);%Inertial force tangential direction
IFSn=zeros(z);%Inertial force normal direction
IFS=zeros(z);%Inertial force total
IF2=zeros(z);
theta=zeros(z);
PDDP=zeros(z);%Presure difference Drill Pipe
PDHWDP=zeros(z);%Presure difference HWDP
PDJar=zeros(z);%Presure difference Jar
PDDC=zeros(z);%Presure difference Drill Collar
DragR=zeros(z);%Drag force for RIH
DragP=zeros(z);%Drag force for POOH
```

```
DragS=zeros(z);%Drag force for Rotating off Bottom
%calculation Re (pipe, ann)

for i=2:z
 if TVDm(i)<110
     temp(i)= (tref+(TVDm(i)*tgrad(1)))*(9/5)+ 32;
 else
     if TVDm(i)<1390
      temp(i)= (tref+(TVDm(i)*tgrad(2)))*(9/5)+ 32;
     else
         if TVDm(i)<1405
       temp(i)= (tref+(TVDm(i)*tgrad(3)))*(9/5)+ 32;
         else
             if TVDm(i)<1550
        temp(i)= (tref+(TVDm(i)*tgrad(4)))*(9/5)+ 32;
             else
        temp(i)= (tref+(TVDm(i)*tgrad(5)))*(9/5)+ 32;
             end
         end
     end
 end

    P(i)=0.052*Rho(i-1)*TVDft(i);%initial guess of pressure
    deltaP(i)=P(i);
while(deltaP(i) > tol)
    P2(i)=P(i);
    Rho(i)=roliq(P(i),temp(i));%recalculate density
    P(i)=0.052*Rho(i)*TVDft(i);%recalculate pressure
    deltaP(i)=abs(P(i)-P2(i));
end

  if md(i)<= 3987.25
       R(i)=IDpipe(5)/2;
       Ao1(i)=(pi*(ODpipe(5))^2)/4;
       Ai1(i)=(pi*(IDpipe(5))^2)/4;
       vpipe(i)=q/(0.0254^2.*Aipipe(5));
       Pwei(i)=(wair(5)*(md(i)-md(i-1))*cosd(mean([Inclin(i),Inclin(i-
1)])))*2.2046226218488;
       atj(i)=(Atj(5));%Area tool joint [in2]
       Recp1(i)=((Rho(i)/0.0083)*((vpipe(i))^(2-
n))*D1(5)^(n))/((Ty/8)*(D1(5)/vpipe(i))^(n) +
k*((3*(n*k*(8*vpipe(i)/D1(5))^(n)/(Ty +
k*(8*vpipe(i)/D1(5))^(n)))+1)/(4*(n*k*(8*vpipe(i)/D1(5))^(n)/(Ty +
k*(8*vpipe(i)/D1(5))^(n)))))^(n) *8^(n-1));
       Pwei(i)=(wair(5)*(md(i)-md(i-1))*cosd(mean([Inclin(i),Inclin(i-
1)])))*2.2046226218488; %Projected weight pipe
       if Recp1(i)<1000
           ktj(i)=0;
       else
           if Recp1(i)<=3000
           ktj(i)=1.91*log10(Recp1(i))-5.64;
           else
               if Recp1(i)<=13000
                   ktj(i)=4.66-(1.05*log10(Recp1(i)));
               else
                   ktj(i)=0.33;
               end
           end

       end
       dptj(i)=((Rho(i)/0.0083)*ktj(i)*(vpipe(i))^2)/2;
```

```
        if Recp1(i)>=3302.45 %turbulent inside pipe
         syms x
         eqn= (4/n)*log10(Recp1(i)*x^(1-n/2)+(e/(3.7*D1(5))))-(0.4*n)-
1/(x^0.5)==0;
         fp1(i)=vpasolve(eqn,x);
        else %Laminar inside pipe
          if Recp1(i)<= 2344.95
         fp1(i)=64/Recp1(i);

          end
          fp1(i)=0.3164/(Recp1(i))^(1/4);
        end

DpDlp1(i)=(fp1(i)*(Rho(i)/0.0083)*(vpipe(i))^(2))/(2*0.0254*IDpipe(5));
      Dpp1(i)=DpDlp1(i)*(md(i)-md(i-1));
      wbp(i)=(9.8*wair(5)+((Rho(i)*119.83)*(Ai(5)-Ao(5)))*9.8)*(md(i)-
md(i-1));
  else

    if md(i)<=4205.25
       R(i)=IDpipe(4)/2;
     vpipe(i)=q/(0.0254^2.*Aipipe(4));
       Ao1(i)=(pi*(ODpipe(4))^2)/4;
       Ai1(i)=(pi*(IDpipe(4))^2)/4;
       Pwei(i)=(wair(4)*(md(i)-md(i-1))*cosd(mean([Inclin(i),Inclin(i-
1)])))*2.2046226218488;
        atj(i)=(Atj(4));
       Recp1(i)=((Rho(i)/0.0083)*((vpipe(i))^(2-
n))*D1(4)^(n))/((Ty/8)*(D1(4)/vpipe(i))^(n) +
k*((3*(n*k*(8*vpipe(i)/D1(4))^(n)/(Ty +
k*(8*vpipe(i)/D1(4))^(n)))+1)/(4*(n*k*(8*vpipe(i)/D1(4))^(n)/(Ty +
k*(8*vpipe(i)/D1(4))^(n)))))^(n) *8^(n-1));
       if Recp1(i)<1000
           ktj(i)=0;
       else
           if Recp1(i)<=3000
           ktj(i)=1.91*log10(Recp1(i))-5.64;
           else
               if Recp1(i)<=13000
                   ktj(i)=4.66-(1.05*log10(Recp1(i)));
               else
                   ktj(i)=0.33;
               end
           end

       end
       dptj(i)=((Rho(i)/0.0083)*ktj(i)*(vpipe(i))^2)/2;
       if Recp1(i)>=3302.45 %turbulent inside pipe
       syms x
      eqn= (4/n)*log10(Recp1(i)*x^(1-n/2)+(e/(3.7*D1(4))))-(0.4*n)-
1/(x^0.5)==0;
        fp1(i)=vpasolve(eqn,x);

       else
          if Recp1(i)<= 2344.95%Laminar inside pipe
        fp1(i)=64/Recp1(i);

          end
          fp1(i)=0.3164/(Recp1(i))^(1/4);
       end
```

```
DpDlp1(i)=(fp1(i)*(Rho(i)/0.0083)*(vpipe(i))^(2))/(2*0.0254*IDpipe(4));
       Dpp1(i)=DpDlp1(i)*(md(i)-md(i-1));

    else
           if md(i)<= 4218.5
       R(i)=IDpipe(3)/2;
      vpipe(i)=q/(0.0254^2.*Aipipe(3));
        Ao1(i)=(pi*(ODpipe(3))^2)/4;
       Ai1(i)=(pi*(IDpipe(3))^2)/4;
       Pwei(i)=(wair(3)*(md(i)-md(i-1))*cosd(mean([Inclin(i),Inclin(i-
1)])))*2.2046226218488 ;
       atj(i)=(Atj(3));
       Recp1(i)=((Rho(i)/0.0083)*((vpipe(i))^(2-
n))*D1(3)^(n))/((Ty/8)*(D1(3)/vpipe(i))^(n) +
k*((3*(n*k*(8*vpipe(i)/D1(3))^(n)/(Ty +
k*(8*vpipe(i)/D1(3))^(n)))+1)/(4*(n*k*(8*vpipe(i)/D1(3))^(n)/(Ty +
k*(8*vpipe(i)/D1(3))^(n)))))^(n) *8^(n-1));
        if Recp1(i)<1000
           ktj(i)=0;
       else
           if Recp1(i)<=3000
           ktj(i)=1.91*log10(Recp1(i))-5.64;
           else
               if Recp1(i)<=13000
                   ktj(i)=4.66-(1.05*log10(Recp1(i)));
               else
                   ktj(i)=0.33;
               end
           end

       end
       dptj(i)=((Rho(i)/0.0083)*ktj(i)*(vpipe(i))^2)/2;
           if Recp1(i)>=3302.45 %turbulent inside pipe
       syms x
       eqn= (4/n)*log10(Recp1(i)*x^(1-n/2)+(e/(3.7*D1(3))))-(0.4*n)-
1/(x^0.5)==0;
       fp1(i)=vpasolve(eqn,x);

       else %Laminar inside pipe
           if Recp1(i)<= 2344.95
        fp1(i)=64/Recp1(i);

           end
           fp1(i)=0.3164/(Recp1(i))^(1/4);
           end

DpDlp1(i)=(fp1(i)*(Rho(i)/0.0083)*(vpipe(i))^(2))/(2*0.0254*IDpipe(3));
        Dpp1(i)=DpDlp1(i)*(md(i)-md(i-1));

          else
          if md(i)<= 4238.17
        Ao1(i)=(pi*(ODpipe(2))^2)/4;
       Ai1(i)=(pi*(IDpipe(2))^2)/4;
        R(i)=IDpipe(2)/2;
        vpipe(i)=q/(0.0254^2.*Aipipe(2));
        Pwei(i)=(wair(2)*(md(i)-md(i-1))*cosd(mean([Inclin(i),Inclin(i-
1)])))*2.2046226218488;
        atj(i)=(Atj(2));
```

```
        Recp1(i)=((Rho(i)/0.0083)*((vpipe(i))^(2-
n))*D1(2)^(n))/((Ty/8)*(D1(2)/vpipe(i))^(n) +
k*((3*(n*k*(8*vpipe(i)/D1(2))^(n)/(Ty +
k*(8*vpipe(i)/D1(2))^(n)))+1)/(4*(n*k*(8*vpipe(i)/D1(2))^(n)/(Ty +
k*(8*vpipe(i)/D1(2))^(n)))))^(n) *8^(n-1));
          if Recp1(i)<1000
           ktj(i)=0;
       else
           if Recp1(i)<=3000
           ktj(i)=1.91*log10(Recp1(i))-5.64;
           else
               if Recp1(i)<=13000
                   ktj(i)=4.66-(1.05*log10(Recp1(i)));
               else
                   ktj(i)=0.33;
               end
           end

       end
        dptj(i)=((Rho(i)/0.0083)*ktj(i)*(vpipe(i))^2)/2;
        if Recp1(i)>=3302.45 %turbulent inside pipe
       syms x

       eqn= (4/n)*log10(Recp1(i)*x^(1-n/2)+(e/(3.7*D1(2))))-(0.4*n)-
1/(x^0.5)==0;
        fp1(i)=vpasolve(eqn,x);

       else %Laminar inside pipe
           if Recp1(i)<= 2344.95
        fp1(i)=64/Recp1(i);

           end
         fp1(i)=0.3164/(Recp1(i))^(1/4);
           end

DpDlp1(i)=(fp1(i)*(Rho(i)/0.0083)*(vpipe(i))^(2))/(2*0.0254*IDpipe(2));
        Dpp1(i)=DpDlp1(i)*(md(i)-md(i-1));

          else
        R(i)=IDpipe(1)/2;
       vpipe(i)=q/(0.0254^2.*Aipipe(1));
       Ao1(i)=(pi*(ODpipe(1))^2)/4;
       Ai1(i)=(pi*(IDpipe(1))^2)/4;
       Pwei(i)=(wair(1)*(md(i)-md(i-1))*cosd(mean([Inclin(i),Inclin(i-
1)])))*2.2046226218488;
         atj(i)=(Atj(1));
         Recp1(i)=((Rho(i)/0.0083)*((vpipe(i))^(2-
n))*D1(1)^(n))/((Ty/8)*(D1(1)/vpipe(i))^(n) +
k*((3*(n*k*(8*vpipe(i)/D1(1))^(n)/(Ty +
k*(8*vpipe(i)/D1(1))^(n)))+1)/(4*(n*k*(8*vpipe(i)/D1(1))^(n)/(Ty +
k*(8*vpipe(i)/D1(1))^(n)))))^(n) *8^(n-1));

        if Recp1(i)>=3302.45 %turbulent inside pipe
       syms x

       eqn= (4/n)*log10(Recp1(i)*x^(1-n/2)+(e/(3.7*D1(1))))-(0.4*n)-
1/(x^0.5)==0;
        fp1(i)=vpasolve(eqn,x);

       else %Laminar inside pipe
```

```
           if Recp1(i)<= 2344.95
        fp1(i)=64/Recp1(i);

           end
           fp1(i)=0.3164/(Recp1(i))^(1/4);
        end

DpDlp1(i)=(fp1(i)*(Rho(i)/0.0083)*(vpipe(i))^(2))/(2*0.0254*IDpipe(1));
        Dpp1(i)=DpDlp1(i)*(md(i)-md(i-1));

           end
            end
    end

  end
   VFp1(i)=(Dpp1(i)*(pi*(R(i)*0.0254)^2))*0.2248090795; %Viscous force
in the wall of the pipe [Pound]

   if md(i)<=180
     R1(i)=(IDann(8)-ODp1(8))/2;
     AIH(i)=((pi*(IDann(8))^2)/4)-Ao1(i);%Area inside the hole [in2]
     vann(i)=q/(Aoann(8));
     Reca1(i)=((Rho(i)/0.0083)*((vann(i))^(2-
n))*D(8)^(n))/((Ty/8)*(D(8)/vann(i))^(n) +
k*((3*(n*k*(8*vann(i)/D(8))^(n)/(Ty +
k*(8*vann(i)/D(8))^(n)))+1)/(4*(n*k*(8*vann(i)/D(8))^(n)/(Ty +
k*(8*vann(i)/D(8))^(n)))))^(n) *8^(n-1));
      if Reca1(i)>=3302.45 %turbulent annuli
       syms x
        eqn3= -2*log10((2.51/((x^0.5)*Reca1(i)))+(e/(3.7*D(8))))-
1/(x^0.5)==0;
        fa1(i)=vpasolve(eqn3,x);

        else %Laminar annuli
        if Reca1(i)<= 2344.95
         fa1(i)=64/Reca1(i);

DpDlann(i)=(fa1(i)*(Rho(i)/0.0083)*(vann(i))^(2))/(2*0.0254*(IDann(8)-
ODp1(8)));
         Dpa1(i)=DpDlann(i)*(md(i)-md(i-1));

        end
        fa1(i)=0.3164/(Reca1(i))^(1/4); %Intermediate flow
    end

DpDlann(i)=(fa1(i)*(Rho(i)/0.0083)*(vann(i))^(2))/(2*0.0254*(IDann(8)-
ODp1(8)));
    Dpa1(i)=DpDlann(i)*(md(i)-md(i-1));
    dfvd(i)=(pi*Dpa1(i)*((0.0254*IDann(8))^(2) -
(0.0254*ODp1(8))^(2))*0.0254*ODp1(8))/(4*0.0254*(IDann(8)-ODp1(8)));
    else
    if md(i)<=1879 %Annular
     AIH(i)=((pi*(IDann(7))^2)/4)-Ao1(i);%Area inside the hole [in2]
     R1(i)=(IDann(7)-ODp1(7))/2;
     vann(i)=q/(Aoann(7));
     Reca1(i)=((Rho(i)/0.0083)*((vann(i))^(2-
n))*D(7)^(n))/((Ty/8)*(D(7)/vann(i))^(n) +
k*((3*(n*k*(8*vann(i)/D(7))^(n)/(Ty +
k*(8*vann(i)/D(7))^(n)))+1)/(4*(n*k*(8*vann(i)/D(7))^(n)/(Ty +
k*(8*vann(i)/D(7))^(n)))))^(n) *8^(n-1));
```

```
    if Reca1(i)>=3302.45 %turbulent annuli
       syms x
        eqn3= -2*log10((2.51/((x^0.5)*Reca1(i)))+(e/(3.7*D(7))))-
1/(x^0.5)==0;
        fa1(i)=vpasolve(eqn3,x);

    else %Laminar annuli
        if Reca1(i)<= 2344.95
         fa1(i)=64/Reca1(i);

DpDlann(i)=(fa1(i)*(Rho(i)/0.0083)*(vann(i))^(2))/(2*0.0254*(IDann(7)-
ODp1(7)));
         Dpa1(i)=DpDlann(i)*(md(i)-md(i-1));

        end
        fa1(i)=0.3164/(Reca1(i))^(1/4); %Intermediate flow
    end

DpDlann(i)=(fa1(i)*(Rho(i)/0.0083)*(vann(i))^(2))/(2*0.0254*(IDann(7)-
ODp1(7)));
    Dpa1(i)=DpDlann(i)*(md(i)-md(i-1));
    dfvd(i)=(pi*Dpa1(i)*((0.0254*IDann(7))^(2) -
(0.0254*ODp1(7))^(2))*0.0254*ODp1(7))/(4*0.0254*(IDann(7)-ODp1(7)));
    else
        if md(i)<= 2917
            R1(i)=(IDann(6)-ODp1(6))/2;
            AIH(i)=((pi*(IDann(6))^2)/4)-Ao1(i);%Area inside the hole
[in2]
            vann(i)=q/(Aoann(6));
            Reca1(i)=((Rho(i)/0.0083)*((vann(i))^(2-
n))*D(6)^(n))/((Ty/8)*(D(6)/vann(i))^(n) +
k*((3*(n*k*(8*vann(i)/D(6))^(n)/(Ty +
k*(8*vann(i)/D(6))^(n)))+1)/(4*(n*k*(8*vann(i)/D(6))^(n)/(Ty +
k*(8*vann(i)/D(6))^(n)))))^(n) *8^(n-1));

        if Reca1(i)>=3302.45 %turbulent annuli
       syms x
        eqn3= -2*log10((2.51/((x^0.5)*Reca1(i)))+(e/(3.7*D(6))))-
1/(x^0.5)==0;
        fa1(i)=vpasolve(eqn3,x);

    else %Laminar annuli
         if Reca1(i)<= 2344.95
         fa1(i)=64/Reca1(i);

DpDlann(i)=(fa1(i)*(Rho(i)/0.0083)*(vann(i))^(2))/(2*0.0254*(IDann(6)-
ODp1(6)));
         Dpa1(i)=DpDlann(i)*(md(i)-md(i-1));
          end
          fa1(i)=0.3164/(Reca1(i))^(1/4); %Intermediate flow
        end

DpDlann(i)=(fa1(i)*(Rho(i)/0.0083)*(vann(i))^(2))/(2*0.0254*(IDann(6)-
ODp1(6)));
        Dpa1(i)=DpDlann(i)*(md(i)-md(i-1));
        dfvd(i)=(pi*Dpa1(i)*((0.0254*IDann(6))^(2) -
(0.0254*ODp1(6))^(2))*0.0254*ODp1(6))/(4*0.0254*(IDann(6)-ODp1(6)));
        else
            if md(i)<3987.25
```

```
            R1(i)=(IDann(5)-ODp1(5))/2;
            AIH(i)=((pi*(IDann(5))^2)/4)-Ao1(i);%Area inside the hole
[in2]
            vann(i)=q/(Aoann(5));
            Reca1(i)=((Rho(i)/0.0083)*((vann(i))^(2-
n))*D(5)^(n))/((Ty/8)*(D(5)/vann(i))^(n) +
k*((3*(n*k*(8*vann(i)/D(5))^(n)/(Ty +
k*(8*vann(i)/D(5))^(n)))+1)/(4*(n*k*(8*vann(i)/D(5))^(n)/(Ty +
k*(8*vann(i)/D(5))^(n)))))^(n) *8^(n-1));

            if Reca1(i)>=3302.45 %turbulent annuli
       syms x
        eqn3= -2*log10((2.51/((x^0.5)*Reca1(i)))+(e/(3.7*D(5))))-
1/(x^0.5)==0;
        fa1(i)=vpasolve(eqn3,x);

            else %Laminar annuli
                  if Reca1(i)<= 2344.95
         fa1(i)=64/Reca1(i);

DpDlann(i)=(fa1(i)*(Rho(i)/0.0083)*(vann(i))^(2))/(2*0.0254*(IDann(5)-
ODp1(5)));
           Dpa1(i)=DpDlann(i)*(md(i)-md(i-1));
                 end
              fa1(i)=0.3164/(Reca1(i))^(1/4);
            end

DpDlann(i)=(fa1(i)*(Rho(i)/0.0083)*(vann(i))^(2))/(2*0.0254*(IDann(5)-
ODp1(5)));
           Dpa1(i)=DpDlann(i)*(md(i)-md(i-1));
            dfvd(i)=(pi*Dpa1(i)*((0.0254*IDann(5))^(2) -
(0.0254*ODp1(5))^(2))*0.0254*ODp1(5))/(4*0.0254*(IDann(5)-ODp1(5)));
            else
               if md(i)<= 4205.25
              R1(i)=(IDann(4)-ODp1(4))/2;
              AIH(i)=((pi*(IDann(4))^2)/4)-Ao1(i);%Area inside the hole
[in2]
             vann(i)=q/(Aoann(4));
             Reca1(i)=((Rho(i)/0.0083)*((vann(i))^(2-
n))*D(4)^(n))/((Ty/8)*(D(4)/vann(i))^(n) +
k*((3*(n*k*(8*vann(i)/D(4))^(n)/(Ty +
k*(8*vann(i)/D(4))^(n)))+1)/(4*(n*k*(8*vann(i)/D(4))^(n)/(Ty +
k*(8*vann(i)/D(4))^(n)))))^(n) *8^(n-1));

                if Reca1(i)>=3302.45 %turbulent annuli
                syms x
                eqn3= -
2*log10((2.51/((x^0.5)*Reca1(i)))+(e/(3.7*D(4))))-1/(x^0.5)==0;
                fa1(i)=vpasolve(eqn3,x);

            else %Laminar annuli
                  if Reca1(i)<= 2344.95
                 fa1(i)=64/Reca1(i);

DpDlann(i)=(fa1(i)*(Rho(i)/0.0083)*(vann(i))^(2))/(2*0.0254*(IDann(4)-
ODp1(4)));
                Dpa1(i)=DpDlann(i)*(md(i)-md(i-1));
                   end
                  fa1(i)=0.3164/(Reca1(i))^(1/4);
                end
```

```
DpDlann(i)=(fa1(i)*(Rho(i)/0.0083)*(vann(i))^(2))/(2*0.0254*(IDann(4)-
ODp1(4)));
                Dpa1(i)=DpDlann(i)*(md(i)-md(i-1));
                dfvd(i)=(pi*Dpa1(i)*((0.0254*IDann(4))^(2) -
(0.0254*ODp1(4))^(2))*0.0254*ODp1(4))/(4*0.0254*(IDann(4)-ODp1(4)));
              else
                   if md(i)<= 4218.5
                      AIH(i)=((pi*(IDann(3))^2)/4)-Ao1(i);%Area inside
the hole [in2]
                       R1(i)=(IDann(3)-ODp1(3))/2;
                       vann(i)=q/(Aoann(3));
                       Reca1(i)=((Rho(i)/0.0083)*((vann(i))^(2-
n))*D(3)^(n))/((Ty/8)*(D(3)/vann(i))^(n) +
k*((3*(n*k*(8*vann(i)/D(3))^(n)/(Ty +
k*(8*vann(i)/D(3))^(n)))+1)/(4*(n*k*(8*vann(i)/D(3))^(n)/(Ty +
k*(8*vann(i)/D(3))^(n)))))^(n) *8^(n-1));

                   if Reca1(i)>=3302.45 %turbulent annuli
                      syms x
                      eqn3= -
2*log10((2.51/((x^0.5)*Reca1(i)))+(e/(3.7*D(3))))-1/(x^0.5)==0;
                       fa1(i)=vpasolve(eqn3,x);

                       else %Laminar annuli
                         if Reca1(i)<= 2344.95
                       fa1(i)=64/Reca1(i);

DpDlann(i)=(fa1(i)*(Rho(i)/0.0083)*(vann(i))^(2))/(2*0.0254*(IDann(3)-
ODp1(3)));
                       Dpa1(i)=DpDlann(i)*(md(i)-md(i-1));

                        end
                       fa1(i)=0.3164/(Reca1(i))^(1/4);
                   end

DpDlann(i)=(fa1(i)*(Rho(i)/0.0083)*(vann(i))^(2))/(2*0.0254*(IDann(3)-
ODp1(3)));
                   Dpa1(i)=DpDlann(i)*(md(i)-md(i-1));

                   dfvd(i)=(pi*Dpa1(i)*((0.0254*IDann(3))^(2) -
(0.0254*ODp1(3))^(2))*0.0254*ODp1(3))/(4*0.0254*(IDann(3)-ODp1(3)));
                   else
                       if md(i)<= 4238.17
                           R1(i)=(IDann(2)-ODp1(2))/2;
                           AIH(i)=((pi*(IDann(2))^2)/4)-Ao1(i);%Area
inside the hole [in2]
                           vann(i)=q/(Aoann(2));
                           Reca1(i)=((Rho(i)/0.0083)*((vann(i))^(2-
n))*D(2)^(n))/((Ty/8)*(D(2)/vann(i))^(n) +
k*((3*(n*k*(8*vann(i)/D(2))^(n)/(Ty +
k*(8*vann(i)/D(2))^(n)))+1)/(4*(n*k*(8*vann(i)/D(2))^(n)/(Ty +
k*(8*vann(i)/D(2))^(n)))))^(n) *8^(n-1));

                           if Reca1(i)>=3302.45 %turbulent annuli
                            syms x
                               eqn3= -
2*log10((2.51/((x^0.5)*Reca1(i)))+(e/(3.7*D(2))))-1/(x^0.5)==0;
                               fa1(i)=vpasolve(eqn3,x);
```

```
                                else %Laminar annuli
                                      if Reca1(i)<= 2344.95
                                    fa1(i)=64/Reca1(i);

DpDlann(i)=(fa1(i)*(Rho(i)/0.0083)*(vann(i))^(2))/(2*0.0254*(IDann(2)-
ODp1(2)));
                                         Dpa1(i)=DpDlann(i)*(md(i)-md(i-1));


                                      end
                                  fa1(i)=0.3164/(Reca1(i))^(1/4);

                                end

DpDlann(i)=(fa1(i)*(Rho(i)/0.0083)*(vann(i))^(2))/(2*0.0254*(IDann(2)-
ODp1(2)));
                               Dpa1(i)=DpDlann(i)*(md(i)-md(i-1));
                               dfvd(i)=(pi*Dpa1(i)*((0.0254*IDann(2))^(2) -
(0.0254*ODp1(2))^(2))*0.0254*ODp1(2))/(4*0.0254*(IDann(2)-ODp1(2)));
                            else
                                R1(i)=(IDann(1)-ODp1(1))/2;
                               AIH(i)=((pi*(IDann(1))^2)/4)-Ao1(i);%Area
inside the hole [in2]

                                vann(i)=q/(Aoann(1));
                                Reca1(i)=((Rho(i)/0.0083)*((vann(i))^(2-
n))*D(1)^(n))/((Ty/8)*(D(1)/vann(i))^(n) +
k*((3*(n*k*(8*vann(i)/D(1))^(n)/(Ty +
k*(8*vann(i)/D(1))^(n)))+1)/(4*(n*k*(8*vann(i)/D(1))^(n)/(Ty +
k*(8*vann(i)/D(1))^(n)))))^(n) *8^(n-1));

                                if Reca1(i)>=3302.45 %turbulent annuli
                                 syms x
                                    eqn3= -
2*log10((2.51/((x^0.5)*Reca1(i)))+(e/(3.7*D(1))))-1/(x^0.5)==0;
                                    fa1(i)=vpasolve(eqn3,x);

                                else %Laminar annuli
                                      if Reca1(i)<= 2344.95
                                    fa1(i)=64/Reca1(i);

DpDlann(i)=(fa1(i)*(Rho(i)/0.0083)*(vann(i))^(2))/(2*0.0254*(IDann(1)-
ODp1(1)));
                                    Dpa1(i)=DpDlann(i)*(md(i)-md(i-1));
                                      end
                                    fa1(i)=0.3164/(Reca1(i))^(1/4);

                                end

DpDlann(i)=(fa1(i)*(Rho(i)/0.0083)*(vann(i))^(2))/(2*0.0254*(IDann(1)-
ODp1(1)));
                               Dpa1(i)=DpDlann(i)*(md(i)-md(i-1));
                              dfvd(i)=(pi*Dpa1(i)*((0.0254*IDann(1))^(2) -
(0.0254*ODp1(1))^(2))*0.0254*ODp1(1))/(4*0.0254*(IDann(1)-ODp1(1)));%[N]
                            end
                        end
                    end
                end
            end
        end
```

```
   end
   %Buoyancy calculations
   if md(i)<= 3987.25
    BFn(i)=(Lpipe(1))*Rho(i)*(ODpipe(5)^2 - IDpipe(5)^2);
    BFd(i)=(Rhopipe*(Lpipe(1))*(ODpipe(5)^2 - IDpipe(5)^2));

else
if md(i)<=4205.25
     BFn(i)=(Lpipe(2))*Rho(i)*(ODpipe(4)^2 - IDpipe(4)^2);
     BFd(i)=(Rhopipe*(Lpipe(2))*(ODpipe(4)^2 - IDpipe(4)^2));

else
 if md(i)<= 4218.5
     BFn(i)=(Lpipe(3))*Rho(i)*(ODpipe(3)^2 - IDpipe(3)^2);
     BFd(i)=(Rhopipe*(Lpipe(3))*(ODpipe(3)^2 - IDpipe(3)^2));
 else
if md(i)<= 4238.17
    BFn(i)=(Lpipe(4))*Rho(i)*(ODpipe(2)^2 - IDpipe(2)^2);
    BFd(i)=(Rhopipe*(Lpipe(4))*(ODpipe(2)^2 - IDpipe(2)^2));
else
    BFn(i)=(Lpipe(5))*Rho(i)*(ODpipe(1)^2 - IDpipe(1)^2);
    BFd(i)=(Rhopipe*(Lpipe(5))*(ODpipe(1)^2 - IDpipe(1)^2));
end
 end
end
end

   VFa1(i)=(Dpa1(i)*(pi*(R1(i)*0.0254)^2))*0.2248090795; %Viscous force
in the wall of the anullar[pound]
   Ptp(i)= P(i)+((Dpp1(i)+dptj(i))*0.000145038);%Dynamic Pressure pipe
   Pta(i)= P(i)+(Dpa1(i)*0.000145038);%Dynamic Pressure annular


  Dfpv(i)=(dfvd(i)*0.22480894244319)/(AIH(i));%Extra pressure generated
due to viscous drag force ANNULAR
  xdp=cumsum(Dfpv,'reverse');
end

PlossBitNoz=((8.3e-05)*Q^(2) * Rho(425))/(Abn^(2)*0.95^(2));%pressure
drop through bit nozzlez psi
Plossi= ((sum(Dpp1)+sum(dptj))*0.000145038)+ PlossBitNoz% Pressure loss
pipe plus bite nozzles[psi]
Plossa=sum(Dpa1)*0.000145038% Pressure loss annuli [psi]
VFann=sum(VFa1);% Total Viscous Force ann [pound]
VFann2=VFa1;
VFpipe=sum(VFp1);% Total Viscous Force pipe [ pound]
VFpipe2=VFp1;
dfvds=sum(dfvd)*0.2248090795;%
Fdrag=(VFp1-VFa1+dfvd)*0.2248090795;%Drag force [pound]
Fbtm= P(425)*Ao1(425);%Bottom pressure force [pound]
drev=fliplr(md);
for i=2:z
    if md(i)<= 3987.25
     PDDP(i)=(Dpa1(i))*0.000145038;

    else
        if md(i)<=4205.25
      PDHWDP(i)=(Dpa1(i))*0.000145038;
        else
            if md(i)<= 4218.5
```

```
            PDJar(i)=(Dpa1(i))*0.000145038;
            else
                if md(i)<= 4238.17
                  PDDC(i)=(Dpa1(i))*0.000145038;
                else

                end
            end
        end
    end

end
DPD=sum(PDDP);
DPHW=sum(PDHWDP);
DPJ=sum(PDJar);
DPDC=sum(PDDC);
PlossBitNoz;
BF= 1-(sum(BFn)/sum(BFd)); %Buoyancy Factor
Dpp=cumsum(Dpp1);%Pressure drop iniside pipe
Dpa=cumsum(Dpa1,'reverse');%Pressure drop annuli
W=cumsum(Pwei,'reverse');%Cumulative weight of the pipe from the Bottom
to the top
  for i=z:-1:2
   Pwem(i)=Ai1(i)*(mdft(i)-mdft(i-
1))*cf*Rho(i)*cosd(mean([Inclin(i),Inclin(i-1)]));
   MW=cumsum(Pwem,'reverse');
   TW=W+MW;
  end
  Pltj=(dptj.*0.000145038);%Pressure losses Tool Joint psi
  Pltjcum=cumsum(Pltj);
  W2=(cumsum(Pwei)+cumsum(Pwem))./10^3;

PP=P(425)+(Dpp(425)*0.000145038)+(Dpa(1)*0.000145038)+PlossBitNoz+xdp(1)
+Pltjcum(425);%Pump pressure [psi]
  VFtj=(Pltj.*atj);%Viscous force tool joint [pound]
  BHP=PP+P(425)-(Dpp(425)*0.000145038)-PlossBitNoz-Pltjcum(425);


  BWF=BF.*(cumsum(Pwei));%Buoyant weight
  Rho1=(Rho).*119.83;%[Kg/m3]

 for i=2:z
   l(i)=md(i)-md(i-1);%Lenght of the section
   P3(i)=BHP+((Dpa(i)*0.000145038))+xdp(i)-P(i);%Pressure profile
without hyd pressure [psi]
   P4(i)=BHP+((Dpa(i)*0.000145038))+xdp(i);
   if Ao1(i)==Ao1(i+1)
   else
   PAF(i)=P3(i)*(Ao1(i+1)-Ao1(i));%Hydraulic pressure due to change of
area
   PAFD(i)=P(i)*(Ao1(i+1)-Ao1(i));
   end

 end
 P3=([P3;P3(425)]).*6894.76;%[Pa]
P4=([P4;P4(425)]).*6894.76;%from bernoulli
 P=([P;0]).*6894.76;
 Ai1=Ai1.*0.0254^2;%[m2]
 var=(Rho1.*q^2)./(Ai1);
```

```
 for i=2:z
        IFSt(i)=(Ai1(i)*(P4(i)-P4(i+1)*cosd(l(i)*DLS(i))))-
(var(i)*(cosd(l(i)*DLS(i))-1));

IFSn(i)=((Ai1(i)*P4(i+1)*sind(l(i)*DLS(i)))+var(i)*sind(l(i)*DLS(i)));
 IF(i)= sqrt(((IFSt(i))^2 + (IFSn(i))^2))*0.2248090795;
 theta(i)=atand(IFSn(i)/IFSt(i));
 DragR(i)=(SFR(i)*(md(i)-md(i-1))*0.2)/10^3;%Drag force for RIH
 DragP(i)=(SFP(i)*(md(i)-md(i-1))*0.2)/10^3;%Drag force for POOH
 DragS(i)=(SFS(i)*(md(i)-md(i-1))*0.2)/10^3;%Drag force for Rotating off
Bottom
 end
VFW=BC-(VFpipe/10^3)+(VFann/10^3)-(VFtj./10^3)-(PlossBitNoz/10^3)-
DragS;%Effect of viscous force
VFM=(VFann/10^3)-(VFpipe/10^3)-(VFtj./10^3)-(PlossBitNoz/10^3)-DragS;
IFC=BC-((IF)./10^3);%Inertial force
PF1=W2+cumsum(PAF./10^3)-DragS;% Pressure area force for Rotatibg Bottom
PAF(425)=0;
Bwei=BF*(sum(Pwei));%Buoyed weight [Lb]
B=(BF.*(cumsum(Pwei))./10^3)-DragS;%Buoyancy for Rotating off Bottom
BD=W2+cumsum(PAFD./10^3);
TF=TW(1)+sum(PAF);
Dif=W2(425)-TF; %Difference between dynamic and static pressure area
AFT=BC+(VFM)-((IF)./10^3)+(((PAF)./10^3)-DragS); %All forces together
effect
AFTR=AFT-DragR;%All forces together effect RIH
AFTP=AFT+DragP;%All forces together effect POOH
BR=B-DragR;%Effect of bouyancy force RIH
BP=B+DragP;%Effect of piston force POOH
PAR=PF1-DragR;%Effect of piston force RIH
PAP=PF1+DragP;%Effect of piston force POOH
IFR=IFC-DragR;%Effect of inertal force RIH
IFP=IFC+DragP;%Effect of inertal force POOH
VFR=VFW-DragR;%Effect of viscous force RIH
VFP=VFW+DragP;%Effect of viscous force POOH
EIF=((BC-IFC)./BC).*100;%Effect of Inertial Force
plot(BC,md,'m',IFC,md,'r',BC2,md,'k')%
set(gca, 'YDir','reverse')
title('HKLD vs MD')
xlabel('Weight [Kpound]')
ylabel('Depth [m]')
legend('Base Case Static','Effect of All Forces','Base Case dynamic')
grid on
%% Effect of inertial force versus inclination
plot(Inclin,md,EIF,md)%
set(gca, 'YDir','reverse')
title('Inclination vs Effect of inertial force')
xlabel('Inclination [degrees]')
ylabel('Depth [m]')
legend('Inclination','Effecf')
grid on
%% Pressure Area
plot(PF1,md,'r',BC2,md,'k',BC,md,'b')
set(gca, 'YDir','reverse')
title('P/A force vs MD')
xlabel('Weight [kpound]')
ylabel('Depth [m]')
legend('P/A force w/ flow effect','Base case Dyn','Base case Stat')
grid on
%% Inertial force
plot(IFC,md,'b',BC2,md,'k',BC,md,'r')
```

```
set(gca, 'YDir','reverse')
title('Inertial force vs MD')
xlabel('Weight [kpound]')
ylabel('Depth [m]')
legend('Inertial force effect','Base Case Dynamic','Base Case Static')
grid on
%% Viscous Force
plot(VFW,md,BC,md,'k',BC2,md,'r')
set(gca, 'YDir','reverse')
title('Viscous force vs MD')
xlabel('Weight [kpound]')
ylabel('Depth [m]')
legend('Effect of Viscous','Base Case Static','Base Case Dyn')
grid on
%% Effect all forces
plot(BC,md,AFT,md,'r',BC2,md,'k')%
set(gca, 'YDir','reverse')
title('HKLD vs MD')
xlabel('Weight [Kpound]')
ylabel('Depth [m]')
legend('Base Case Static','Effect of All Forces','Base Case Dynamic')
grid on
%% Buoyancy vs BC
plot(B,md,'b',BC,md,'r')
set(gca, 'YDir','reverse')
title('HKLD vs MD')
xlabel('Weight [kpound]')
ylabel('Depth [m]')
legend('Buoyant weight','Base Case')
grid on
%% Effect all forces td
plot(BC,md,'m',AFT,md,'r',AFTR,md,'k',AFTP,md,'b')%
set(gca, 'YDir','reverse')
title('HKLD vs MD')
xlabel('Weight [Kpound]')
ylabel('Depth [m]')
legend('Base Case Static','Effect of All Forces','RIH','POOH')
grid on
%% buoyancy T&D
plot(BC,md,'m',B,md,'r',BR,md,'k',BP,md,'b')%
set(gca, 'YDir','reverse')
title('HKLD vs MD')
xlabel('Weight [Kpound]')
ylabel('Depth [m]')
legend('Base Case Static','Buoyancy','RIH','POOH')
grid on
%% P/A T&D
plot(BC,md,'m',PF1,md,'r',PAR,md,'k',PAP,md,'b')%
set(gca, 'YDir','reverse')
title('HKLD vs MD')
xlabel('Weight [Kpound]')
ylabel('Depth [m]')
legend('Base Case Static','Pressure Area','RIH','POOH')
grid on
%% IF T&D
plot(BC,md,'m',IFC,md,'r',IFR,md,'k',IFP,md,'b')%
set(gca, 'YDir','reverse')
title('HKLD vs MD')
xlabel('Weight [Kpound]')
ylabel('Depth [m]')
legend('Base Case Static','Inertial Force','RIH','POOH')
```

```
grid on
%% Viscous T&D
plot(BC,md,'m',VFW,md,'r',VFR,md,'k',VFP,md,'b')%
set(gca, 'YDir','reverse')
title('HKLD vs MD')
xlabel('Weight [Kpound]')
ylabel('Depth [m]')
legend('Base Case Static','Viscous','RIH','POOH')
grid on
%%
plot(BC,md,'m',AFT,md,'r',BC2,md,'k')%
set(gca, 'YDir','reverse')
title('HKLD vs MD')
xlabel('Weight [Kpound]')
ylabel('Depth [m]')
legend('Base Case Static','Effect of All Forces','Base Case dynamic')
grid on
%%
plot(BC,md,'m',VFW,md,'r',BC2,md,'k')%
set(gca, 'YDir','reverse')
title('HKLD vs MD')
xlabel('Weight [Kpound]')
ylabel('Depth [m]')
legend('Base Case Static','Effect of viscous force','Base Case dynamic')
grid on
```